Universidad Autónoma de Madrid

Facultad de Ciencias

Departamento de Biología Molecular

"*In vivo* and *in vitro* studies of the *lrpC-topB* operon of *Bacillus subtilis*"

Tesis Doctoral

Esther Patricia García Tirado

Madrid 2011

UAM UNIVERSIDAD AUTONOMA DE MADRID

CNB CENTRO NACIONAL DE BIOTECNOLOGIA

Memoria presentada por Esther Patricia García Tirado para optar al título de Doctor en Ciencias por la Universidad Autónoma de Madrid

El trabajo ha sido realizado en el Centro Nacional de Biotecnología (CNB-CSIC) bajo la dirección de la Dra. Silvia Ayora Hirsch y del Prof. Juan Carlos Alonso.

INDEX

INDEX

FIGURES AND TABLES INDEX

FIGURE INDEX

TABLE INDEX

ABBREVIATIONS

ABBREVIATIONS

ATP: adenosin triphosphate
BSA: bovine serum albumin
bp: base pair
Cm: chloramphenicol
DAPI: 4´, 6´-diamino-2-phenylindole
DNA: deoxyribonucleic acid
dsDNA: double strand DNA
DSB: double strand break
dsDNA: double-strand DNA
DSS: disuccinyl suberate
DTT: dithiothreitol
FPLC: fast protein liquid chromatography
HJ: Holliday Junction
HR: homologous recombination
Kbp: kilobase pair
KDa: kilodaltons
LB: Luria-Bertani rich medium
min: minutes
MMC: mitomycin C
MMS: methyl methanesulfonate
PAGE: polyachrylamide gel electrophoresis
RC: repair center
RNA: riboxynucleic acid
RT: retrotranscriptase
scDNA: supercoiled DNA
SDS: sodium dodecyl sulfate
SDS-PAGE: polyacrylamide gel electrophoresis in presence of SDS
Sp: spectinomycin
ssDNA: single-strand DNA

TE: Tris-acetate

TBE: Tris-borate

SUMMARY

INTRODUCCIÓN

El gen *lrpC* de *Bacillus subtilis*, que ha sido caracterizado como un gen no esencial, posiblemente regula el metabolismo de aminoácidos celular y disminuye el tiempo de entrada en fase de esporulación (Beloin et al., 1997). LrpC es capaz de autoregular su propia expresión (Beloin et al., 2000). LrpC es una proteína de unión a DNA independiente de secuencia, presentando una mayor afinidad por DNA de doble cadena curvado, aunque es capaz de unirse a un amplio rango de tipos de DNA. Teniendo en cuenta estos datos bioquímicos se ha propuesto un posible papel de LrpC como proteína arquitectural, lo que viene avalado por los datos de microscopía de fuerzas atómicas que revelan la unión de LrpC al DNA formando los denominados "nucleosomas" celulares (Beloin et al., 2003). La resolución del cristal de LrpC revela un octámero en estructura cruciforme, que se uniría al DNA curvándolo y compactándolo (Thaw et al., 2006). En *B.subtilis*, el gen *topB*, que se encuentra aguas abajo del gen *lrpC*, codifica para la proteína Topoisomerasa III. Esta proteína pertenece a la superfamilia de las topoisomerasas tipo IA. El mecanismo de acción de las topoisomerasas en general consiste en la ruptura de una o las dos hebras del DNA mediante el ataque nucleofílico de la tirosina del centro activo de la enzima al fosfato del esqueleto del DNA. La forma en la que se lleva a cabo dicha función ha llevado a clasificar a las topoisomerasas en dos familias denominadas tipo I (cortan una hebra del DNA) y tipo II (cortan las dos hebras del DNA). Nos centraremos en las topoisomerasas tipo IA, que comprenden Topo I y III de procariotas y Topo III de eucariotas. Estas enzimas crean un enlace 5´-fosfotirosil con el DNA, cortando una de las hebras del DNA, lo que les permite relajar un DNA inicialmente superenrollado (Depew et al., 1978; Liu and Wang, 1979; Tse et al., 1980). Topo III de *E.coli* ha sido caracterizada como una enzima capaz de decatenar intermediarios tardíos de tipo θ del plásmido pBR322 (DiGate and Marians, 1988). Sin embargo, a diferencia de Topo I, relaja probremente un DNA superenrollado, a una temperatura óptima de 52°C (DiGate and Marians, 1988). Junto con la helicasa RecQ, Topo III es capaz de resolver horquillas de replicación convergentes, y esto se ha demostrado que se realiza por interacción física entre ambas, mediada por la interacción por separado de cada una de ellas con la proteína SSB (Suski and Marians, 2008). La proteína más similar a Topo III de *B.subtilis* es Topo IIIβ de *Bacillus cereus*, con la que presenta un 64% de identidad de secuencia. Esta enzima presenta un máximo de actividad de relajación a 52ºC y pH óptimo de 9.8 y no es capaz de relajar totalmente un DNA superenrollado (Li et al., 2006). Topo IIIβ no es capaz de compensar la pérdida de Topo III de *E.coli in vivo*, lo que probablemente indica que se trata de una nueva topoisomerasa con una función distinta en la célula. En general, las topoisomerasas tipo III han sido asociadas a procesos de recombinación de DNA, como en el caso de Topo III de *E.coli*, la cual podría tener un papel *in vivo* como ruta alternativa de disolución de la Holliday Junction (Lopez et al., 2005). El proceso de recombinación homóloga en *B.subtilis* es un proceso altamente organizado. Una de las razones por las que se activa es como consecuencia de un daño en el DNA, como roturas de doble cadena. Cuando esto ocurre, el daño es reconocido y procesado por nucleasas específicas, generando un extremo de cadena sencilla, que será reconocido por la proteína central de la recombinación, RecA, que se encarga del intercambio de cadenas entre dos DNA homólogos. Como consecuencia de su acción, se formará un intermediario de recombinación denominado Holliday Junction, que deberá ser procesado por el resolvasoma RuvAB-RecU. De esta forma se generan dos moléculas hijas donde ha ocurrido un intercambio de material genético para reparar el daño. Se desconoce si Topo III tiene algún papel en una ruta alternativa a la resolución de RuvAB-RecU (al igual que en *E.coli*), en la cual y con la ayuda de una helicasa tipo RecQ (RecQ o RecS) la Holliday Junction sería disuelta y como consecuencia las dos moléculas hijas no intercambiarían material genético (fig. 9). El proceso de recombinación homóloga en *B.subtilis* se encuentra asociado al de competencia celular, con proteínas que participan en ambos procesos, como RecA, SSB, RecO, RecU y RecN. Durante el estado de competencia natural de *B.subtilis*, el DNA exógeno es incorporado al interior de la célula mediante la maquinaria localizada en la pared celular conocida como proteínas "com". El DNA, que entra en forma de cadena sencilla, es recubierto por SSB y procesado por RecA para comenzar con un evento de recombinación (Chen et al., 2005)

RESULTADOS Y DISCUSION

Uno de los objetivos propuestos para la presente Tesis Doctoral fue el de dilucidar el papel *in vivo* de LrpC. Para ello, se determinaron los niveles intracelulares de la proteína en distintos momentos del ciclo celular y en diferentes medios de crecimiento. LrpC presenta una mayor abundancia al final de la fase exponencial, pero no se encuentran diferencias entre medio rico o medio mínimo. Los resultados obtenidos descartan que LrpC sea un regulador global en *B.subtilis*, inclinándose más bien hacia un papel en regulación local. La fusión fluorescente GFP-LrpC ha permitido determinar la localización *in vivo* de dicha proteína. En crecimiento vegetativo, en fases exponencial y estacionaria, LrpC se encuentra formando un patrón específico de foci dentro o en los bordes del nucleoide, y en algunos casos formando agregados coincidentes con el mismo. Esta localización en foci y no decorando todo el nucleoide, cuyo patrón además varía según el crecimiento y medios de cultivo empleados, indica que LrpC puede tener un papel específico durante el crecimiento celular, presentando una localización cercana a los centros de transcripción situados en la periferia del nucleoide. Sin embargo, en competencia celular, LrpC presenta un patrón de localización polar en la célula, lo cual sugiere un rol en transformación. Esto se ha visto confirmado con el descenso al 50% en transformación plasmídica del mutante nulo *lrpC* en comparación con la cepa silvestre. Por lo tanto LrpC podría presentar un pequeño papel en competencia celular. Los genes *lrpC* y *topB* se encuentran localizados en el mismo operón y se transcriben bajo el mismo promotor. LrpC estimula la actividad relaxasa de Topoisomerasa III, aunque no se ha detectado una interacción directa proteína-proteína.

El gen *topB* de *B.subtilis* ha sido caracterizado por primera vez. La morfología celular y del nucleoide del mutante nulo *topB* no presenta diferencias respecto a la cepa silvestre. El mutante nulo *topB* presenta una viabilidad celular muy similar a la de la cepa silvestre tras inducir daño por MMS. Sin embargo, tras la inducción de daño por dicha droga, la mutación sencilla *topB* combinada con mutación en algunos genes implicados en rutas presinápticas de la recombinación (*recF, recO, addAB* y *recJ*) recuperan parcialmente su viabilidad respecto a la de cada mutante sencillo por separado más sensible. El doble mutante *recUtopB*, sin embargo, presenta una viabilidad más reducida que la del mutante sencillo *recU*, lo cual lleva a sugerir que ambos genes se encuentran actuando en la última etapa de la recombinación homóloga participando en distintas vías de resolución. Esta hipótesis se ha visto reforzada por el hecho de que el mutante doble *recUtopB* presenta un mayor número de células anucleadas y filamentadas respecto al mutante sencillo *recU*. Cuando se utiliza otro compuesto que causa daños en el DNA como el H_2O_2, el mutante sencillo *topB* presenta una ligera disminución de la viabilidad celular con respecto a la cepa silvestre. Los dobles mutantes *addABtopB*, *recFtopB* y *recOtopB* recuperan parcialmente la viabilidad celular respecto a la de los mutantes sencillos por separado *addAB*, *recF* y *recO*. El doble mutante *recQtopB* presenta el mismo fenotipo que el mutante sencillo *recQ*, mientras que *recStopB* es menos sensible que el mutante sencillo *recS*, lo cual sugiera que Topo III actuaría en la misma ruta que RecQ y distinta de RecS. El doble mutante *recUtopB* presenta un fenotipo sinérgico respecto al mutante sencillo *recU*, al igual que en presencia de MMS. Todos estos datos llevan a proponer un papel de TopoIII en etapas tardías de la recombinación homóloga. La fusión fluorescente TopoIII-YFP presenta una localización celular citosólica o polar, y no se observan foci específicos en los centros de reparación tras la inducción de daño del DNA por MMC. La proteína Topoisomerasa III de *B.subtilis* ha sido purificada y caracterizada por primera vez. Se trata de una proteína monomérica de 80 KDa aproximadamente. La actividad relacionada con dicha proteína permite clasificarla como una relaxasa de DNA superenrollado, que presenta dicha actividad a pH 9.8 y una temperatura de 52ºC. TopoIII es capaz de unirse con mayor afinidad a cualquier tipo de DNA en presencia de 1 mM $MgCl_2$. También se une con mayor afinidad a las estructuras de recombinación que a un DNA de cadena doble o sencilla, indicando un posible papel en recombinación homóloga. Topo III por sí sola no puede cortar el intermediario de cuatro cadenas que se produce en recombinación, la Holliday Junction, por lo que se estima necesaria la participación de una proteína accesoria para dicha actividad, en caso de que Topo III pudiera disolver dicha estructura. Sin embargo, Topo III corta específicamente el primer intermediario de recombinación, producto de la invasión de un DNA de cadena sencilla en un DNA homólogo de cadena doble (denominado D-loop).

CONCLUSIONES

Las conclusiones obtenidas durante la presente tesis doctoral son:

1. Los niveles proteicos de LrpC no presentan una variación entre medio rico y medio mínimo, pero sí entre fases de crecimiento, presentando un máximo al final de la fase exponencial. LrpC no puede ser considerado un regulador global como su homólogo en *E.coli*. Al final de la fase exponencial en medio rico, LrpC modula la expresión de tan solo 26 genes, lo que supone un 0.6% del genoma total.
2. La localización *in vivo* de GFP-LrpC durante el crecimiento vegetativo muestra dos patrones principales, presentando foci discretos o agregados coincidentes con el nucleoide, que a su vez varían según el medio de crecimiento empleado. En medio mínimo en crecimiento exponencial, GFP-LrpC presenta dos focos simétricos coincidentes con el nucleoide o uno asimétrico en los bordes del nucleoide. Este patrón de focos está situado más cerca de los polos celulares en crecimiento estacionario. En medio mínimo de competencia, GFP-LrpC se localiza mayoritariamente en focos polares.
3. LrpC no es una proteína reclutada a los centros de reparación después de daño por MMC. La localización polar de GFP-LrpC en fase de competencia natural permite sugerir un papel en dicho proceso, confirmado por el defecto en transformación plasmídica presentado por el mutante nulo *lrpC*.
4. Los genes *lrpC* y *topB* de *B.subtilis* conforman un único operón y por lo tanto son transcritos a partir del mismo promotor. LrpC estimula la actividad de relajación de Topo III, aunque no se pudo detectar una interacción directa entre ambas.
5. El mutante nulo *topB* presenta una morfología celular y de nucleoide similar a la cepa silvestre. El doble mutante *recUtopB* presenta 3 veces más de células enucleadas en comparación con el mutante sencillo *recU*.
6. Cuando se introduce un daño de DNA por MMS o por H_2O_2, la viabilidad celular del mutante sencillo *topB* es similar a la de la cepa silvestre. Dobles mutantes de *topB* con genes presinápticos *addAB*, *recJ*, *recO* y *recF* recuperan su viabilidad parcialmente respecto a la de los mutantes sencillos *addAB, recJ, recO* y *recF*, respectivamente. El doble mutante *recUtopB* presenta una mayor sensibilidad al daño por MMS que el mutante sencillo *recU*. TopoIII está implicada en reparación de DNA por recombinación homóloga, pudiendo desarrollar una actividad antirecombinasa y de resolución de D-loops. El análisis genético parece indicar que TopoIII sería epistático con RecQ, mientras que con RecS sólo sería epistático en caso de daño por MMS.
7. La fusión Topo III-YFP se encuentra localizada en el citosol celular, a diferencia de RecQ y RecS que localizan en foci discretos coincidentes con el nucleoide. Topo III no forma parte de las proteínas que son reclutadas a los centros de reparación tras inducir daño por MMC.
8. Topoisomerasa III de *B.subtilis* es un polipéptido monomérico de 80 kDa. Presenta actividad característica de relajación parcial de plásmido superenrollado con unas condiciones de 52ºC y pH 9.8.
9. TopoIII se une a intermediarios de recombinación con 6 veces más de afinidad que a DNA de cadena doble o sencilla en presencia de Mg^{2+}. En presencia de EDTA, TopoIII se une con menor afinidad a estas estructuras. TopoIII no realiza el corte de la HJ *in vitro* en las condiciones probadas.
10. TopoIII corta específicamente D-loops, intermediarios de recombinación que se forman durante la sinapsis. El mutante nulo *topB* presenta un defecto en transformación cromosomal que apoya.

INTRODUCTION

1. *Bacillus subtilis* LrpC

1.1 Genetic and biochemical properties of *B. subtilis* LrpC (Leucine-responsive regulatory protein C)

1.1.1 Genetic studies of LrpC

The *Bacillus subtilis lrpC* gene was first discovered in the course of the genome sequencing project. Theoretical studies revealed a putative ORF at 37º in the *Bacillus* chromosome that coded for a 231 amino acid polypeptide (Beloin et al., 1997). This region showed three possible internal ATG initiation codons, one of them being properly placed near the RBS site. This region named *orf144* codes for a 144 amino acid polypeptide that shows 34% identity to *Escherichia coli* Lrp and 25% when compared to *E. coli* AsnC (Kolling and Lother, 1985; Willins et al., 1991). Using western blot technique with antibodies against *E. coli* Lrp, a polypeptide of 16 kDa suggesting a *bona fide* Lrp-like protein was identified in *B.subtilis* (Beloin et al., 1997). Right after the coding sequence of *lrpC*, there is an ORF named "*topB*" that codes for Topoisomerase III. This gene has never been studied and it is unknown if both are transcribed under the same operon. Later on in the introduction antecedents of *topB* will be discussed.

The genome of *B. subtilis* comprises seven genes that are putative Lrp homologs, with a range of identity that varies from 25-34% in comparison with *E.coli* Lrp (figure 1).

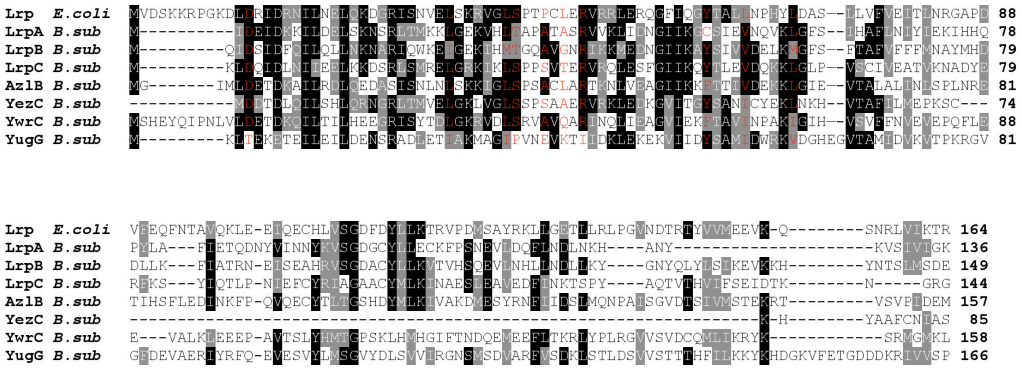

Figure 1: Putative *E.coli* Lrp homologs found in *B. subtilis*. Black shaded background shows identical residues. Grey background shows conserved residues. *E. coli: Escherichia coli; B. sub: Bacillus subtilis*. Identified DNA binding residues of *E. coli* Lrp, and the corresponding residues in the *B.subtilis* homologs are colored in red. The Alignment was made with ClustalW software and edited using box-shade Server.

In addition to *lrpC*, there are two homologous genes at position 47º in the chromosome that have been named *lrpA* and *lrpB,* with 33% and 29% of sequence identity, respectively. The products of these proteins are implicated in KinB-dependent sporulation (Dartois et al., 1997). Another partially characterized homolog is *azlB*, with 35% of sequence identity, which is implicated in branched-chain aminoacid transport (Belitsky et al., 1997).

The *lrpC* gene was proved to be non-essential, and its characterization showed a possible role in amino acid metabolism due to the behaviour of the null mutant *lrpC* in growth medium containing different amino acid combinations. It was shown that a null mutant *lrpC* enters sporulation earlier than the wildtype strain, which led the authors to propose a possible role for LrpC in regulation of early sporulation (Beloin et al., 1997).

LrpC *in vivo* complementation of *E. coli* Lrp was studied by analyzing the expression of the *ilvH* operon (Beloin et al., 1997). *B. subtilis* LrpC was shown to be able to bind to the *ilvH* operon region and to weakly down-regulate it, in contrast to its counterpart *E. coli* Lrp, which activates its transcription (Wang et al., 1994). Computer based analysis of the 5´ non-coding region of *lrpC* showed two putative promoters P1 and P2, with a region between them that has been shown to be intrinsically curved, being P1 the major *in vivo* lrpC promoter (Beloin et al., 2000). This group also showed that LrpC is able to autoregulate its own promoter *in vivo* in a very weak positive manner, which is a new feature for proteins belonging to the Lrp/AsnC family, that are in general down-regulators of their own gene expression. LrpC intracellular levels have been shown to be variable. In rich media, LrpC shows a 6-7 fold reduction in exponential phase compared to the levels in minimal medium. These results led the authors to propose a role for LrpC in nutrition starvation (Beloin et al., 2000).

1.1.2 Biochemical properties of LrpC

1.1.2.1 Binding to the DNA

LrpC protein was expressed and purified in an *E.coli* system (Beloin et al., 2000; Tapias et al., 2000). LrpC has a predicted molecular mass of 16.4 KDa and it is a tetramer in solution. LrpC is able to bind to multiple sites on its own promoter in a cooperative way (forming two types of complexes), in a leucine-independent manner (Beloin et al., 2000; Tapias et al., 2000). In fact, LrpC binds to the DNA in a sequence independent manner and shows a greater affinity for curved dsDNA (Kap ≅ 35 nM) when compared to non curved dsDNA (Kap ≅ 350 nM) (Tapias et al., 2000). The fact that LrpC is binding to the DNA in a sequence-independent manner is a new feature inside the family, whose members normally bind to a consensus sequence (reviewed in Kawashima et al., 2008). LrpC promotes DNA bending, revealed by DNase I footprint assay and circularization assays. There are other proteins that have this behaviour in *B. subtilis*, like the chromatin-associated Hbsu protein. This protein shows a 52% and 57% of identity with HU-1 and HU-2 from *E. coli*, respectively. Hbsu binds DNA in a sequence-independent manner (Groch et al., 1992) and its role is essential for cellular growth (Micka et al., 1991; Micka and Marahiel, 1992). Hbsu and LrpC bind together to the DNA in a mutually cooperative manner (Tapias et al., 2000). This is consistent with the fact that Hbsu also binds preferently curved DNA and promotes DNA bending (Alonso et al., 1995a; Alonso et al., 1995b; Fernandez and Alonso, 1999). These results suggest that, in contrast to other members of its family, LrpC could act preferently as an architectural protein instead of behaving as a specific regulator.

Other biochemical properties of LrpC have been described, as the *in vitro* binding to a wide range of types of DNA, as ssDNA, linear dsDNA and supercoiled dsDNA (Lopez-Torrejon et al., 2006) and several recombination intermediates: the Holliday Junction, or 4-way junction; the 3-way or 3-branched junction, with 3 double helical arms, that resembles a replicated fork and the forked substrate, consisting of a duplex region with a double ssDNA arm, that resembles a non-replicated fork (Lopez-Torrejon et al., 2006)(table 1). LrpC binds to the Holliday Junction in its open conformation 4 to 5-fold higher when compared to other recombination intermediates, in the presence of EDTA (Lopez-Torrejon et al., 2006). The apparent binding constant Kapp ≅ 5nM for this structure is very similar to the one showed for HU (Kamashev and Rouviere-Yaniv, 2000). In table 1 it is shown the apparent binding constants of LrpC to the different substrates, proving that LrpC binds with the highest affinity to 4-way junction. The addition of leucine to the reaction did not affect the binding of LrpC to the DNA, in contrast to *E.coli* Lrp (Ricca et al., 1989)

DNA substrate	Kapp (in nM) EDTA	$MgCl_2$
4-way junction	5	22
Y-junction	7	30
forked substrate	21	40
50-bp	17	42
50-nt	>400	>400
31-bp curved DNA	17	35

Table 1: **Apparent binding constants of LrpC to different DNAs**. Kapp (constant of apparent binding) indicates the affinity of LrpC to the DNA, measured by the LrpC concentration to reach half saturation with the different DNA substrates. The values are an average of 3 independent experiments. Table extracted from López-Torrejón et al, 2006.

LrpC is not only binding to the DNA, but it is able to make high-molecular weight complexes by bridging either linear or circular dsDNA (Tapias et al., 2000). This bridging results in a large network of compacted DNA molecules. LrpC constrains DNA supercoils on a partially relaxed plasmid (Tapias et al., 2000), that is also needed for compactation. The architectural role of LrpC is confirmed by electron microscopy and AFM experiments. LrpC forms the so called "nucleosome structures" with the DNA, which are visible by electron microscopy (EM) and atom force microscopy (AFM) (fig.2) (Beloin et al., 2003). In these EM pictures, LrpC would wrap a linear DNA molecule containing promoters P1 and P2, with the curved region between them, to form different types of complexes due to the different steps in the wrapping mechanism (fig.2). The DNA is wrapped around LrpC as a right-handed superhelix. This structure was visible not only with the promoter region of *lrpC*, but for a plasmid containing phased A tracks.

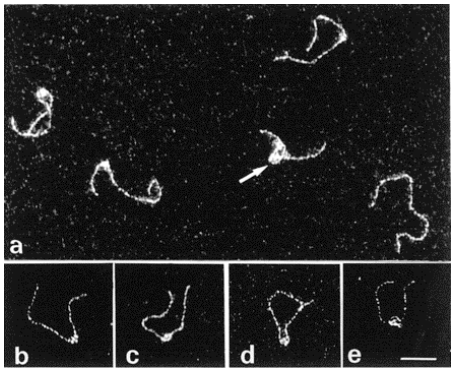

Figure 2: Visualization of nucleosome-like structures of LrpC-DNA complexes. A linear DNA fragment containing P1 and P2 promoters was mixed with purified LrpC at a protein/DNA molar ratio of 6:1. LrpC/DNA complexes were visualized by EM. **a:** different types of complexes that can be formed, compared to uncomplexed DNA (molecule at bottom right). The presence of the protein correlates with thickening at some parts (showed by an **arrow**) indicating highly condensed DNA caused by successive wrapping. **b-e:** representative LrpC/DNA complexes indicating the different steps in the wrapping mechanism. In e, a tight wrapping of more than one superhelical turn of DNA is shown. **Scale bar**, 50 nm. Figure adapted from Beloin *et al*, 2003.

As a consequence of bridging/compactation, LrpC is also able to perform DNA annealing of two complementary DNA strands (Lopez-Torrejon et al., 2006). This feature of LrpC suggests a possible role in DNA recombination. Another architectural proteins have been to shown to have a role in DNA recombination, like the histone-like protein HU from *E. coli* (Kamashev and Rouviere-Yaniv, 2000) and also its homolog in *B.subtilis* Hbsu (Fernandez et al., 1997).

1.1.2.2 LrpC structure

The crystal resolution of LrpC reveals a stable octamer in a cruciform-like structure with an angle of 90º between each dimer (Thaw et al., 2006) (fig.3). The monomer shows the characteristic helix-turn-helix motif, where DNA binds, located in the N-terminal domain (fig.3).

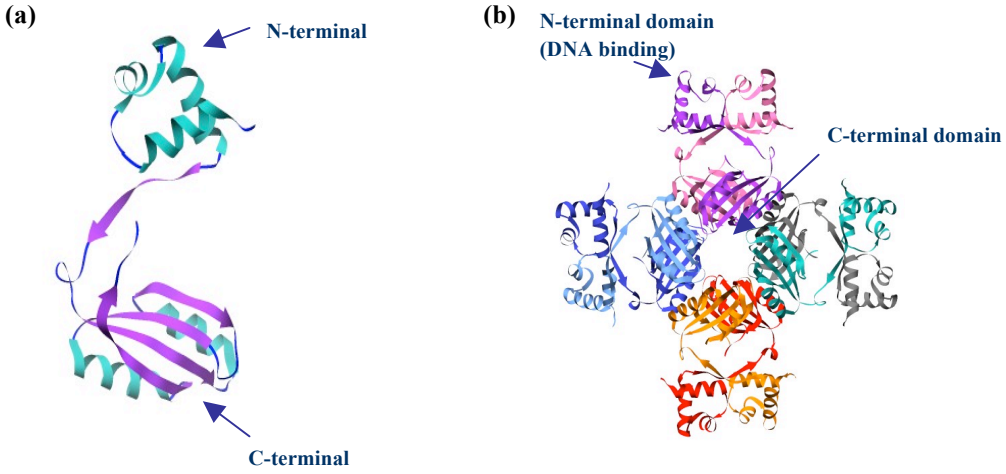

Figure 3: Schematic representation of LrpC structure. (a) LrpC monomer representing the secondary structure of the protein. In green, α-helix are showed. In purple, β-sheets. The position of the N and C-terminal of the protein is shown**. (b)** Cartoon representation of the octameric form of LrpC. Each monomer is represented in a different color. The arrows are pointing to the position of the N and C-terminal of the protein in the final conformation. In the C-terminal domain, several residues form the binding pocket of the protein. Protein coordinates was obtained form PDB database (2CFX) and images were made using Chimera software.

The C-terminal domain contains the binding pocket for the effector aminoacid, as it is been shown for the case of *E.coli* AsnC (Thaw et al., 2006). In the case of LrpC, the size of the binding pocket does not allow the binding of any aminoacid. This confirms the independence of leucine for the binding of LrpC to the DNA that was shown by the biochemistry studies.

The proposed model for binding of LrpC to the DNA is shown in figure 4. In this model, the octamer binds the DNA changing the degree of curvature (fig.4). Several octamers would bind to the DNA in distinct steps, compacting it. This allows the wrapping of the DNA into a solenoid form that is consistent with EM previous data of nucleosome like structures.

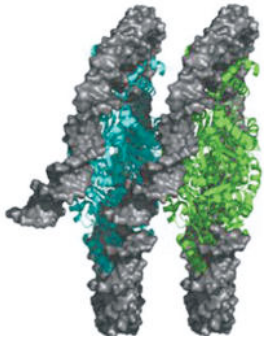

Figure 4: Representative model of *B. subtilis* LrpC bound to the DNA. LrpC could wrap the DNA in a nucleosome-like structure. Cooperative binding of LrpC to the DNA forms a right-handed super-helix. Two octamers are represented in cyan and green. DNA is represented in grey based on existing crystal structures of wrapped DNA (PDB code 1AOI) and electron microscopy studies of LrpC (Beloin *et al*, 2003). Figure adapted from Thaw *et al*, 2006.

1.2 Genetic and biochemical properties of the Feast/Famine Regulatory Proteins (FFRPs)

As already mentioned, LrpC shows structure and sequence homology with *E.coli* AsnC and Lrp, both well known members of FFRPs. Members belonging to the FFRPs family comprise transcriptional regulator proteins from *Bacteria* and *Archaea*. The term FFRP was initially proposed by Calvo and Matthews in 1994 to define how Lrp was positively regulating genes during environmental starvation conditions (famine) and downregulating another genes during optimal nutritional conditions (feast). The transition from one growth condition to the other is highly regulated by Lrp in response to extracellular levels of leucine (Calvo and Matthews, 1994).

FFRPs members show a structural unit conforming a dimer, that can assemble and present high-order structures (octamer in the case of *E.coli* Lrp and AsnC and *B.subtilis* LrpA, see figure 6) or a disk of six consecutive dimers (in the case of the Archaea Pyrococcus OT3 FL11). Members of this family are usually small DNA binding proteins, some of them considered as transcriptional regulators, which show a molecular weight around 15 KDa and form multimeric species in solution, including dimmers, tetramers, octamers and hexadecamers. The assembly of these structures is often influenced by the presence of aminoacids (leucine for Lrp, lysine or arginine for FL11) (reviewed in Kawashima et al., 2008; Yokoyama et al., 2006). The property of forming multiple association states is the key to understand regulation by FFRPs. In the case of *E.coli* Lrp, two octamers interact to form a hexadecamer in the absence of leucine. This new conformation is able to recruit RNA polymerase to the target promoter of the *ilvIH* operon, directly or indirectly. In the presence of leucine, the hexadecamer conformation is split up in two octamers, reducing transcriptional activation of this operon (Kawashima et al., 2008; Platko et al., 1990).

Crystallized structures for these proteins described for now and their similarities can be seen in figure 5. A sequence alignment of these five representative proteins is shown in figure 6.

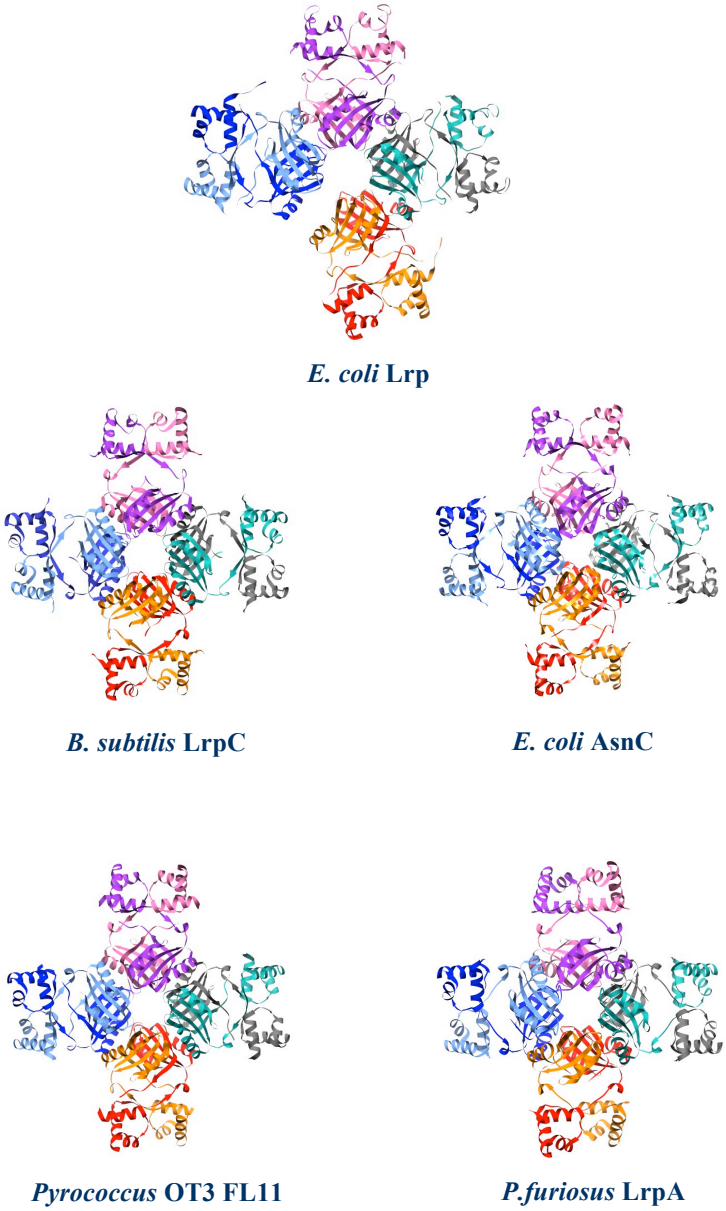

Figure 5: Schematic representation of the structure of some members of Lrp/AsnC family of transcriptional regulators. Each monomer is represented in a different color. Protein information was collected from PDB database and images were created using Chimera software. All structures show very similar overall structures in the shape of octamers. PDB codes: Lrp (2GQQ), LrpC (2CFX), AsnC (2CG4), Fl11 (1R17) and LrpA (1I1G).

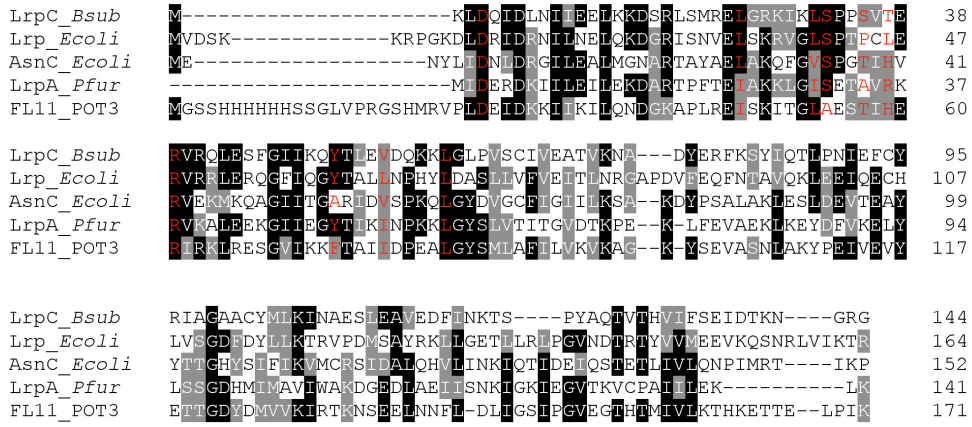

Figure 6: Sequence alignment of bacterial and archaeal members of the FFRP family with a known structure. Black shaded background shows conserved residues. Grey background shows similar residues. *E. coli: Escherichia coli; B.sub: Bacillus subtilis*; *P fur*: *Pyrococcus furiosus*; P OT3: *Pyrococcus* OT3. Identified DNA binding residues of *E. coli* Lrp are noted in red, as well as the corresponding residues of the other members of the family. Alignment was made with ClustalW software and edited using box-shade Server.

The overall structures of the FFRPs studied up to now are very similar, showing that all of them are stable octamers, suggesting a similar mechanism for the binding to the DNA (fig.6). In addition, FL11 can also form a right-handed helix of six consecutive dimmers (Koike et al., 2004). In general, a FFRP shows a N-terminal domain containing the DNA binding domain (fig 5, red residues) (DBD), and a C-terminal domain that contains the effector domain. In some members of the family, presence of effectors such as aminoacids is changing the conformation of the protein, as it is the case for *E.coli* Lrp with leucine (Chen and Calvo, 2002) or *Pyrococcus* OT3 FL11 with lysine (Yokoyama et al., 2007). LrpA from *P.furiosus* has been shown to negatively autoregulate its own promoter in an independent effector manner (Brinkman et al., 2000)

1.2.1 *E.coli* Lrp and AsnC

The best studied member of the Lrp/AsnC family is Lrp from *E. coli*. It shares 34% of sequence identity with the *B.subtilis* LrpC (fig.5) and their overall structures are very similar (fig.6). LrpC crystal structure shows a stable octamer (fig.3b), but in solution it forms a tetramer (Beloin et al., 1997), so probably the final conformation depends on protein concentration. In the case of Lrp, octamer or hexadecamers are present in a leucine dependent manner, both *in vivo* (Chen et al., 2001) and *in vitro* (Chen and Calvo, 2002). Lrp is a global regulator that has been shown to regulate several operons in *E. coli*, what was called early as the Lrp regulon (Newman et al., 1992). This regulon includes operons related with aminoacid biosynthesis, aminoacid degradation, peptide transport and pilin biosynthesis (reviewed by Calvo and Matthews, 1994). Microarray data have revealed that Lrp controls at least 10% of the total genome of *E. coli* (Tani et al., 2002). It has been shown that there are 138 binding sites for Lrp all over across the *E.coli* genome (Cho et al., 2008). Most of the regulon of Lrp is likely to be regulated under stationary growth conditions, and this regulation is affected by the presence or absence of leucine (Cho et al., 2008). Lrp binds to the DNA in a specific manner (Cui et al., 1995) and its abundance in the cell at 0.9 O.D in minimal medium at 37ºC is around 3000 dimers per cell (Willins et al., 1991). The X-ray structure shows that the N-terminal domain of the protein contains the helix-turn-helix domain

that is responsible for DNA binding. The C-terminal region contains the binding site for the aminoacid leucine, what has been demonstrated also by mutational analysis, which maped in these two areas (Platko and Calvo, 1993). Lrp binds DNA cooperatively and bends it upon binding, and DNase I foot print assay using six distinct regions upstream of the *ilvH* promoter showed that Lrp binding facilitates the formation of high-order nucleoprotein structure (Wang and Calvo, 1993). A null mutation in *lrp* causes a slow growth in minimal media, when compared to the isogenic strain lrp^+, but this effect is very mild and can be eliminated by the addition of isoleucine and valine (Ernsting et al., 1992).

AsnC from *E. coli* shows 25% of sequence identity with *B.subtilis* LrpC. Its gene *asnC* is in an operon together with *asnA*, which encodes for asparagine synthase A. AsnC is able to stimulate the expression of the operon in an asparagine-dependent manner (de Wind et al., 1985). The operon *asnA-asnC* is located in the proximities of the origin of replication *oriC* . Based on *in vivo* transcription studies, some authors have proposed an implication of AsnC in the regulation of genes located next to the origin of replication, as *gidA* and *mioC* (Kolling et al., 1988). AsnC has never been proposed as a global regulator so far.

1.3 *B. subtilis* nucleoid associated proteins (NAPs)

DNA inside the cell must be organized and stored in a compacted way that must be compatible with DNA replication, chromosome segregation and gene expression. For this purpose there are several architectural proteins that bind to the DNA and compact it. This group of proteins, previously named "histone-like" due to the resemblance to eukaryotic histones, are now termed as NAPs (nucleoid-associated proteins). This large family comprises proteins from the three domains *Eukarya*, *Archaea* and *Bacteria*. Most of the proteins of this family have the ability of bridging, wrapping or bending the DNA (reviewed in Dillon and Dorman, 2010) . Here it will be focused on the relevant *B. subtilis* Hbsu and SMC proteins.

1.3.1 *B.subtilis* Hbsu

B. subtilis Hbsu is the homolog of *E. coli* HU. It is the major chromosomal protein in vegetative cells of *B. subtilis*, and shows 52% and 57% of identity with subunits HU-α and HU-β from *E. coli*, respectively. Mutations in gene *hbsu* are inviable (Micka et al., 1991), so that the gene resulted to be essential (Micka and Marahiel, 1992). Hbsu is able to bind dsDNA with moderate affinity (Groch et al., 1992). This protein is also implicated in different processes in the cell. Hbsu has been shown to be the accessory factor for *in vitro* beta-mediated DNA recombination (Alonso et al., 1995b). The role if Hbsu in DNA repair and recombination has also been addressed. By the obtention of partial mutations in the *hbs* gene and in combination with mutants in DNA repair and homologous recombination, Hbsu was shown to be required for recombination and repair (Fernandez et al., 1997). The *in vivo* localization of GFP-Hbsu has been reported, showing a tight link to the nucleoid (Kohler and Marahiel, 1997).

1.3.2 *B.subtilis* SMC

SMC-like proteins (structural maintenance of chromosomes) are a large family of proteins involved in chromosome organization, sister chromatid cohesion as well as in DNA repair and recombination. The SMC-like proteins are homodimers that show dimerization through their hinge domains, being this feature essential for proper binding to the DNA, and therefore, for its role in condensation (Hirano and Hirano, 2002). The *B. subtilis* SMC complex consists of three proteins: SMC and two non-SMC subunits named ScpA and ScpB (segregation and condensation

protein A and B). By using the yeast two-hybrid system, a physical interaction between SMC and ScpA has been showed (Soppa et al., 2002).

In vivo microscopy using FRET techniques and inmunoprecipitation have shown that ScpA and ScpB interact with each other and with SMC (Mascarenhas et al., 2002). A null mutation in the *B. subtilis smc* gene leads to a severe decrease of growth rate, a high number of anucleate cells and decondensation of the nucleoid (Britton et al., 1998; Graumann et al., 1998; Moriya et al., 1998). SMC-GFP forms foci at the outer border of the nucleoids (Britton et al., 1998). Inmunofluorescence studies show that SMC localizes in foci that are close to the cell poles (Graumann et al., 1998). Western blot analysis reveals a natural depletion of SMC occurring two hours upon entrance on stationary phase (Graumann et al., 1998). The other components of the SMC complex ScpA and ScpB colocalize with each other and in the DNA, in a SMC dependent manner (Mascarenhas et al., 2002).

SMC has been proposed to be a link protein between two important processes in the cell: DNA replication and chromosome segregation. SMC was recently shown to be specifically recruited to a large region around the origin of replication. This recruitment is done by the Par-B homolog and regulator of early sporulation Spo0J, which could by this way connect chromosome replication (by regulating the Par-A homolog Soj that promotes initiation of replication) with segregation (via SMC) (Gruber and Errington, 2009). The ParB-homolog Spo0J is required for proper chromosome segregation in *B.subtilis* (Ireton et al., 1994) and SMC is required for the correct segregation of newly duplicated chromosomes *in vivo* (Graumann, 2000)

Other well characterized NAPs in *E.coli*, as IHF or H-NS do not have their counterparts in *B.subtilis*, which opens the question for LrpC to cover these functions. *B.subtilis* Hbsu or SMC have not been shown to be global regulators in the cell. Other well known global regulators in the cell are CodY and AbrB. CodY controls the expression of 100 genes, many of them implied in nitrogen or carbon metabolism (Fisher, 1999), and its binding to the DNA is increase by interaction with branched aminoacids (Shivers and Sonenshein, 2004). AbrB is one of the key regulators of gene expression during the transition from exponential to stationary phase (Phillips and Strauch, 2002).

2. *Bacillus subtilis* Topoisomerase III

2.1 Bacterial and Eukaryotic DNA type III topoisomerases

Downstream the *lrpC* ORF is located the gene *topB*. In the region of 67-bp that separates both genes, no Shine-Dalgarno sequence can be found. The gene *topB* has never been studied before in *B.subtilis*. The product of gene *topB* shares 27% of sequence identity with Topo I from *E.coli* and 33% with *E.coli* Topo III. This identity classifies *B.subtilis* Topo III as a member of type IA topoisomerase family, whose members are able to relax a supercoiled DNA by introducing one nick in one of the DNA strands (Depew et al., 1978; Liu and Wang, 1979; Tse et al., 1980). Topo III homologs have been exhaustively studied in *E.coli*, *B.cereus* and humans, as well as its relation with the RecQ-like helicases.

.

2.1.1 *E. coli* Topoisomerase III

E. coli Topo III, encoded by the gene *topB*, was initially identified in the crude extract of cells lacking gene *topA*, that is, the gene that encodes Topo I. These cells extracts are still able to perform decatenation and segregation of two daughter molecules that arise from *in vitro* replication of a supercoiled plasmid pBR322 (DiGate and Marians, 1988). For performing this reaction, Topo III needs a single-stranded region in the DNA. Topo III is also able to relax supercoiled DNA, with an optimal temperature of 52ºC, and its activity is not affected by the type II enzyme-specific inhibitor norfloxacin (DiGate and Marians, 1988).

Relaxation activity of Topo III is enhanced by the presence of the single-strand binding protein Ssb (Harmon et al., 2003). Biochemical assays with the purified enzyme show that Topo III may act behind the replication fork, where precatenates of the two daughter chromosomes are formed (Nurse et al., 2003). During bacterial θ replication, two replication forks are formed that will converge in the termination sites, so in this moment Topo III will be needed for the total separation or segregation of the two daughter chromosomes. In the resolution of these converging replication forks and with the help of SSB, Topo III acts together with the helicase RecQ. Both Topo III and RecQ directly interact with SSB (Harmon et al., 2003; Harmon et al., 1999; Suski and Marians, 2008).

Other *in vivo* assays show that Topo III could have additional roles in the cell: overexpression of Topo III can partly substitute the suppression of subunits ParC or ParE from Topo IV, which indicates a probable cellular role in decatenation *in vivo* (Nurse et al., 2003). Topo III is also been shown to perform a role in DNA recombination. In the presence of compensatory mutations, Topo I deletion strains grow normally; however, if Topo III activity is repressed in these cells, they filament extensively and possess an abnormal nucleoid structure. These defects can be suppressed by the deletion of the *recA* gene, suggesting that these enzymes may be involved in RecA-mediated recombination and may specifically resolve recombination intermediates before partitioning (Zhu et al., 2001). It was proposed that *E. coli* Topo III could have a role in resolution of homologous recombination intermediates, as an alternative and non-resolutive pathway to the known one mediated by RuvABC, as indicated by *in vivo* studies. These studies show that a double mutant *ruvCtopB* shows a synergic effect when compared to single mutant *ruvC*, therefore suggesting that resolvase RuvC and Topo III would be in two separate pathways (Lopez et al., 2005).

In *Bacteria*, as well as in humans and yeasts, there is a cooperation between a TopoIII-like protein and a RecQ-like helicase. *E. coli* Topo III is able to form fully catenates between two different DNA molecules only in the presence of RecQ and Ssb (Harmon et al., 1999). A model of how this could be done is showed in figure 7a, in which RecQ could unwind a covalently closed dsDNA molecule, creating single-stranded regions as a substrate for Topo III to perform strand passage.

This could be done in one direction, that is, promoting the fully catenation of two different DNA molecules, or in the other direction, by decatenation of these molecules.

The concerted single-strand DNA passage activity showed by Topo III and RecQ has been proved to be mediated by a physical interaction via Ssb, in which Topo III and RecQ would interact separately with the C-terminal domain of Ssb for this purpose (Suski and Marians, 2008). Furthermore, as already mentioned, Topo III is specifically acting with RecQ and SSB in the resolution of the two converging replication forks that are formed during θ replication (fig.7b) (Suski and Marians, 2008).

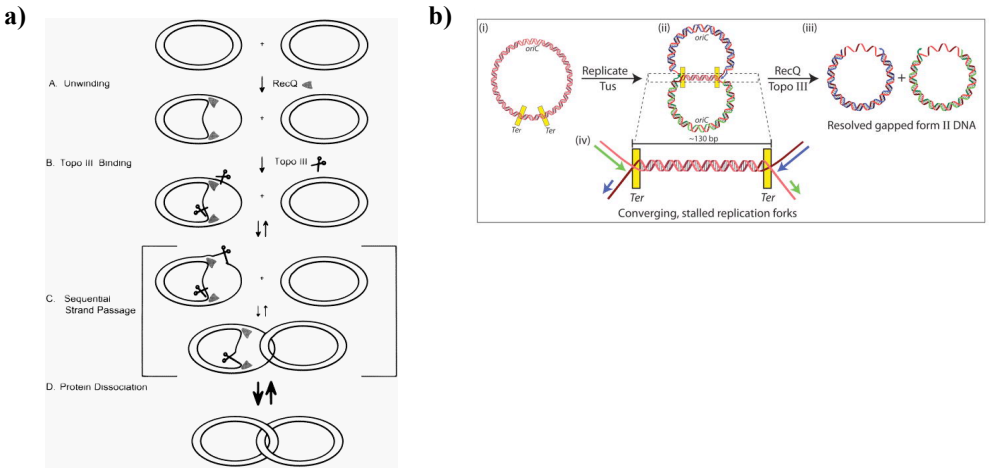

Figure 7: Concerted action of Topo III-RecQ in DNA decatenation and resolution of converging replication forks. a) Model for catenation of two DNA molecules by the concerted action of Topo III and RecQ in *E. coli*. **A:** RecQ helicase unwinds covalently closed dsDNA molecule to create a region of ssDNA as a substrate for Topo III. **B:** two Topo III monomers bind to opposite strands. Each of these monomers will perform an independent strand passage event. **C:** sequential strand passage by each Topo III monomer leads to catenation of two DNA molecules. **D:** catenated dsDNA molecules result after the dissociation of the proteins. Decatenation process occurs exactly in the opposite direction. This could be the case of two converging replication forks that, in the end of replication would become close and would generate the two daughter chromosomes topologically linked. Figure adapted from Harmon *et al*, 1999**. b)** Schematic representation of resolution of converging replication forks by Topo III and RecQ (i) A plasmid containing oriC and two termination sites Ter is incubated with replication proteins and latter with protein Tus, that blocks replication (ii), this creates two DNA daughter molecules linked together by a region of 130 pb (iv) and (iii) this stalled replication forks can be resolved by the concerted action of both RecQ helicase and Topo III, generating two daughter molecules that are now separated and contain a gap, that are named "form II". Figure adapted from Suski and Marians, 2008.

2.1.2 *Bacillus cereus* Topoisomerase IIIα

B.cereus has two type III topoisomerases: Topo IIIα and Topo IIIβ. *E.coli* Topo III shares 33% identity with both *B.cereus* Topo IIIα and *B.cereus* Topo IIIβ. Topo IIIα shows a putative zinc finger motif that is not present in *E.coli* Topo III. This enzyme is able to partially relax a supercoiled DNA in the presence of 2.5 mM $MgCl_2$ with and optimum pH range of 8-9.8 and it can perform *in vitro* decatenation of two oriC-based plasmids, in a similar way to *E.coli* Topo III (Li et al., 2005). Consistent with this, *B.cereus* Topo IIIα is able to compensate the loss of *E.coli* Topo III *in vivo*, suggesting that they could have a similar role in the cell (Li et al., 2005).

2.1.3 *Bacillus cereus* Topoisomerase IIIβ

B.cereus Topo IIIβ shows 64% of sequence identity with *B. subtilis* Topo III. This is the highest resemblance of *B.subtilis* Topo III with the studied bacterial Topo III homologs. This protein can partially relax supercoiled DNA, with an optimum of pH of 9.8 and 52ºC (Li et al., 2006).

This enzyme is not able to perform decatenation of daughter molecules or compensate the loss of *E. coli* Topo III *in vivo*, suggesting that Topo IIIβ is having a different and unknown role in the cell (Li et al., 2006).

2.1.4 Eukaryotic Topoisomerase III

In higher eukaryotes, there are two types of Topo III-like enzymes: Topo IIIα and Topo IIIβ. *In vivo* studies show that in mice, the loss of Topo IIIα is lethal during early embryogenesis (Li and Wang, 1998) and the loss of Topo IIIβ results in infertility and chromosomal defects, such as aneuploidy (Kwan et al., 2003). In the case of humans, Topo IIIβ has recently started to be studied. Expression of Topo IIIβ is correlated with breast cancer distant metastasis and death (Oliveira-Costa et al., 2010).

In all eukaryotes studied for now, type III topoisomerases are directly or indirectly involved in DNA recombination processes. *In vitro* studies support this idea. In the case of Drosophila, Topo IIIβ is binding and cleaving plasmid-based D-loops, an intermediate that is forming in the initial steps of DNA recombination (Wilson-Sali and Hsieh, 2002). Human Topo IIIα is able to resolve a double Holliday Junction with the presence of helicase BLM (Wu and Hickson, 2003), suggesting an anti-recombination role for the action of these two proteins. Human Topo IIIβ has not been yet studied *in vitro*.

In humans, Topo IIIα interacts with a RecQ-like helicase, and this interaction has been studied deeply due to the implications in cancer and aging (reviewed in Bernstein et al., 2010). In these organisms, there are five RecQ-like helicases: BLM, whose name derives from Bloom´s syndrome; WRN, from Werner Syndrome; RTS, from Rothmund-Thomson syndrome and helicases RECQ1 and REQ5. The best studied among these are helicases BLM, WRN and RTS, that lead to different genetic diseases (Seki et al., 2008). Focusing, on BLM, the loss of *blm* gene during embryogenesis is lethal (Chester et al., 1998). The truncated version of *blm*, found in several Bloom´s patients, shows an increase of sister chromatid exchange (SCE), making these organisms particularly susceptible to a wide range of cancers (Luo et al., 2000). Helicase BLM is interacting *in vitro* specifically to hTOPO IIIα (Wu et al., 2000). BLM, Topo IIIα and RMI1 act together in the dissolution of a double Holliday Junction, as a mechanism to preserve genome integrity (Raynard et al., 2006; Wu et al., 2006; Wu and Hickson, 2003). In this case, Topo IIIα acts as a DNA decatenase and it is specifically stimulated by BLM and RMI1 (Yang et al., 2010).

Human RecQ-like helicases WRN, RECQ1 and RECQ5 are also interacting with a Topo III-like protein. In the case of WRN helicase, it is physically interacting with *Saccharomyces cerevisiae* Top3 (Aggarwal and Brosh, 2009). A large isomer of RECQ5, termed RecQ5β, interacts both with human Topo IIIα and Topo IIIβ, separately (Shimamoto et al., 2000). It also has been proposed that RECQ1 might interact with Topo IIIβ (Wu and Brosh, 2010).

Experiments with other eukaryotes as yeasts also show an interaction between Topo III and a RecQ-like helicase. In the case of *S.cerevisiae*, the *E.coli* RecQ-homolog Sgs1 is interacting with both Topo1 and Topo3, in the latter case mediated by DNA binding protein Rmi1 (Watt et al., 1995). Moreover, it appears that interactions between topoisomerases and helicases are conserved among different organisms and must be essential for type III topoisomerases.

3. Homologous recombination in *B. subtilis*

Survival of all living organisms relies on faithful DNA replication and maintenance of chromosomes. During these cellular processes or by exposition to natural exogenous mutagens, DNA can be damaged. For repairing these damages, *Bacteria* have developed a wide range of DNA repair mechanisms: NER (nucleotide excision repair), BER (base excision repair) and MMR (mismatch repair). When some of these specific pathways fail, the only possibility of repairing DNA is by homologous recombination (HR). This mechanism is also activated specifically when there is a double strand break (DSB), which can be caused by natural mutagens as X-rays or spontaneously during cellular processes, when replication is impaired and the fork collapses. The generation of DSBs leads to the recruitment of recombination proteins to the site of the damage, in a highly controlled and time-dependent manner.

DNA repair by HR in *B. subtilis* has been characterized genetic and biochemically, and it can be divided into five general steps (reviewed in Ayora et al., 2011)

A. Break site recognition of DNA damage.

B. Generation of ssDNA tail by end-processing.

C. Loading of RecA protein onto the DNA.

D. Strand exchange mediated by RecA between damaged and non-damaged DNA strands

E. Branch migration and resolution of recombination intermediate.

In *B.subtilis*, the genes involved in the different steps of HR have been classified in ten epistatic groups due to different response to DNA damaging agents, in which genes belonging to the same group share the same phenotype (Fernandez et al., 2000) (Sanchez et al., 2007) (figure 8). In all living organisms, there is a central recombinase (RecA in *Bacteria*, RadA in *Archaea* and Rad51 in *Eukarya*) that catalyzes strand exchange as a central step in HR. For this reason, RecA is not classified within any epistatic group of genes.

Products of genes belonging to groups β, γ, δ, ζ, and κ are involved in early stages of HR. Intermediate stages are performed by genes belonging to groups α, θ, and ι while late stages are performed by genes belonging to groups ε and η. A null mutation *recA* renders cells strongly sensitive to DNA damaging agents. Mutants of genes involved in epistatic groups α (*recF, recO* and *recR*), δ (*recN*), ε (*ruvA*, *ruvB* and *recU*) and η (*recG*) show a strong reduction of cell viability when cells are exposed to DNA damaging agents. In the case of epistatic groups β (*addA* and *addB*), γ (*recH* and *recP*) and ζ (*recS*, *recQ* and *recJ*), the viability of cells exposed to DNA damaging agent MMS is slightly reduced (Fernandez et al., 2000).

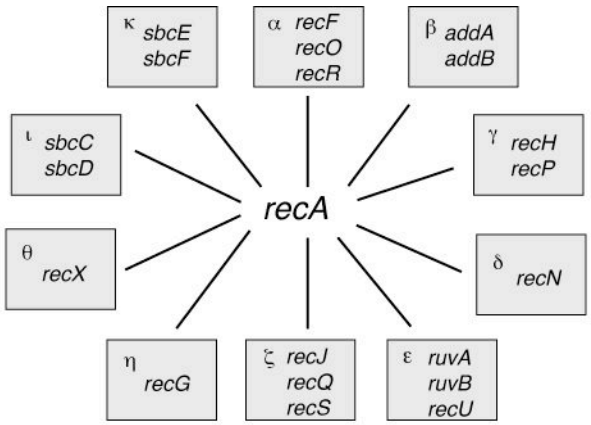

Figure 8: Epistatic groups of classified genes belonging to DNA repair by HR in *B. subtilis*. RecA is placed in the center of the recombination groups indicating its central step in HR. Several genes have not been yet classified, including essential genes (*pcrA, smc/scpA/scpB, ssbA, dnaB, dnaD, topA, gyrAB* and *hbs*) and non-essential genes (*cbfA, held, lrpC, mfd, mutS2, pnpA, priA, rarA, recD2, recK, polA, ripX/codV, sms/radA, topB* and *ypcP*). Figure adapted from Ayora et al, 2011.

The general mechanism of HR process for repairing a DSB is schematically represented in figure 9 and occurs as follows: in step A, RecN (δ group) protein is required for the recognition of DNA damage. Step B involves DNA end-processing performed by the AddAB complex (β group) or by the helicases RecS/RecQ or PcrA/UvrD, together with the nuclease RecJ (ζ group) and probably with SsbA. If Topo III has a role at this step remains unknown. The final product of this step is a ssDNA that is covered by Ssb. In step C, loading of RecA onto this ssDNA requires displacement of Ssb and it needs RecFOR (α group) or AddAB (β group). Step D is basically performed by RecA mediated strand exchange, and this step can be regulated by RecA modulators RecFOR, RecX, RecU and PcrA/UvrD. In *E.coli*, the helicase UvrD is known as a RecA modulator (Veaute et al., 2005), but it is still unknown if PcrA has a similar role in *B.subtilis*. Step E comprises resolution of the recombination intermediate by the resolvasome RuvAB- RecU (ε group) or branch migration by RecG (η group). Depending on the orientation of the cleavage of this recombination intermediate, two types of products can be formed: cross-over (CO) and non-crossover (NCO) (fig. 9).

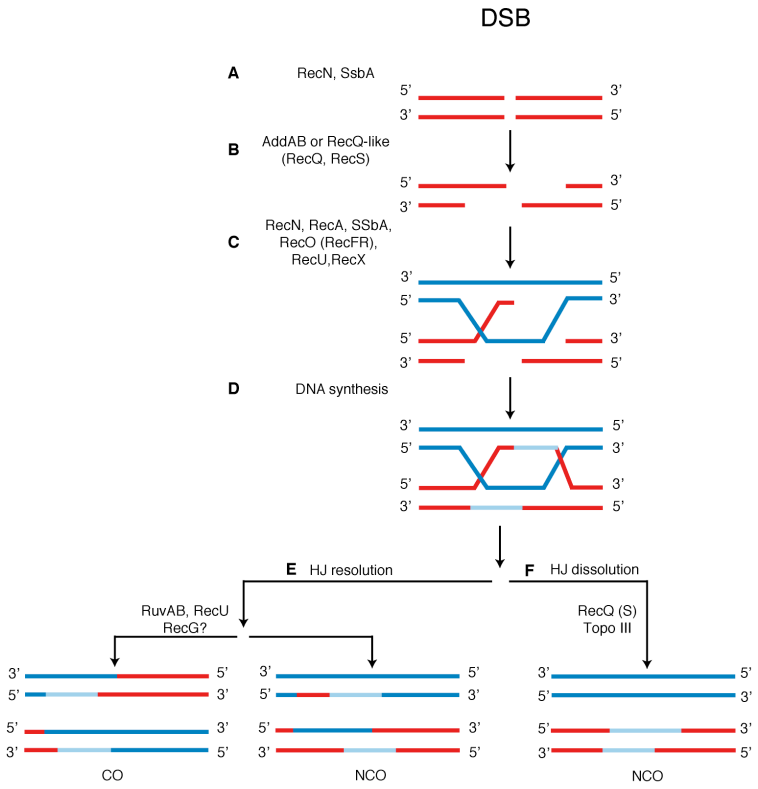

Figure 9: Schematic model of homologous recombination in *B. subtilis*. A: After the formation of a DSB, RecN recognizes the damaged ends. SsbA will be also recruited to the damaged site when there is formation of ssDNA region. **B:** the 5´ends of DNA are resected by the AddAB complex or by the RecJ exonuclease, in concert with a RecQ-like helicase, with SsbA bound to the ssDNA region. DNA ends are tethered by RecN, which promotes loading of RecA mediators (RecFOR, RecU, RecX, PcrA). **C:** disassembly of SsbA and loading of RecA onto DNA is promoted by RecO or RecO-RecR-RecN complex. RecA polymerizes onto SsbA-coated ssDNA and promotes the search for a homologous template, followed by DNA invasion. Extension of RecA filament is controlled by its modulators (RecFOR, RecU, RecX, PcrA. **D:** The invading strand is used for primosome loading. Replication starts using the intact homologous chromosome as a template to restore lost information. Capture of the second DNA derived from the other end of DSB leads to the formation of a double Holliday Junction. This structure can be resolved by migration of the HJ by the action of RuvAB or RecG **(E)**, and the differential cleavage of resolvase RecU will determined a cross-over (CO) or non-crossover (NCO) event. In the absence of RuvAB-RecU, the double HJ can be dissolved **(F)** by the concerted action of Topo III and a RecQ-like helicase. Step F has not been yet demonstrated *in vivo*. Figure adapted from Ayora et al, 2011.

The recombination intermediate is not always leading to a crossover event: in the absence of RuvAB-RecU or RecG, it could be dissolved by the potential action of Topo III in concert with a RecQ-like helicase (figure 9, step F). In *B.subtilis*, there are two recQ-like helicases: RecQ and RecS. Both helicases are known to interact directly with SSB, as proved by fluorescence microscopy and TAP-tag purification (Costes et al., 2010; Lecointe et al., 2007). In this organism is still unknown whether RecQ or RecS interacts somehow with TopoIII. TAP-tag affinity purification of RecQ did not show any detectable traces of Topo III (Lecointe et al., 2007).

RecS is interacting with SSB and with YpbB, a protein of unknown function that is coded in the same operon (Costes et al., 2010). The alternative resolution pathway Topo III-RecQ/S still remains elusive for *B.subtilis* and its one of the objectives of the present Thesis.

Fluorescence microscopy studies have shown the localization of some recombination proteins during a DSB repair in living cells (Kidane and Graumann, 2005a) (Kidane et al., 2004; Mascarenhas et al., 2002; Mascarenhas et al., 2005) (summarized in fig.10). In minimal medium at 30ºC, about 15 minutes after the induction of DNA damage caused by mitomycin C (MMC) or a site specific HO-endonuclease, some recombination proteins are recruited to the site of the damage, known as the repair center (RC). The fusion RecN-YFP is one of the first to be detected in these RCs, at 15-20 minutes after the damage (Kidane et al., 2004) (Krishnamurthy et al., 2010). Around 30-45 minutes after induction of damage, RecO-YFP, RecR-YFP and GFP-RecA are simultaneously recruited to the RC, and their fluorescent fusions co-localize with that of RecN-YFP. RecF is recruited to the RC around 60-90 minutes after induction and the RecA-modulator RecX is also recruited to the RC (Graumann P and Alonso JC, personal communication). Replication proteins PriA, DnaA, DnaB, DnaC and DnaI start to re-assemble between 60-90 minutes after the damage. The presence of resolvase RecU, which acts in a late step during HR, is detected in the RCs around 100-110 minutes after the damage, in a RuvAB dependent manner. Growth resumes under these conditions around 180 minutes after induction of DNA damage.

Not all proteins involved in DNA repair localize at the RCs during DNA damage, as it is the case of RecG, RecQ and RecS. *In vivo* GFP-RecQ and GFP-RecG fusions colocalize continuously with the replication factory (Lecointe et al., 2007). Fusions GFP-RecS or GFP-YpbB localize largely dispersed throughout the cell, but a fusion GFP-YpbB-RecS forms a regular pattern of foci, inside the nucleoid (Costes et al., 2010).

At the same time that damage recognition is taking place, different proteins involved in other processes are detected. Architectural proteins SMC (together with ScpA and ScpB), SbcC and SbcE play a role in maintenance of chromatin structure and their fluorescent fusions show discrete foci linked to the DNA, while SbcC co-localizes with the replication machinery (Krishnamurthy et al., 2010; Mascarenhas et al., 2006; Mascarenhas et al., 2002). When DNA replication is ended, formation of dimeric chromosomes is resolved by the tyrosine recombinase RipX/CodV in concert with translocases SpoIIIE or SftA (Kaimer et al., 2009; Ptacin et al., 2008; Sherratt, 2003). Cellular growth is restarted around 180 minutes after detection of DNA lesion (Kidane et al., 2004). All these data show that DNA repair by HR is a well organized process that requires the sequential recruitment of recombination proteins.

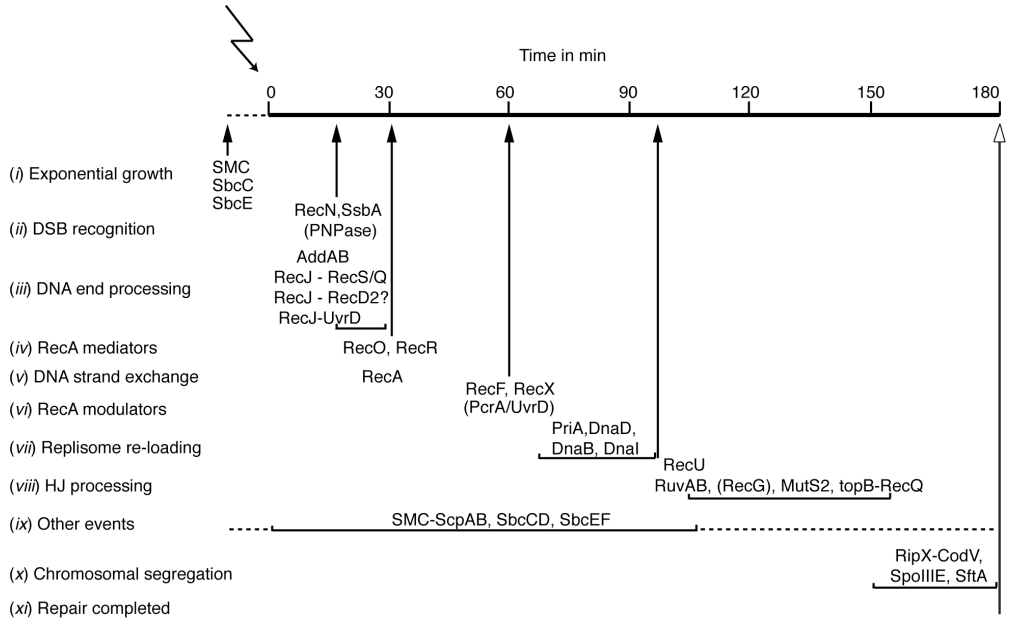

Figure 10: Temporal order of protein assembly at DSBs in exponential growing *B. subtilis* cells. SMC, SbcC andSbcE form discrete foci during exponential growth (stage *i*). Upon induction of damage (time 0), the RecN sensor recognizes it, and in concert with PNPase, assembles on DNA forming few repair centres (RCs) (stage *ii*). After basal resection, the 5´ ends are resected either by the nuclease-helicase AddAB (AdnAB or RecBCD) complex or by the RecJ ssDNA exonuclease in concert with a RecQ-like (RecQ and/or RecS) or an UrvD-like (RecD2, PcrA?) DNA helicase in association with SsbA(SSB) (stage *iii*). Stages *ii* to *iii* are closely integrated *in vivo*. The long-range end resection leads to SsbA binding and protection of the ssDNA and to RecN tethering of the DNA ends leading to a discrete RC (15 – 30 min) and "DSB coordination". The stages *iv* to *vi* are visualized by the temporal RecO, RecR and RecA recruitment (30 – 45 min). These proteins are directly or indirectly recruited to RecN-promoted RC. At a later stage RecF (min 60) is recruited to the RecN-mediated RC and RecX modulates RecA threads. Replisome assembly via PriA, (PcrA?), DnaD, DnaB, DnaI, DnaC might take place during 60 and 90 min after DNA damage (stage *vii*). The recruitment of RecU to a recombination intermediate, in the presence of RuvAB, was visualized at min 100 – 110 after DNA damage (stage *viii*). Concomitant with stages *ii* to *viii*, other processes as SMC maintenance of the chromosome condensation and SbcCD- and SbcEF-dependent repair take place (stage *ix*). Once DNA replication is ended and cell division begins, the RipX/CodV(XerCD, XerS) tyrosine recombinase in concert with SpoIIIA(FtsK) or SftA resolves the accumulated dimeric chromosomes (stage *x*). Growth resumption in minimal medium at 22 ºC takes place ~ 180 min upon DNA damage in wt cells. Figure adapted from Ayora et al, 2011.

4. Natural competence in *B. subtilis*

B. subtilis shows a highly regulated physiological state in which it is possible to internalize exogenous DNA, in a process called DNA transformation. Other Bacteria, as *Streptococcus pneumoniae*, *Neisseria gonorrhoeae* and *Haemophilus influenzae* also exhibit natural competence. In the case of *B. subtilis*, this state is reached in a natural way depending on the growth phase and the lack of nutrients. In general, natural DNA transformation pathway involves 3 main steps: binding, fragmentation/transport, degradation and recombination (reviewed in Chen et al., 2005). In the binding step, the double stranded DNA is attached to the cell surface, in one of the ≈50 potencial binding sites that do exist per cell (Dubnau and Cirigliano, 1972b; Singh, 1972). Binding shows no sequence preference, and it occurs in a molecular weight independent manner.

In the fragmentation step, the initial bound donor molecule of DNA is cleaved in a limited way, consisting of nicks and double strand breaks (Arwert and Venema, 1973; Dubnau and Cirigliano, 1972a). In the step of transport and degradation, one of the strands of the DNA is degraded outside the cell surface, while one of the strands is transported inside the cell through the competence pilli. The average length of the single-stranded fragments is 6-15 kb (Davidoff-Abelson and Dubnau, 1973).

When there is homology between exogenous DNA and bacterial chromosome, the internalized ssDNA is able to interact with the chromosome, forming heteroduplex DNA and therefore initiating a DNA recombination event (Arwert and Venema, 1973; Dubnau and Cirigliano, 1973).

Natural DNA transformation is a well characterized process that involves specific competence proteins belonging to the operons *comG*, *comC*, *comF* and *comE*. Other proteins that do not belong to the "com" operons are also involved in DNA transformation. Among these ones, there are single stranded DNA binding proteins as Smf (ortholog of DprA, DNA processing protein from *S.pneumoniae*), YwpH/SsbB, RecA and YjbF (ortholog of *S.pneumoniae* CoiA). Smf has been shown to bind to ssDNA and protect it from the action of nucleases (Mortier-Barriere et al., 2007). Smf physically interacts with RecA (Mortier-Barriere et al., 2007). All these findings suggest a role for Smf in DNA transformation, in which Smf would load RecA into the incoming DNA. A null mutant *smf* shows a 10-fold decrease in chromosomal and 60 fold decrease in plasmid DNA transformation efficiency (Tadesse and Graumann, 2007). The role of YjbF remains elusive**,** though it is shown to be needed for optimal DNA transformation (Eschevins, 2003, PhD Thesis).

The regulation of competence in *B. subtilis* is mainly performed by ComK (Dubnau and Roggiani, 1990) (van Sinderen et al., 1995). Microarrays data have shown that ComK upregulates at least 165 genes, that include not only all the *com* loci, but also its own gene, *smf*, *recA*, *ssb* and the operon *soj-spo0J* (Berka et al., 2002; Hamoen et al., 1998).

Several proteins involved in DNA transformation have been localized *in vivo* in *B. subtilis* for a better understanding of this process. ComGA, SsbB (YwpH) and ComFA have been localized at one cell pole during competence (Hahn et al., 2005). RecA is also located at one cell pole prior to competence, and when DNA is added, it forms dynamic structures called "threads" that can tract along the DNA in its search for homology (Kidane and Graumann, 2005b) (Kidane et al., 2009). Other recombination proteins have been shown to localize at the cell poles during competence. That is the case of RecN, that oscillates between each cell pole, but in the presence of DNA it stays fixed at the competent pole (Kidane and Graumann, 2005b). RecO localizes to the competent pole in response to incoming plasmid DNA and RecU is present at the competent pole prior to the addition of DNA (Kidane et al., 2009). ComK-dependent DNA binding proteins Smf (Tadesse and Graumann, 2007) and YjbF (CoiA) also localize at one cell pole (Hahn et al., 2005). Data obtained from fluorescence microscopy, FRET and studies of "com" genes knockout strains (Kramer et al., 2007) have determined a model of localization and interaction between all of them (Chen et al., 2005) (fig.11).

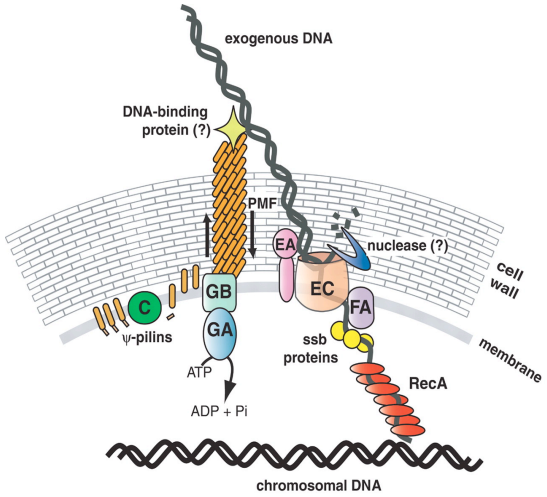

Figure 11: DNA uptake during transformation in *B. subtilis*. The uptake machinery is preferentially located at the cell poles. The pseudo-prepilins are processed by the peptidase ComC and translocate to the outer face of the membrane. With the aid of the other ComG proteins, the major pseudo-pilin ComGC assembles into the pseudo-pilus, which attaches exogenous DNA via a hypothetical DNA binding protein. Retraction of the pseudo-pilus, driven by the proton motive force, and DNA binding to the receptor (ComEA) are required to transport one strand of DNA through the membrane channel (ComEC) while the other is degraded by an unidentified nuclease. The helicase/DNA translocase (ComFA) assists the process, along with ssDNA binding proteins that interact with the incoming DNA. RecA forms a filament around the ssDNA, and mediates a search for homology with chromosomal DNA. ssb, single-stranded DNA binding proteins (YwpH or Smf). ADP: adenosine diphosphate; Pi, inorganic phosphate; PMF, proton motive force. Figure adapted from Chen et al, 2005.

In this model, based on results obtained from *B.subtilis* and *P.pneumoniae*, the exogenous incoming DNA would bind to a DNA-binding protein, with the help of the ATPase comGA, and would pass through the channel conformed by ComEC and ComEA, together with the action of translocase ComFA. After degradation into ssDNA, DNA binding proteins Ssb or Smf would bind to protect the donor DNA. RecA would be loaded in the DNA and would perform search for homology in order to start with a DNA recombination event. If the incoming ssDNA does not present homology sequence with the chromosome, it is reannealed and it should be self-replicative for inheritance in daughter cells. The role of other "rec" proteins in DNA transformation, apart from RecA or Ssb, still remains elusive.

OBJECTIVES

The purpose of this thesis was to decipher the *in vivo* role of *B.subtilis* LrpC and Topoisomerase III.

1. Determination of intracellular levels of LrpC and role of LrpC in global gene expression

2. *In vivo* localization of GFP-LrpC to analyze its role as nucleoid associated protein

3. Genetic and biochemical characterization of the operon *lrpC-topB*: gene expression, *in vitro* protein interaction and modulation of activity

4. Characterization by genetic analysis, and protein localization of the role of TopoIII in HR, individually and in combination with different genes with a genuine HR defect

5. Biochemical characterization of Topoisomerase III

MATERIALS AND METHODS

1. MATERIALS

1.1 Bacterial strains

B.subtilis and *E.coli* strains used and/or constructed in this work are shown in tables 2 and 3.

Strain	Relevant genotype	Reference
BG214	wildtype[a]	Yasbin *et al*, 1980
SB19	*met*$^+$	Rottländer and Trautner, 1970
BG963	*lrpC::Cm*	this work
BG855	*ΔrecU*	Cañas *et al*, 2008
BS1529	*recO::six*	this work
BS1516	*lrpC::Cm ΔrecU*	this work
BS1528	*lrpC::Cm recO::six*	this work
BG1163	*smf::Em*	this work
BS1527	*lrpC::Cm smf::Em*	this work
BS158	*lrpC::Cm gfp-lrpC*	this work
BS1525	*lrpC::Cm gfp-lrpC ΔcomK*	this work
BS1526	*lrpC::Cm gfp-lrpC ΔcomA*	this work
BG935	*topB::six-cat-six*	this work
BG955	*topB::six*	this work
BG775	*recJ::six*	Sánchez *et al*, 2006
BS151	*recJ::six topB::six-cat-six*	this work
BG129	*recF15*	Alonso *et al* 1988
BS153	*recF15 topB::six-cat-six*	this work
BG107	*recO::Cm*	Alonso *et al*, 1988
BS154	*ΔrecO topB::six-cat-six*	this work
BG1095	*ΔaddAB::six-cat-six*	this work
BS1511	*ΔaddAB::six-cat-six topB::six*	this work
BG703	*ruvAB::six*	Sánchez *et al* (2005)
BG991	*ruvAB::six topB::six-cat-six*	this work
BG691	*recG::six-cat-six*	Sánchez *et al* (2005)
BS1515	*recG::six-cat-six topB::six*	this work
BS1517	*ΔrecU topB::six-cat-six*	this work
BG425	*recS::cat*	Fernández *et al* (1998)
BG983	*recS::cat topB::six*	this work
BG939	*recQ::six-cat-six*	Sánchez et al, 2005
BG981	*recQ::six-cat-six topB::six*	this work
BS1512	*topB-yfp*	this work
BS1530	*ΔrecU topB-yfp*	this work
PK9C8	*hbsu-gfp;Pspac (his)$_6$ Hbsu*	Kohler *et al* (1997)
8G32	*ΔcomK*	van Sinderen *et al*, 1994
BD1243	*ΔcomA*	Guillen *et al*, 1989

Table 2: *B.subtilis* strains used in the present work.
[a]Phenotype of the wildtype strain is: *amyE, attSPβ, aatICEBs1, metB5, sigB37, trpC2*, *xin-1*.

Strain	Relevant genotype	utilization
XL1-Blue	*recA1 endA1 gyrA96 thi-1 hsdR17 supE44 relA1 lac* [F′*proAB lacI*^{q}*ZΔM15 Tn10* (Tet)] from Strategene	construction and maintenance of plasmids
Bl21(DE3)	plysS B F- *dcm ompT hdS* (rB-mB-) *gal* (DE3) [plysS Cat] from Stratagene; contains plasmid pTOPhis	overexpression of recombinant protein TopoIII(his_6)

Table 3: *E.coli* strains used in the present work.

1.2 Buffers

Buffers used for this work in biochemistry assays are specified in table 4.

buffer	composition
A	50 mM Tris-HCl pH 9.8, 15 mM NaCl, 1 mM DTT, 0.1 mg/ml BSA, 1mM $MgCl_2$, 30% glycerol.
B	50 mM Tris-HCl pH 7.5, 50 mM NaCl, 1 mM DTT, 0.05 mg/ml BSA, 1 mM $MgCl_2$.
C	50 mM Tris-HCl pH 7.5, 50 mM NaCl, 1 mM DTT, 0.05 mg/ml BSA, 10 mM $MgCl_2$.
D	50 mM Tris-HCl pH 7.5, 50 mM NaCl, 1 mM DTT, 0.05 mg/ml BSA, 1 mM EDTA.
F	50 mM Tris-HCl pH 9.8, 30 mM NaCl, 1 mM $MgCl_2$, 5% glycerol

Table 4: Buffers used in this work

1.3 Reagents and materials

Product	Manufacturer
[α^{32}P]-dATP, [γ^{32}P]-ATP	Perkin-Elmer
PVDF membrane, Sephadex G-50 DNA grade, PCR DNA Gel Band Purification Kit, Ni-Sepharose High Performance	GE-healthcare
Micro Bio-spin columns	Bio-Rad
Litte Ablot Chemiluminiscent substrate for western blotting	Euroclone
Ammonium sulfate, Urea	ICN
Methanol, casein hydrolysate	Fluka
Wizard Plus Miniprep Kit	Promega
Sodium-dodecyl-sulfate (SDS), Mytomycin C (MMC), methyl methanesulfonate (MMS), Hydrogen peroxide (H_2O_2), 1,4-dithiothreitol (DTT), 2-mercaptoetanol, Triton X-100, lysozyme, antibiotics, ethidium bromide, deoxynucleotides diphosphate (dNTPs), imidazole, D-fructose	Sigma
Anti-rabbit IgG-Horseradish peroxidase	Jackson Inmunoresearch laboratories
Rifampicin	Calbiochem
Restriction enzymes, T4 polynucleotide kinase, T4 DNA ligase, DNA polymerase I (Klenow fragment)	New England biolabs
DNA taq polymerase	Biotools
LB broth	USB
Proteinase K, Tris, ribonuclease A (RNase A)	Roche
Coomasie blue, xylencyanol, bromophenol blue, magnesium chloride, calcium chloride, dimethyl sulfoxide, absolute ethanol, isopropanol, sodium hydroxide, D/L Tryptophan, L-methionine, zinc chloride, ferric choride, titriplex (EDTA)	Merck
Millex filters (0.22 μm and 0.45 μm), VM filters (0.05 μm)	Millipore
Acetic acid, vaseline	Panreac
Mounting medium	Vector
Agarose, tryptone, European agar, yeast extract	Pronadisa
Plasmid extraction quit	Quiagen
Acrylamide, bisacrylamide	Serva
Dialysis membranes	Spectrum

Table 5: Reagents and materials used in this work

1.4 Growth media and antibiotics

B.subtilis or *E.coli* strains were grown in rich medium LB (Luria Bertani). *B.subtilis* was also grown in minimal medium S750 (Vasantha and Freese, 1979): K_2HPO_4-KH_2PO_4 5 mM pH 7.0, ammonium sulphate 10 mM, $MgCl_2$ 2mM, $CaCl_2$ 0,7 mM, $MnCl_2$ 5 μM, $FeCl_3$ 5 μM, $ZnCl_2$ 1 μM, tryptophan 0,04 mg/ml, methionine 0,04 mg/ml, fructose 0,5%, glutamate 1mg/ml and MOPS 10 mg/ml) or *B.subtilis* competence medium GMI (Davidoff-Abelson and Dubnau, 1971) (ammonium sulphate 15 mM, K_2HPO_4 60 mM, KH_2PO_4 45 mM pH 7.0, sodium citrate 3,4 mM, glucose 0,5% o xylose 0,5%, yeast extract 0,1%, hydrolysate casein 0,02%, $MgSO_4$ 800 mM, tryptophan 0,025 mg/ml and methionine 0,02 mg/ml) or GMII (GMI supplemented with $CaCl_2$ 0,5 mM and $MgSO_4$ 3,5 mM). Antibiotics used for *E.coli* were: ampicilin (100 μg/ml) and chloramphenicol 15 μg/ml; for *B.subtilis*: chloramphenicol 5 μg/ml, spectinomycin (100 μg/ml), kanamycin (10 μg/ml), erythromycin (1 μg/ml) and neomycin (10 μg/ml). Strain PK9C8 requires 1mM IPTG for the expression of $(his)_6$ Hbsu.

2. METHODS

2.1 Cell manipulation

2.1.1 Competent cells preparation

E.coli competent cells were obtained by the chemical treatment method with $CaCl_2$ (Hanahan, 1983). XL1-Blue or BL21 pLysS strains were grown at 37ºC in LB medium with constant shaking till exponential phase (0.4 O.D), moment in which the culture was centrifuged and resuspended in ice-cold 50 mM $CaCl_2$. This compound is able to make cell walls permeable, so that these cells are able to uptake exogenous DNA. Competent cells are kept at -80ºC with 15% glycerol.
B.subtilis wildtype strain is naturally competent under certain growth conditions (by using GMI competence medium). Competent cells were obtained by incubation of a single fresh colony into GMI medium at 30ºC overnight without shaking. The next morning, the culture was diluted in GMI to obtain an O.D. of 0.05. This culture was incubated at 37ºC with constant shaking till the O.D. is stable (the cells have reached stationary phase). 90 minutes after reaching stationary phase, 15% glycerol was added and cells rapidly frozen at -80ºC (Wilson and Bott, 1968).

2.1.2 Bacterial transformation

E.coli cells (XL1-Blue and BL21 pLysS were transformed using the heat shock protocol (Hanahan, 1983). 200 μl of cells were incubated with 10-100 ng of plasmid DNA on ice for 15 minutes. Then the mixture was incubated at 42ºC for 90 seconds and placed in ice again for 2-3 minutes. After this, 400-500 μl of LB was added to the samples and incubated at 37ºC with constant shaking for 30 minutes. Then, cells were plated in LB-Agar Petri dishes with the proper antibiotic.
B.subtilis competent cells were diluted 1:10 in fresh GMII medium and incubated 1 hour at 37ºC with constant shaking. After this, 200 μl of the cells were added to 100-300 ng of plasmid DNA or 10-50 ng of chromosomal DNA and incubated at 37ºC for one hour.
Then cells were plated in Lb-Agar Petri dishes with the proper antibiotic (Wilson and Bott, 1968). Transformation efficiency assays are detailed in part 2.3.5.

2.2 DNA manipulation

2.2.1 DNA isolation and quantification

Plasmid DNA from *E.coli* or *B.subtilis* was isolated using the method of alkaline lysis (Birnboim and Doly, 1979) using kits from Quiagen or Promega. Chromosomal DNA from *B.subtilis* strains was isolated as follows: overnight culture from fresh colony was centrifuged and the pellet resuspended in TE buffer containing 1 mg/ml of lysozyme and 0.5 mg/ml RNase A. The mixture was incubated at 37ºC with a slight shaking for 20-30 minutes, till the observation of a clear lysate. Then, proteinase K was added at a final concentration of 2 mg/ml and incubated at 37ºC for additional 10 minutes. Samples were then incubated with 0.01% SDS for 5 minutes at room temperature. The samples were poured on ice-cold 100% ethanol and the cell lysate containing chromosomal DNA was taken with a sterile pipette and resuspended in water. DNA concentration was measured using nanodrop software for Windows, which measures absorbance at 260 nm and 280 nm. The ratio between both values gives the purity of the sample.

2.2.2 Plasmids and mutants construction

2.2.2.1 LrpC plasmids and strains

Plasmids used and constructed in this work are described in table 6. A deletion of the 432 bp gene *lrpC* was obtained by substitution of the central part of the gene by chloramphenicol resistance cassette in vector pCB266 (Sanchez et al., 2007). Around 400 bp of the upstream part of *lrpC* plus 60 bp of the N-terminal gene were cloned in pCB266 using enzymes EcoRI and KpnI. Around 400 bp downstream of gene *lrpC* plus 60 bp of the C-terminal part of the gene were cloned in pCB266 using enzymes BamHI and HindIII. In the final construction (pCB739), *lrpC* gene was deleted from nt +60 to nt +372, and this part of the gene replaced by Cm cassette. Strain *lrpC::Cm* (BG963) was obtained by transformation of plasmid pCB739 in wildtype strain YB886, selected for chloramphenicol, double crossover checked by PCR and confirmed by Western Blott with polyclonal antibodies against LrpC. Double mutants BS1516, BS1527 and BS1528 were obtained by phage SPP1 transduction as follows: strain BG963 (donor strain) was infected with wildtype phage SPP1. The supernatant obtained from this infection was used to infect (with a MOI of 1,5 or 10) the strains BG855, BS1529 and BG1163 (acceptor strains).
For LrpC localization experiments, a N-terminal fusion GFP-LrpC was obtained by cloning with PCR the entire gene *lrpC* in vector pSG1729 with restriction enzymes ApaI and EcoRI using primers 5´GAA GGA GGG CCC CAT ATG AAA CTT GAC 3´ and 5´ CCT TTC GGG AAT TCT TAG CAGC 3´, respectively. Plasmid pSG1729-*gfp-lrpC* was used to transform in a strain BG963, so that the only copy of the gene is the one carrying the fusion inserted in the *amy* locus, expressed under xylose promoter. The fusion was confirmed by PCR and Western Blott with polyclonal antibodies against LrpC.
Strains BS1525 (GFP-LrpC *ΔcomK*) and BS1525 (GFP-LrpC *ΔcomA*) were obtained by transforming chromosomal DNA from strains 8G32 (*Δ*comK) and BD1243 (*Δ*comA) in strain BS158 (GFP-LrpC). These constructions were checked by PCR, and the *lrpC* locus remained intact as *lrpC::Cm*.

2.2.2.2 Topo III plasmids and strains

The 2181 bp gene *topB* was cloned by PCR in pUC18 with restriction enzymes BamHI and EcoRI using primers 5´ TTA TAA TAA CG GGA TCC GCG 3´ and 5´ GGACC GAATTC CAA TAA AAA ACC TGT GCG 3´, respectively, resulting in pCB725. To interrupt the gene, pCB725 was digested with NruI (that cuts inside *topB* at nt +307).

Plasmid pCB266 carrying the cassette six-cat-six was digested with EcoRI and HindIII, blunted and ligated to pCB725 digested vector to obtain pCB726. Linear plasmid pCB726 was transformed in wildtype YB886 strain and selected with chloramphenicol to obtain strain *topB::six-cat-six* (BG935). Strain BG935 was transformed with plasmid pBT353-1 that carries the β-recombinase and performs recombination of both "six" sites to liberate cloramfenicol resistance (Sanchez et al., 2007), resulting in strain *topB::six* (BG955).

For obtaining double mutants BG983(*recStopB*) and BG981(*recQtopB*), strain BG955 (*topB::six*) was transformed with plasmids pCB176 (*recS::cat*) y pCB714 (*recQ::six-cat-six*), selected for chloramphenicol and checked by PCR. Double mutants BS151(*recJtopB*), BS153(*recFtopB*), BS154(*recOtopB*) and BG991(*ruvABtopB*) were obtained by transforming plasmid pCB726 in the strains BG775 (*recJ::six*), BG129 (*recF15*), BG107 (*recO::Cm*) and BG703(*ruvAB::six*), respectively. Double mutants BS1515 (*recGtopB*) and BS1511 (*addABtopB*) were obtained by phage SPP1 transduction, being BG691(*recG::six-cat-six*) and BG1095 (*ΔaddAB::six-cat-six*) the donor strains and BG955 (*topB::six*) the acceptor strain. Double mutant BS1517 (*recUtopB*) was also obtained by transduction, being BG855 (*ΔrecU*) the donor strain and BG935 (*topB::six-cat-six*) the acceptor strain. In all cases, single or double mutants in the chromosome of *B.subtilis* were confirmed by PCR.
For Topoisomerase III localization experiments, a C-terminal fusion TopoIII-YFP was obtained by cloning the 300 pb of the 3´end of *topB* in vector pSG1164 with restriction enzymes ApaI and ClaI using primers 5´ GCC TCG GGC CCG TGG C 3´ and 5´ CAG GTT TTT ATC GAT TTT ATC CAA ACC G 5´. Vector pSG1164-*topB-yfp* was transformed in wildtype strain YB886 with one cross-over event in the original locus under the native promoter. The fusion was confirmed by PCR and Western Blott with polyclonal antibodies against GFP.

For overexpression of Topoisomerase III, the entire gene *topB* was cloned into pET21b using restriction enzymes NdeI and XhoI, resulting in vector pTOPhis. In this vector, the C-terminal part of the gene was fused to a 6 histidines tag. Vector was checked by sequencing. Plasmid pTOPhis was transformed into *E.coli* BL21 plysS for protein overexpression.

Plasmid	Description and Reference
pET21b	Plasmid for overexpression that contains the promoter region of phage T7 polymerase (Novagen)
pUB110	Replicative vector for *B.subtilis* (Gryczan and Dubnau, 1978)
pGEM-3Zf (-/+)	Contains the origin of replication of phage f1 in a different orientation (-) and (+) (Promega)
pCB266	Contains a cloramfenicol cassette flanked by two identical copies in direct orientation of β-recombinase recognition sites (Sanchez et al., 2007)
pSG1729	Suicide vector for N-terminal GFP fusions in *B.subtilis* (Lewis and Marston, 1999)
pSG1164	Suicide vector used for C-terminal GFP fusions in *B.subtilis* (Lewis and Marston, 1999)
pBT353-1	Contains β-recombinase for excision of the antibiotic resistance in between of two identical six sites in the *B.subtilis* chromosome (Sanchez et al., 2007)
pET21b	Contains the promoter region of phage T7 polymerase and introduces 6 histidines in the 3´end of the target gene (Novagen)
pCB739	Contains the N and C-terminal parts of the gene *lrpC* interrupted by Cm^R gene (this work)
pSG1729 *gfp-lrpC*	Contains the N-terminal fusion GFP-LrpC. Suicide vector for integration in the chromosome by double crossover in the *amy* site (this work)
pCB725	Contains gene *topB* for cloning in *E.coli* (this work)
pCB726	Contains gene *topB* with an insertion in the NruI site of the cassette six-cat-six (this work)
pCB176	Contains gene *recS* interrupted by gene Cm^R (Fernandez et al., 1998)
pCB714	Contains gene *recQ* interrupted by cassette six-cat-six (Sanchez et al., 2005)
pSG1164 *topB-yfp*	Contains the C-terminal fusion TopoIII-YFP into the suicide vector that is integrated in the original locus by single crossover (this work)
pTOPhis	Contains gene *topB* with a fusion of six histidines in the C-terminal part for overexpression of recombinant Topo III protein (this work)

Table 6: Plasmids used in the present work.

2.3 *In vivo* assays

2.3.1 Drug survival assays

B.subtilis strains were grown from fresh colonies in LB medium at 37ºC till exponential phase (0.4 O.D) with constant shaking. At this moment of growth, cells are incubated with 10 mM methyl-methanosulfonate (MMS) at different times or the indicated concentration of H_2O_2 for 15 minutes, then serially diluted and plated in LB agar overnight at 37ºC, followed by colony quantification as previously described (Friedman and Yasbin, 1983).

2.3.2 LrpC *in vivo* quantification

Strain YB886 was grown in LB or minimal medium at 37ºC and O.D. of the culture was followed from exponential to stationary phase. Aliquots of 2 ml were taken at the indicated O.D: 0.4 for exponential phase, 0.8 and 1.6 for early stationary phase and 2.2 for late stationary phase. These aliquots were centrifuged and concentrated in 200 µl in buffer Tris-EDTA and incubated with lysozyme (1 mg/ml) at 37ºC for 30 minutes, followed by sonication. SDS-loading buffer was added to the samples and incubated at 95ºC for 5 minutes. Samples were run in 15% SDS-PAGE followed by Western Blott with polyclonal antibodies against LrpC. Protein bands were analyzed and quantified with Quantity One software (BioRad).
For the quantification of levels of GFP-LrpC during vegetative growth, strain BS158 was grown in minimal medium supplied with 0.01, 0.02, 0.03 or 0.04% of xylose at 30°C till early exponential phase (0.2 O.D), middle exponential phase (0.4O.D) or till stationary phase (0.8 O.D). As a control, BS158 and wildtype strain YB886 were grown in the same conditions without xylose. Aliquots of 2 ml were taken at the indicated optical densities and processed for western blott as described above.
For quantification of levels of GFP-LrpC during competence, strain BS158 was grown in LB or in GMI medium at 37°C till different growth states during stationary phase, as stated in the experiment. Aliquots of 2 ml were taken at the indicated optical densities and processed for western blott as described above.

2.3.3 *B.subtilis* microarray analysis of the null mutant *lrpC*

Microarrays were performed and analyzed in Centro de Astrobiología (CAB), Madrid, under the supervision of Dr. Eduardo González Pastor. *B.subtilis* wildtype strain YB886 and BG963 were grown till the end of exponential phase (0.9 O.D) or to stationary phase (1.8 O.D) in LB medium at 37ºC. At his moment, 25 ml of the culture was taken and 1 volume of ice-cold 100% methanol was added to the sample and centrifuged at 4000 rpm for 30 minutes. The pellet was frozen at -80ºC for storage. Total RNA was extracted from the cells using hot acid phenol extraction (Fawcett et al., 2000).
This RNA was visualized on 0.8% agarose gel stained by ethidium bromide and the concentration was measured by Nanodrop equipment. The complementary cDNA was obtained from the extracted RNA by the retrotranscriptase (RT) reaction using nucleotides labelled with fluorophores Cy3 (wildtype strain) or Cy5 (mutant strain BG963). Labelled cDNA was hibridyzed in the *B.subtilis* microarray chip. Data obtained from 3 independent experiments for each moment of growth were analyzed and processed.

2.3.4 Fluorescence microscopy analysis

For nucleoid visualization, strains were grown in LB rich medium at 37ºC with constant shaking till exponential phase (0.4 O.D), moment in which cells were fixed with 2% formaldehyde, stained with 1 µg/ml of 4,6-diamino-2-fenilindol (DAPI) followed by addition of mounting medium and visualized by fluorescence microscopy. *In vivo* fluorescence microscopy was performed in Albert-Ludwig Universität Freiburg (Germany) under the supervision of Pr.Dr. Peter Graumann. For *in vivo* localization of fluorescent fusion proteins, strains were grown in minimal medium S750 at 30ºC with constant shaking till exponential phase (0.4 O.D), or till stationary phase (≈ 6 O.D) when stated.
In the case of visualization of cells in competence, strains were grown in GMI medium till the beginning of stationary phase (when the O.D starts to stabilize), moment in which the cells are transferred to GMII medium for approximately 2 hours and 30 minutes. In this moment, an aliquot of the cell culture is stained with DAPI, mounted in agarose gel slides containing minimal medium S750 and visualized with the proper fluorescent filter, or one sample of the culture was incubated with 150 ng of plasmid DNA (pDG148) or 200 ng of chrosomosomal DNA (YB886) for 30 min at 37ºC, followed by DAPI staining as stated above.
Images were taken using microscopes Zeiss AX10 Observer A.1, Observer Z.1 and Zeiss AX10 Imager A.1 with cameras Cool Snap ES^2 or HQ from Photometrics. Pictures were processed with Metamorph 7.5.5.0 and VisiView 1.7.4 software for Windows.

2.3.5 Transformation efficiency assays

B.subtilis strains YB886, BG963, BS1529, BG855, BG1163, BS1528, BS1516, BS1527 and BG955 were transformed with two types of DNA: religated plasmid pUB110 or chromosomal DNA from strain SB19 (met^+). Transformants were selected in LB plates containing neomycin 10 µg/ml for plasmid DNA or minimal medium met^- plates for chromosomal DNA. Quantification of colonies was corrected by cell viability in the moment of transformation, plating in LB serial dilutions of each strain as described before (Alonso et al., 1988) and by measurement of the entrance of DNA. For this last purpose, EcoRI-linearized plasmid pHP13 was radio labelled with [α^{32}P]-dATP and transformed in the strains at the same time as the other DNAs, followed by incubation at 37ºC for 30 minutes and centrifugation. Cell pellets were washed twice in PBS buffer and radioactivity measured with scillitation counter. For each experiment, quantification values were corrected to the wildtype strain, which is considered 100%.

2.3.6 Analysis of the expression of the *lrpC-topB* operon

In order to determine the expression of the genes *lrpC* and *topB*, a reverse transcription followed by PCR (RT-PCR) experiment was performed. Total RNA was extracted from strains YB886 and BG963 as described above. This RNA was visualized on 0.8% agarose gel stained by ethidium bromide and concentration was measured. To get rid of contaminating DNA in the sample, total RNA was treated with DNase (TURBO DNA-free from IMBION).

DNA free total RNA was used as a template for 3 different RT reactions (Applied Biosystems) containing: 700 ng of RNA, 2mM of dNTP mixture, 1 unit of Multiscribe Reverse Transcriptase and primers "top3", "top2" or "lrp2" for the 3 independent experiments. Three different primers were used due to the two different possibilities of expression of *lrpC* and *topB* (fig.12)
The resulting cDNAs were treated with 1 unit RNase H (IMBION) in order to get rid of RNA::DNA hybrids. Finally, the cDNAs were used for a PCR reaction containing: 10 ng cDNA or chromosomal DNA, 1µM of different pairs of primers, 0.4 mM dNTP mixture, 1x polymerase reaction buffer and 1 unit of BIOTOOLS DNA polymerase.

PCR fragments were run in 0.8% agarose gels in TAE buffer and were visualized by ethidium bromide staining. The expected length of the PCR reaction is: 350 bp with pairs lrp1-lrp2; 400 bp with pairs topB1-topB2; 600 bp with pairs topB2-lrp3 and 250 bp with pairs topB3-lrp3.

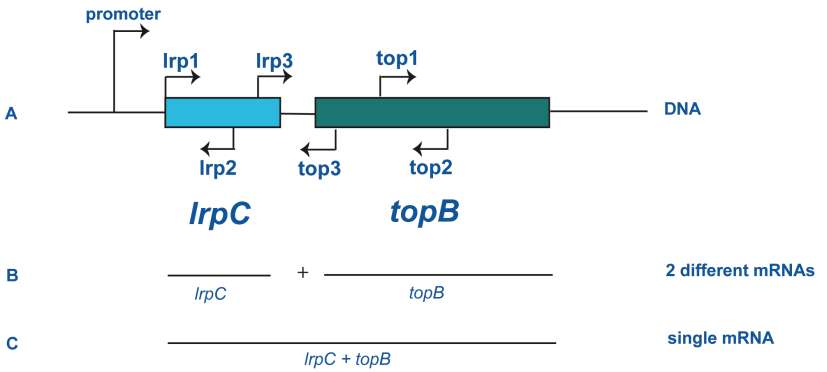

Figure 12: Design of the RT-PCR experiment. A: *B.subtilis* DNA locus coding for LrpC and Topoisomerase III (located in 475.440- 478.400 chromosomal region) showing the primers used for the experiment. Primers lrp2, top3 and top2 were used in an independent manner in order to cover the two possibilities of expression. **B**: shows the expected RNAs obtained if the genes *lrpC* and *topB* were transcribed separately (covered by using primers lrp2 or top2) or **C:** shows the expected RNA obtained if both genes were transcribed in conjunction (covered by using top3). If the two genes are transcribed under the same promoter, cDNA obtained from RT reaction with primers top2 or topB3 should have a length corresponding to the whole *lrpC* gen plus a fragment of *topB*. The gene *lrpC* shows two putative promoters P1 and P2, resumed in the figure as "promoter".

2.4 Purification and analysis of proteins

2.4.1 Overexpression of Topoisomerase III

Bacillus subtilis Topoisomerase III was overexpressed from *E.coli* BL21 plysS strain containing plasmid pTOPhis, which is transcribed under the T7 phage promoter. This strain was grown in LB at 37ºC till an optical density of 0.8, moment in which 2 mM IPTG was added. After 30 minutes, general transcription of the strain was stopped with 250 µg/ml rifampicin followed by further incubation for 90 minutes. Cells were then harvested and stored at -20ºC.

2.4.2 Purification of Topoisomerase III

Cell mass containing overexpressed Topo III was resuspended in buffer 50 mM potassium phosphate pH 7.5, 500 mM NaCl, 5% glycerol, 2.5 mM imidazol and lysed by sonication, followed by centrifugation at 18000 rpm for 35 minutes. The 80 KDa Topo III protein was found in the soluble fraction. Supernatant containing Topo III was loaded onto a Ni-Sepharose column equilibrated with the same buffer. Column was washed with equilibration buffer 50 mM potassium phosphate pH 7.5, 500 mM NaCl, 5% glycerol in a step gradient from 2.5 to 30 mM imidazol. Fractions containing Topo III, which elutes at 30 mM imidazol were recovered, dialyzed and loaded onto a phosphocelulose column equilibrated with buffer 50 mM Tris-HCl pH 7.5, 200 mM NaCl and 5% glycerol. Phosphocelulose column was extensively washed with a step gradient from 200 to 400 mM NaCl. Fractions containing Topo III, which elutes at 400 mM NaCl, were recovered and loaded onto a second Ni-Sepharose equilibrated with 50 mM potassium phosphate pH 7.5, 500 mM NaCl, 5% glycerol, 2.5 mM imidazol. Ni-Sepharose column was washed extensively at 5 mM imidazol to get rid of further contaminants.

Topo III was finally eluted with buffer 50 mM Tris-HCl pH 7.5, 300 mM NaCl, 50% glycerol and 50 mM imidazol, aliquoted and stored at -20ºC. Final protein concentration was determined by nanodrop equipment and 15% SDS-PAGE.

B.subtilis LrpC, SsbA and RecU proteins were a kind gift of Dr.Silvia Ayora, Tribhuwan Yadav and Cristina Cañas, respectively.

2.4.3 Molecular mass determination of Topoisomerase III

Molecular mass determination of Topo III was analyzed by gel filtration using FPLC (fast protein liquid chromatography, GE-Healthcare). Superose 12 10/300 GL column was used and the chromatography was carried out in buffer 50 mM Tris-HCL pH 7.5, 100 mM NaCl and 5% glycerol, at a flow rate of 0.3 ml/min. Around 0.14 mg of pure Topo III were injected to the column and the O.D. at 280 nm was measured. Collected fractions were analyzed by 15% SDS-PAGE. A standard curve of K_{av} versus $\log_{10}$ relative mobility was determined as recommended by the manufacturer. Protein standards for this column were: RNase 13KDa, Chymotripsine A 25 KDa, Ovoalbumin 43 KDa, Albumin 6 KDa, Aldolase 158 KDa, Catalase 232 KDa, Ferritin 440 KDa and Thyroglobulin 669 KDa.

2.5 *In vitro* assays

2.5.1 Crosslinking experiments

In vitro interaction of purified proteins LrpC and Topo III, or SsbA and Topo III was studied. For the LrpC-Topo III interaction, LrpC (0.5 μM in octamer) and Topo III (0.5 μM in monomer) were incubated in a buffer containing 50 mM Na-P pH 7.5, 50 mM NaCl, 1 mM $MgCl_2$ in a final volume of 30 μl. After 10 minutes of preincubation at 37ºC, DSS (0.5 or 1 μM) was added to the samples and put at 37ºC for an additional 15 minutes. SDS loading buffer was added and samples run in a 12 % SDS-PAGE. A western blott using polyclonal antibodies anti-LrpC or anti-his was carried out.

For the SsbA-Topo III interaction, SsbA (0.25 μM in tetramer) and Topo III (0.25 μM in monomer) were incubated in a buffer containing 50 mM Na-P pH 7.5, 50 mM NaCl, 1 mM $MgCl_2$ in a final volume of 25 μl. After 10 minutes of preincubation at 37ºC, DSS (0.1 or 0.5 mM) was added to the samples and put at 37ºC for an additional 15 minutes. SDS loading buffer was added and samples run in a 12 % SDS-PAGE. A western blott using polyclonal antibodies anti-G36P (a SSB-like homolog from *B.subtilis* bacteriophage SPP1) was carried out.

2.5.2 Supercoiled DNA relaxation assays

Supercoiled DNA relaxation assays were performed as previously described for *B.cereus* (Li et al., 2006). In general, supercoiled pUC18 plasmid DNA (200 ng) was incubated with increasing amounts of Topo III (0.6, 6, 12, 30, 60 and 90 nM) with buffer A in 20 μl of final volume. Reaction was incubated at 52ºC for 10 minutes and deproteinized by adding 2% SDS, 30 mM EDTA and 2 mg/ml proteinase K at 37ºC for 20 minutes. Reaction mixtures were run through 1% agarose gels in TBE buffer at 2 V/Cm for 22 hours approximately. Topoisomers were visualized by staining with ethidium bromide.

As a control, 1 unit of Topoisomerase I from *E.coli* (USB) was incubated at 37ºC for 15 minutes with the same amount of DNA, in buffer 1x provided by the supplier.
For experiments using LrpC, pUC18 (400 ng) was pre-incubated with 90 nM of Topo III with buffer A in 20 μl of final volume at 52ºC for 10 minutes. LrpC (1.5 or 0.3 μM) was added to the samples and incubated for additional 10 minutes at 52ºC. Reaction was stopped and processed as described above.

2.5.3 Electrophoretic Mobility Shift Assay (EMSA)

For performing these assays, several oligonucleotides were labelled using [γ-^{32}P]-ATP.
Linear oligonucleotides and dsDNA formed by annealing of ssDNA with its complementary sequences were 5´-end labelled using [γ-^{32}P]-ATP and polynucleotide kinase. Recombination intermediates Holliday Junction (HJ), 3-branched and forked substrate were formed by annealing of different combinations of oligonucleotides J3.1, J3.2, J3.3 and J3.4.
For obtention of forked substrate, oligos J3.1 and J3.2 were annealed. For obtention of 3-branched substrate, oligos J3.1, J3.2 and J3.4 were annealed. For obtention of the HJ, oligos J3.1, J3.2, J3.3 and J3.4 were annealed.
The oligonucleotides used in this work for DNA binding and cleavage analysis are listed in table 7.
Different DNA structures labelled in the 5´end using [γ^{32}P]-ATP were incubated with increasing amounts of Topo III (range of 6-240 nM) in a final volume of 20 μl in buffer B or D at 37ºC for 15 minutes, or in buffer A at 52°C for 10 minutes. Loading buffer was added to the samples. Formation of protein-DNA complexes was observed in non-denaturing PAGE 6% in buffer TAE 1X. Gels were dried and revealed by autoradiography.

name	sequence
$ssDNA_{polydT}$	5´-$(T)_{40}$-3´
$ssDNA_{60}$	5´-CTCCTATTATGCTCAACTTAAATGACCTACTCTATAAA GCTATGTACTGCTATCTAATC-3´
$ssDNA_{60comp}$	5´GATTAGATAGCAGTACTATAGCTTTATAGAGTAGGTCA TTTAAGTTGAGCATAATAGGAG-3´
J3.1	5´-CGCAAGCGACAGGAACCTCGAGAAGCTTCCGGTAGCA GCCtgagcggtggttgaattcctcgaggttcctgtcgcttgcg-3´
J3.2	5´-CGCAAGCGACAGGAACCTCGAGGAATTCAACCACCGC TCAactcaactgcagtctagactcgaggttcctgtcgcttgcg-3´
J3.3	5´-cgcaagcgacaggaacctcgagtctagactgcagttgagTCCTTGCTAGGAC GGATCCCTCGAGGTTCCTGTCGCTTGCG-3´
J3.4	5´-cgcaagcgacaggaacctcgagggatccgtcctagcaaggGGCTGCTACCG GAAGCTTCTCGAGGTTCCTGTCGCTTGCG-3´
16-M	5' -GACGCTGCCGAATTCTACCAGTGCCTTGCTAGGACAT CAGTCCTTACCTGCAGGTTCAC-3'
17-M	5'-GGGTGAACCTGCAGGTaaggGGCTGCTCATCGTAGGTTA GTTGGTAGAATTCGGCAGC-3'
19-M	5'-TAAGAGCAAGATGTTCctcAActGATGTCCTAGCAAGGC AC-3'
22-M	5'-TGAGGAACATCTTGCTCTTA-3'
23-M	5´-actaacctacgatgagcagcctgaggaacatcttgctctta-3´
fork-21	5-actaacctacgatgagcagcc-3'

Table 7: Oligonucleotides used in the present work

2.5.4 Topo III-mediated cleavage of recombination intermediates

Holliday Junction structure labelled in the 5´end using [γ^{32}P]-ATP in the four different oligonucleotides was incubated with 400 nM of Topo III in a final volume of 10 µl, in buffer B or C at 37ºC for 15 minutes, or in buffer A at 52°C for 10 minutes. An equal volume of loading buffer containing 90% formamide and 25 mM EDTA was added to the samples and incubated at 95ºC for 5 minutes. Samples were immediately stored on ice and loaded into a 15% PAGE denaturing gel containing 7.6 M urea. Gel was revealed by autoradiography.

As a positive control, the *B.subtilis* HJ resolvase RecU (100 nM) was incubated with HJ labelled in oligonucleotide J3.4 in buffer C in a final volume of 10 μl at 37ºC for 10 minutes. Samples were processed as described above.
For obtention of recombination intermediates D-loop, oligos 16-M, 17-M and 19-M were annealed. Structure RC-Dloop (recessed D-loop, resembling a D-loop where one of strands of the invading molecules was processed) was obtained by annealing oligos 16-M, 17-M, 19-M and 22-M. HJ was obtained by annealing oligos 16-M, 17-M, 19-M, 22-M and fork-21. Structure r-Dloop (replicated d-loop, resembling a D-loop where the lagging strand has been fully replicated) was obtained by annealing oligos 16-M, 17-M, 19-M and fork-21. The bona-fide D-loop was formed by the annealing of oligos 16M, 17M and 19M. The different structures labelled in the 5´end of oligo 19-M or 17-M and were incubated with 90 nM of Topo III in a final volume of 10 μl in buffer F at 37ºC for 30 minutes. An equal volume of loading buffer containing 90% formamide and 25 mM EDTA was added to the samples and incubated at 95ºC for 5 minutes. Samples were immediately stored on ice and loaded into a 15% PAGE denaturing gel containing 7.6 M urea. Gel was revealed by autoradiography.

RESULTS

1. *In vivo* studies of *Bacillus subtilis* LrpC

1.1 *In vivo* quantification of LrpC

To study the amount of LrpC in the cell at different growth stages and growth media, an *in vivo* quantification experiment was performed by the Western Blot technique. The experiment was done in LB and minimal medium S750 (see material and methods for further details) to check whether the influence of the nutritional environment could affect the expression of LrpC in the cell, as it was published before (Beloin et al., 2000). Average LrpC levels in mid-exponential phase (0.4 O.D) are nearly the same in LB (422 octamers/cell) and in minimal medium S750 (420 octamers/cell), while in late exponential phase (0.8 O.D) this number increases in both media, showing 1251 (LB) and 1306 (minimal medium S750) octamers/cell (fig.13). In early stationary phase (1.6 O.D) there is a decrease in the amount of LrpC to 292 (LB) and 316 (minimal medium S750) octamers/cell. In late stationary phase (O.D 2.2), LrpC shows a slight increase in LB (460 octamers/cell) and in minimal medium S750 (566 octamers/cell) (fig. 13).

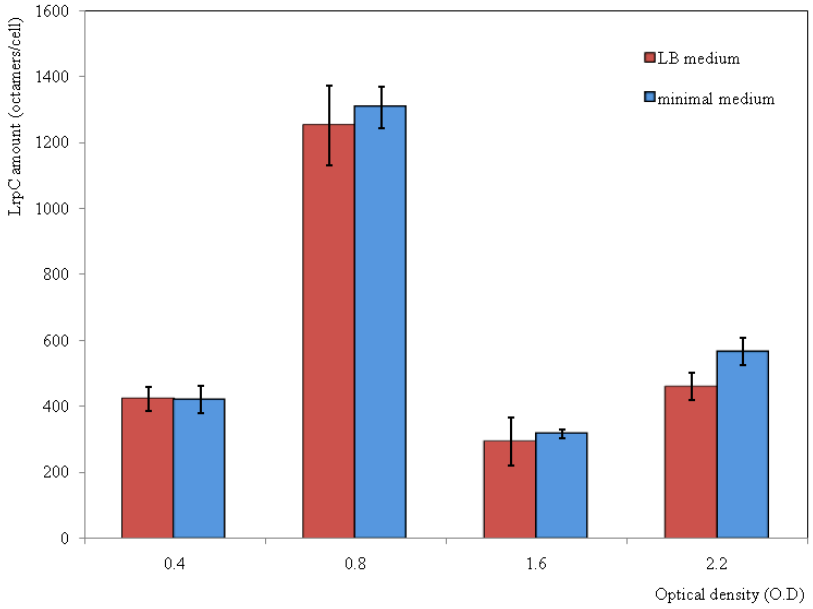

Figure 13: *In vivo* quantification of LrpC in *B.subtilis*. Wildtype strain YB886 was grown in rich (LB, red bars) or minimal medium S750 (MM, blue bars) at 37ºC. Samples were taken at indicated O.D, harvested, lysed and analyzed by western blot using rabbit polyclonal anti-LrpC antibodies. Graphic shows the amount of LrpC in octamers/cell at the different O.Ds analyzed. Bars indicate the average of three independent experiments.

1.2 Influence of LrpC in global gene expression

E.coli Lrp has been shown to regulate the expression of at least 10% of the whole genome during stationary phase (Cho et al., 2008; Tani et al., 2002). One of the objectives of the present Thesis was to determine the possible role of LrpC in global gene expression. For this purpose, microarray experiments were performed (in collaboration with Eduardo González-Pastor, CAB).

Microarrays experiments were done for two strains: wildtype and null *lrpC* mutant, in order to compare the results of the presence or absence of LrpC in the cell, and how this could affect gene expression.
Due to the results obtained in the *in vivo* quantification, microarrays were performed at the end of exponential phase in LB medium (0.9 O.D), when the LrpC amount in the cell is higher, or in stationary phase (1.8 O.D), when LrpC shows its minimum levels, and also because it is in stationary phase when a higher number of genes are regulated by *E.coli* Lrp (Cho et al., 2008; Tani et al., 2002). Data reveal that only 26 genes in the end of exponential phase and 15 in stationary phase of the whole *B.subtilis* genome are affected, which is only 0.65-0.9% of the genome (genes are summarized in tables 8, 9, 10 and 11). Genes whose expression is affected a significant fold change of 2.5 times or more, and with a p-value inferior to 0.2 were considered and classified in two groups: metabolic and unknown genes. At one glance it is clear that LrpC is not affecting the global gene expression of the genome, leading to discard the hypothesis of a role in global regulation for LrpC.

gene name	protein	general features	fold change	p-value
purH	inosine-monophosphate cyclohydrolase	purine biosynthesis	-2.50	0.14
ybbE	similar to beta-lactamase	unknown	-2.50	0.14
spoIVCA	site-specific DNA recombinase	required for excision of the skin element	-2.54	0.18
licB	PTS lichenan-specific enzyme	lichenan degradation product utilization	-2.59	0.11
yogA	similar to alcohol dehydrogenase	unknown	-2.59	0.17
mtlA	PTS mannitol-specific enzyme	mannitol metabolism	-2.64	0.02
kipR	Kinase protein regulator	transcriptional regulator of the Kip operon	-2.75	0.20
purL	phosphoribosylformylglycinamidine synthetase II	purine biosynthesis	-2.77	0.18
radA	DNA repair protein homolog	possible role in recombination	-2.81	0.19
mtlD	mannitol-1-phosphate dehydrogenase	mannitol metabolism	-2.92	0.06
purS	phosphoribosylformylglycinamidine synthetase	purine biosynthesis	-2.97	0.19
clpE	Clp protease E	part of the heat shock regulon	-3.12	0.03
ycsF	similar to lactam utilization protein	unknown	-3.42	0.11
kipI	Kinase protein inhibitor	inhibitor of KinA	-3.49	0.17
ilvB	Acetolactate synthase	biosynthesis of valine/isoleucine	-3.60	0.16
ilvD	Dihydroxy-acid dehydratase	biosynthesis of valine/isoleucine	-3.76	0.17
cydC	Cytochrome bd transporter	ABC transporter required for expression of cytochrome bd	-4.30	0.14
yvkC	unknown	unknown	-4.44	0.16
idH	myo-inositol 2-dehydrogenase	myo-inositol catabolism	-4.68	0.14
ytiB	similar to carbonic anhydrase	unknown	-5.80	0.19
lctP	L-lactate permease	fermentative metabolism	-6.05	0.20

Table 8: Genes downregulated by LrpC at the end of exponential phase. Genes with a significant fold change of 2.5 or more are shown. P-value (≤0.2) establishes the reliability of the experiment. Strains wildtype and *lrpC* mutant were grown in LB till the end of stationary phase (0.9 O.D), cells were treated with ice-cold methanol, centrifuged and stored. Total RNA was extracted with an acid phenol-chloroform protocol (see material and methods).

gene name	protein	general features	fold change	p-value
ywtD	similar to murein hydrolase	unknown	2.43	0.03
yutJ	similar to NADH dehydrogenase	unknown	2.54	0.19
gntK	gluconate kinase	gluconate utilization	2.60	0.11
yjeA	similar to chitooligosaccharide deacetylase	unknown	3.60	0.01
lrpC	leucine responsive protein C	transcriptional regulator	8.41	0.02

Table 9: Genes upregulated by LrpC at the end of exponential phase. Genes with a significant fold change of 2.5 or more are shown. P-value (≤0.2) establishes the reliability of the experiment. Strains wildtype and *lrpC* mutant were grown in LB till the end of stationary phase (0.9 O.D), cells were treated with ice-cold methanol, centrifuged and stored. Total RNA was extracted with an acid phenol-chloroform protocol (see material and methods).

gene name	protein	general features	fold change	p-value
yhgB	unknown	unknown	-2.63	0.07
levD	PTS fructose-specific enzyme IIA component	metabolism of fructose	-2.82	0.07
opuCD	glycine betaine/carnitine/choline ABC transporter	membrane transport protein	-2.91	0.16
yoeB	unknown	unknown	-3.03	0.08
yxjJ	unknown	unknown	-3.09	0.06
yqhO	unknown	unknown	-3.22	0.05
yvgW	similar to heavy metal-transporting ATPase	unknown	-3.23	0.04
ytiB	similar to carbonic anhydrase	unknown	-3.42	0.02

Table 10: Genes downregulated by LrpC in stationary phase. Genes with a significant fold change of 2.5 or more are shown. P-value (≤0.2) establishes the reliability of the experiment. Strains wildtype and *lrpC* mutant were grown in LB till stationary phase (1.8 O.D) and processed as above mentioned.

gene name	protein	general features	fold change	p-value
ywjI	similar to glycerol-inducible protein	unknown	2.54	0,13
ybfE	unknown	unknown	2.56	0.13
hutH	histidase	histidine utilization	2.83	0.08
yefC	similar to resolvase	unknown	3.17	0.01
gntK	gluconate kinase	gluconate utilization	3.22	0.20
yybK	unknown	unknown	3.33	0.08
yxjA	similar to pyrimidine nucleoside transport	unknown	5.59	0.18

Table 11: Genes upregulated by LrpC in stationary phase. Genes with a significant fold change of 2.5 or more are shown. P-value (≤0.2) establishes the reliability of the experiment. Strains wildtype and *lrpC* mutant were grown in LB till stationary phase (1.8 O.D) and processed as above mentioned.

1.3 *In vivo* localization of GFP-LrpC

1.3.1 LrpC localization in vegetative growth

In order to look for a specific role if LrpC has a specific role in the cell or is an architectural protein as other nucleoid associated proteins as Hbsu, a fluorescent GFP-LrpC fusion was obtained. The fusion is located on the N-terminus of LrpC and the resulting gene was placed in the *amy* locus. The original locus has a deletion in the *lrpC* gene, so that the only copy of the protein produced in the cell is the one carrying the fusion (figure 14). An attempt to localize LrpC expressed from its own promoter was done, by replacing the original gene by a GFP fusion located in the C-terminus of LrpC, which resulted in no detectable fluorescence (data not shown). This is in accordance with the LrpC crystal structure, which shows that the GFP protein can probably be fused to the N-terminus without affecting the protein activity, because the N-terminus is exposed and placed outside the core, and not in the C-terminus, that is placed inside the protein, so that a fusion in this terminus will probably disrupt the octameric structure of LrpC and thereby its activity (Thaw et al., 2006).

Due to the fact that the GFP-LrpC fusion is expressed under the xylose promoter and not from its own promoter, a first assay was done to determine the amount of xylose needed for having similar GFP-LrpC levels from the xylose promoter and from its original promoter. For this purpose, a wildtype strain YB886 and the strain BS158 (expressing GFP-LrpC) were grown in minimal medium S750 supplied with 0, 0.01, 0.02, 0.03 or 0.04% of xylose at 30°C till exponential phase (0.4 O.D). At this moment, 2 ml samples were taken from each culture and a western blot anti-LrpC was carried out (figure 14). The recombinant protein GFP-LrpC showed the correct full length (fig. 14 lanes 3-8). Strain BS158 grown without any xylose showed that levels of GFP-LrpC without induction are enough for having *in vivo* levels of this protein, due to escapes in the promoter (fig.14, compare lanes 3 with 4).

Similar results were obtained when cells were grown in minimal medium S750 till early exponential phase (0.2 O.D) or when cells were collected at late exponential phase (0.8 O.D) (data not shown), proving that without xylose, the amount of GFP-LrpC expressed from the xylose promoter in the cell is comparable to that of LrpC expressed from its own promoter.

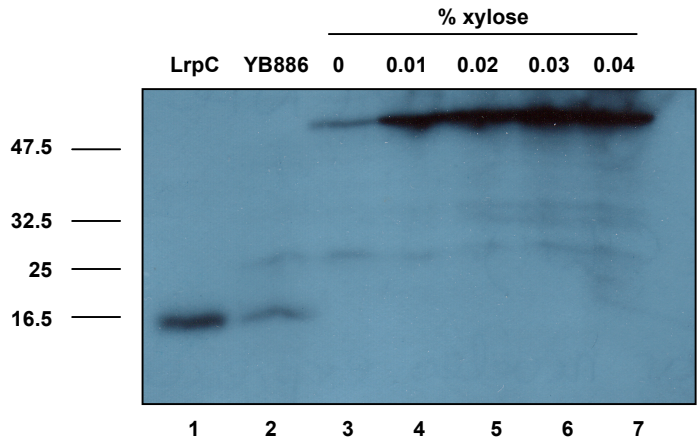

Figure 14*: In vivo* quantification of GFP-LrpC expression. Strain BS158 (GFP-LrpC) was grown in minimal medium S750 supplied with 0.01, 0.02, 0.03 or 0.04% of xylose at 30°C till exponential phase (0.4 O.D). As a control, BS158 and wildtype strain YB886 were grown in the same conditions without xylose. Aliquots of 2 ml were taken at 0.4 O.D and processed for western blot as described in material and methods. Lane 1: 10 ng of purified wildtype LrpC. Lane 2: cell extract from YB886 without xylose. Lane 3-7: cell extract from BS158 with increasing amounts of xylose (0-0.04%). In the left part of the figure, lines indicate the migration of molecular weight marker (in Kda).

LrpC has been localized for the first time in the cell, showing a specific pattern in exponential (0.4 O.D) and stationary phase (2.5 O.D). Around 86% of total cells were showing specific foci in exponential and stationary phase (table 12). In minimal medium S750 during exponential phase, this pattern consists of two symmetric foci that are located inside the nucleoid (fig. 15, white triangles), in the borders of the nucleoid, close to the cell poles (fig.15, orange triangles), or one asymmetric focus located in the borders of the nucleoid, that is not placed in the center of it (figure 15, green triangles). The percentage of cells showing two foci inside the nucleoid was higher than the number of cells showing two foci at the border of the nucleoid near the poles (table 12). GFP-LrpC also shows another distinct pattern, showing some fluorescence without a specific localization in terms of foci, but forming aggregates that are coincident with the nucleoid, and that are expectable for an architectural protein decorating the DNA (figure 15, blue triangles; table 12). This pattern is only seen in 7% of cells in the case of exponential phase.

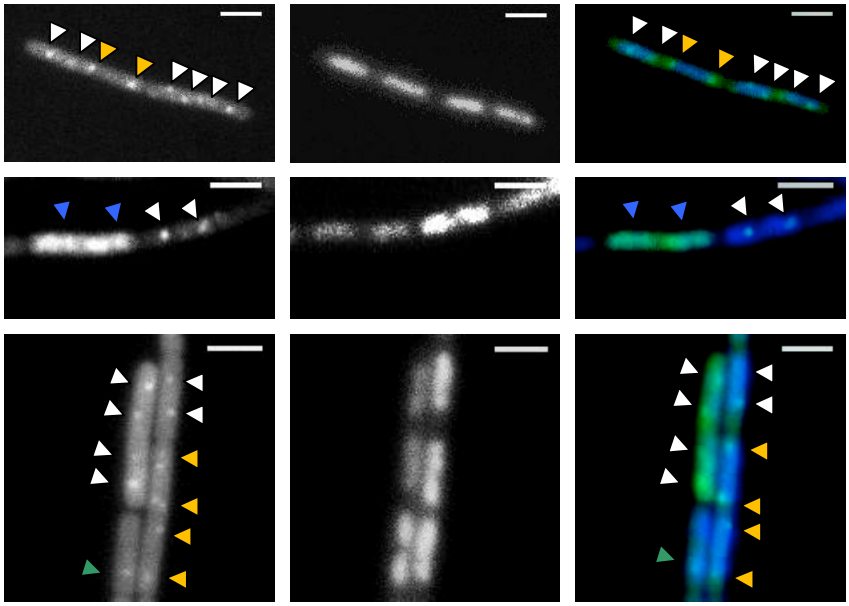

Figure 15: Localization of GFP-LrpC in minimal medium S750 during exponential phase. Strain GFP-LrpC was grown in minimal medium S750 at 30ºC till exponential phase (0.4 O.D). Cells were stained with 1 µg/µl DAPI and mounted in agarose slides. White triangles show two symmetric foci per cell inside the nucleoid. Orange triangles show two symmetric foci per cell located in the borders of the nucleoid and near to the cell poles. Green triangles show one single asymmetric focus per cell in the borders of the nucleoid. Blue triangles indicate LrpC aggregates. White bar: 2 µm.

In stationary phase (2.5 O.D) number of cells showing two foci in the borders of the nucleoid near the cell pole is higher than cells showing two foci inside the nucleoid (fig. 16, table 12). Also these foci seem to be closer to the cell pole than the same foci observed in exponential phase (compare orange triangles in fig. 15 and 16). The number of cells showing one focus at the pole is higher in stationary phase than in exponential phase (table 12). In stationary phase aggregates seem to dissipate during stationary phase, so that their number is decreased to 1% (table 12).

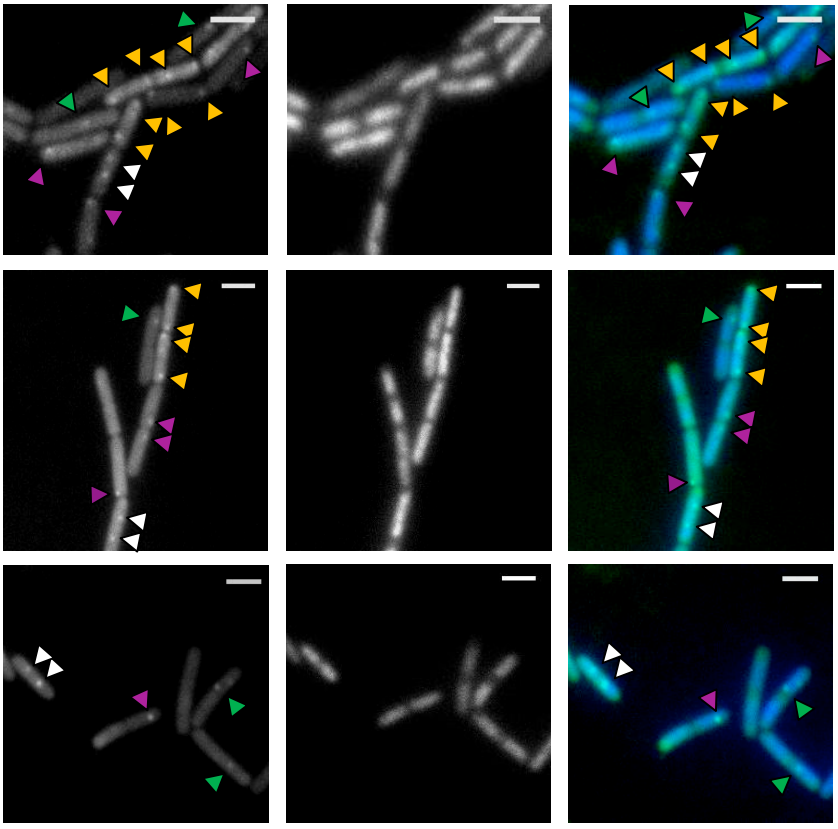

Figure 16: Localization of GFP-LrpC in minimal medium S750 during stationary phase. Strain GFP-LrpC was grown in minimal medium S750 at 30ºC till late stationary phase (2 O.D). Cells were stained with 1 μg/μl DAPI and mounted in agarose slides. Orange triangles show two symmetric foci per cell located in the borders of the nucleoid or at the cell poles. Green triangles show one single asymmetric focus per cell in the borders of the nucleoid. Blue triangles indicate LrpC aggregates. Purple triangles point to one single asymmetric focus close to the cell pole. White bar: 2 μm.

	one focus per cell (near cell pole)	one focus per cell (borders of nucleoid)	two foci per cell (nucleoid)	two foci per cell (near cell poles)	aggregates	total cells
exponential	15 (2.9%)	44 (8.6%)	241 (47.2%)	103 (20.1%)	38 (7.4%)	510
stationary	169 (32.5%)	85 (16.3%)	69 (13.2%)	120 (23.1%)	6 (1.1%)	519

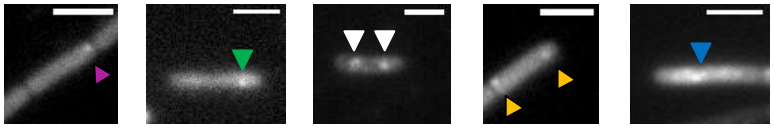

Table 12: *In vivo* quantification data of GFP-LrpC foci in minimal medium S750 during exponential and stationary phase. Around 500 cells were counted for each growth phase. Out of the parenthesis, number of cells showing distinct pattern of localization, and inside the parenthesis the calculated percentage related to the total cells counted. Pictures show an example of each different localization pattern: two symmetric foci inside nucleoid (white triangles), two symmetric foci in the borders of the nucleoid close to cell pole (orange triangles), one asymmetric focus per cell in the borders of the nucleoid (green triangle), one asymmetric focus per cell near cell pole (purple triangle) and aggregates (blue triangle). White bar: 2μm.

The pattern of localization of GFP-LrpC is similar to the one found for SMC, an architectural protein in charge of the maintenance of the chromosome. In this case, SMC-GFP is forming foci that are located in the outer borders of the nucleoid during exponential phase (Britton et al., 1998). Due to the fact that SMC and LrpC show similar localization during vegetative growth and that they are both considered as architectural proteins, an attempt of colocalization was made by bimolecular fluorescence complementation. LrpC was fused to the C-terminal part of the YFP protein (YC), while SMC was fused to the N-terminal part of the YFP (YN). Both fusions were transformed in the same background and checked for complementation YC-YN, which restores the entire YFP protein, though emitting fluorescence. This experiment did not show any detectable fluorescence, showing that SMC and LrpC might not interact *in vivo* (data not shown). Another experiment was done in order to determine if the presence or absence of LrpC was affecting SMC localization, showing that SMC-YFP is not changing its localization in an *lrpC* mutant background (data not shown).

1.3.2 Effect of MMC on the *in vivo* localization of GFP-LrpC

In *B.subtilis*, when cells are exposed to certain types of DNA damage, as mitomycin C (MMC). Some proteins involved in DNA repair by homologous recombination are specifically recruited to the so called repair centers, RCs (Kidane et al., 2004). RecN has been shown to be the first protein that is recruited to the RCs, after 20-30 minutes of the induction of DNA damage with MMC, followed by RecO at 60 minutes and RecF at 90 (Kidane et al., 2004). Other proteins, as the resolvase RecU, are fully recruited at 120 min after the induction (Sanchez et al., 2005). However, not all *rec* proteins are recruited to the RCs after damage induction, as it is the case for AddAB (Mascarenhas et al., 2006).
In order to check for the possible implication of LrpC in DNA repair processes and to determine the influence of MMC addition in the formation of GFP-LrpC foci, strain BS158 was exposed to 50 ng/ml MMC for 30, 60 and 120 min during exponential phase (fig. 17).
A quantification of GFP-LrpC foci was also performed during this MMC treatment. Before MMC addition, 56.6% of cells showed two foci per cell and 8% of cells showed one single focus per cell at or near the cell pole (table 13).

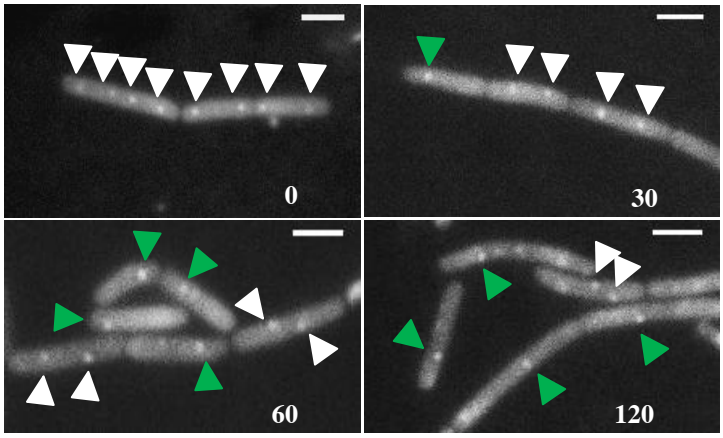

Figure 17: Induction of DNA damage alters the pattern of localization of GFP-LrpC. Strain BS158 (GFP-LrpC) was grown in minimal medium S750 at 30ºC until exponential phase (0.4 O.D.). In this moment, an aliquot of the sample was incubated with 50 ng/ml MMC. Samples were taken the indicated times after MMC addition, mounted on agarose slides and visualized under fluorescence microscopy. White triangles indicate two foci per cell. Green triangles point to one focus per cell. White bar: 2 μm.

Table 13 shows that in general, by prolonging the time of MMC treatment, the number of cells showing foci decay. The number of cells showing two foci in the nucleoid or near cell poles decreases. At the same time, the number of cells showing one focus in the nucleoid or near the cell poles increases by prolonging the time of MMC treatment. This shows that the treatment with 50 ng/ml MMC is affecting localization of GFP-LrpC strain. Also, the general amount of cells showing foci decreases from 68% to 33% after MMC treatment (table 13).

	one focus per cell (near cell pole)	one focus per cell (borders of nucleoid)	two foci per cell (nucleoid)	two foci per cell (near cell poles)	aggregates	total cells
time zero	3 (1.3%)	15 (8%)	123 (54.9 %)	4 (1.7%)	7 (3.1%)	224
30 min	7 (2.9%)	26 (10.9 %)	95 (40.0 %)	3 (1.2%)	3 (1.2%)	237
60 min	7 (3.1%)	27 (12.1 %)	63 (28.4 %)	3 (13.6%)	2 (0.9%)	222
120 min	8 (3.6%)	33 (15.1 %)	25 (11.4 %)	6 (2.7%)	2 (0.91%)	219

	cells showing foci	cells without foci	total cells
time zero	152 (67.8%)	72 (32.1%)	224
30 min	134 (56.5%)	103 (43.4%)	237
60 min	102 (45.9%)	120 (54.0%)	222
120 min	74 (33.7%)	145 (66.2%)	219

Table 13: *In vivo* quantification data of GFP-LrpC foci in minimal medium S750 after treatment with 50 ng/ml MMC. Upper part: quantification of different patterns observed after treatment with MMC. **Down part:** general quantification of cells with or without foci. Around 200 cells were counted for each time. Out of the parenthesis, number of cells showing distinct pattern of localization, and inside the parenthesis the calculated percentage related to the total cells counted.

1.3.3 Localization of GFP- LrpC in competence

During the general competence process in *B.subtilis*, certain proteins are recruited to the cell poles to conform the DNA uptake machinery (Dubnau, 1999). Recently it has been shown that some, but not all, proteins implicated in DNA recombination processes localize at the cell poles during natural competence in the cell. Among these proteins there are two, RecO and RecU, which show *in vitro* DNA annealing activity (Kidane et al., 2009; Kidane and Graumann, 2005) and RecA-independent DNA annealing is believed to be an important step in the establishment of a plasmid after transformation (Kidane et al., 2009). Due to the fact that biochemistry studies showed that LrpC possesses strand annealing activity (Lopez-Torrejon et al., 2006), GFP-LrpC foci were analyzed during competence. In the case of *B.subtilis*, at the beginning of stationary phase, cells start to be competent, and after 1.5-2 hours, around 10-20 % of the whole population is fully competent when the cells are incubated in a starvation medium (Young, 1967). BS158 strain was grown in GMI till the beginning of stationary phase (approx. 4 hours), then cells were incubated in the second medium (GMII) and the incubation continued for 150 minutes approx. At this moment, that is when cells reach the maximum level of competence, the GFP-LrpC fusion was observed at the cell poles (fig. 18, orange and yellow triangles). Around 8-10% of the total population was showing foci at each (orange triangles) or at one (yellow triangles) cell pole (fig. 18).

Around 3% of total cells show one focus located in the borders of the nucleoid (fig. 18, green triangles). Only around 0.5% of total cells were showing two foci per cell, as it was seen in exponential or stationary phase of vegetative growth.

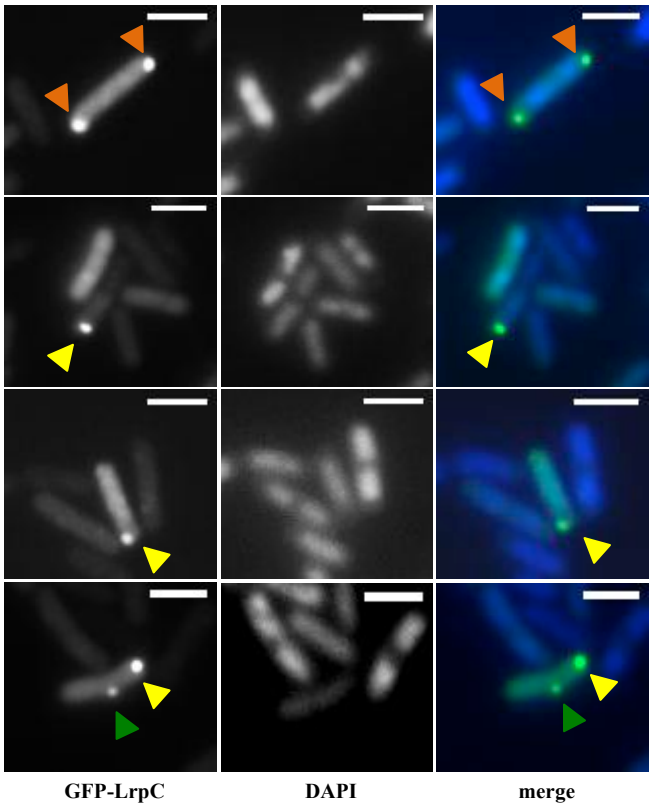

Figure 18: Localization of GFP-LrpC during competence. Strain BS158 carrying the GFP-LrpC fusion was grown in GMI media at 37ºC until stationary phase, switch to GMII medium and further incubated for 150 minutes. In this moment, an aliquot of the sample was stained with 1 μg/μl DAPI, mounted on agarose slides and visualized under fluorescence microscopy**.** Orange triangles point to GFP-LrpC two polar foci per cell, each of them located at one cell pole. Yellow triangles point to one single polar foci per cell. Green triangles show one focus located in the borders of the nucleoid. White bar: 2 μm.

These polar foci are brighter than the ones observed in exponential or stationary phase. For this reason, a western blot experiment was performed to determine if the amount of the GFP-LrpC fusion was higher in GMII than in LB (figure 19). Levels of GFP-LrpC are approximately the same in competence medium GMI than in LB, in different stages of growth: in late exponential phase (0.6 O.D), in the moment in which cells are shifted to the second competence medium GMII (1.1 O.D) and in the moment of fully competence (150 minutes later). Figure 19 shows that polar foci observed cannot be an artifact due to the excess of protein in the cell.

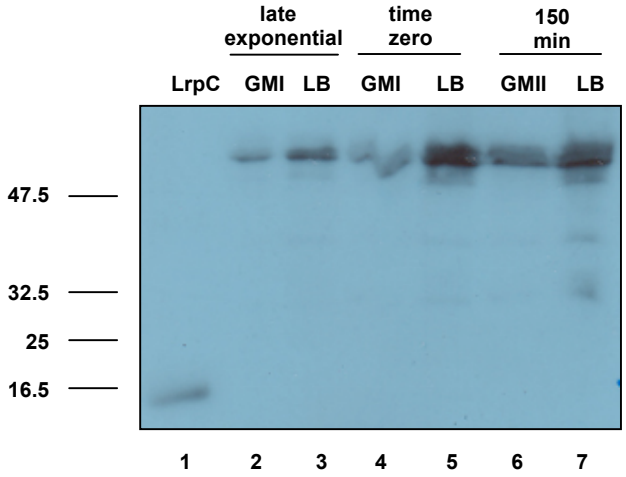

Figure 19: Determination of GFP-LrpC levels during competence. Strain BS158 was grown in LB medium or GMI medium at 37°C till stationary phase. Aliquots of 2 ml were taken from each culture at different stages of growth: at late exponential phase (0.6 O.D, lanes 2 and 3), in the moment in which cells growing in GMI are shifted to GMII for the case of competence medium, denoted as time zero (1.1 O.D, lanes 4 and 5), and at 150 minutes after this shifting (lanes 6 and 7). Aliquots were processed for western blot developed with antibodies anti-LrpC as described in materials and methods. Lanes 2, 4 and 6 correspond to samples from competence media (GMI-GMII) and lanes 3, 5 and 7 of LB medium. Lane 1: 10 ng of purified wildtype LrpC. In the left part of the figure, lines indicate the running positions of molecular weight marker (in Kda).

Time lapse experiments were done to observe entrance in competence and appearance of GFP-LrpC foci at the cell pole. Considering time zero the moment in which cells are shifted to the medium GMII, cells were grown up to 150 minutes, taking aliquots for analysis at 45, 90 and 150 minutes (fig.20). At time zero, almost no foci of GFP-LrpC were visible at any cell pole (0.2- 0.4 % of total cells), while the fusion appeared to be located in the nucleoid, forming aggregates (fig 20, blue arrows). In GMII medium, the percentage of GFP-LrpC with this pattern is around 50% of total cells (table 14), a number much higher than during vegetative growth. At time 45 minutes, the number of cells showing foci at the poles is increased to 0.4% (fig. 20, yellow and orange triangles), while at 90 minutes it reaches 1.4 %. At 150 minutes, around 10% of total cells show foci at one or two poles (fig 20, orange and yellow triangles), which corresponds to the percentage of cells expected to be at competent state (Young, 1967). Concomitant with this behavior, the aggregates of GFP-LrpC decrease in number as competent stage is reached, from 50 % to 4.5% (table 14, blue triangles in figure 20). A different pattern of GFP-LrpC foci is also detected during this time lapse, consisting of foci located in the borders of the nucleoid (fig.20, green triangles). These foci start to appear at 45 min and 90 minutes, but their presence is quite rare (table 14: 0.6-0.8 %). At 150 min, the number is increased to 2.9%. This suggests that, as the competent stage is reached, GFP-LrpC starts to be recruited at the cell poles and disappearing from the nucleoid. The pattern of two symmetric foci that is showed during exponential phase in vegetative growth is in this case diminished from 5% to 0.7% (table 14), as the cell reaches its competent state.

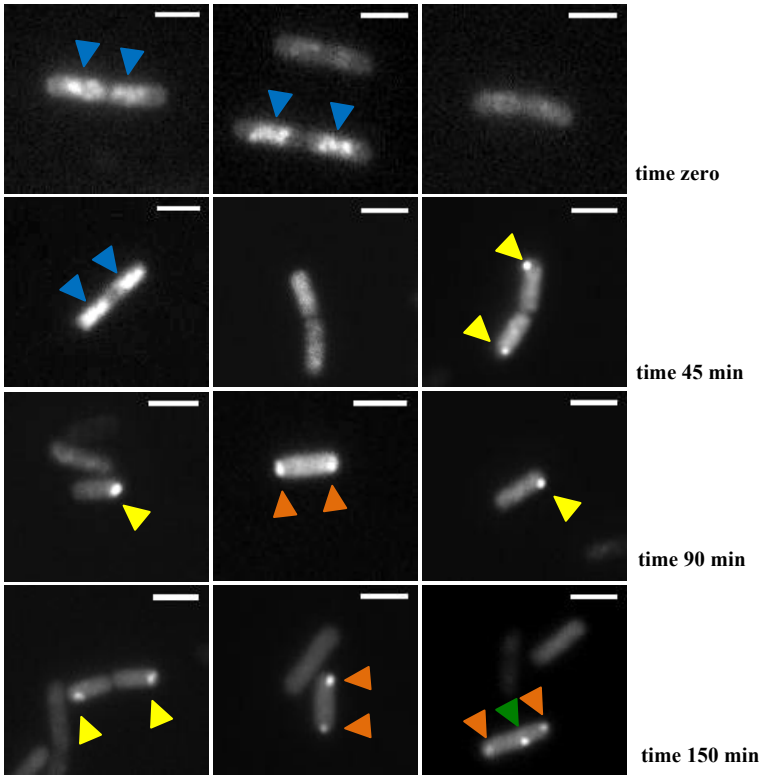

Figure 20: **Experiment of localization of GFP-LrpC during development of competence**. Strain GFP-LrpC was grown in GMI medium at 37ºC until stationary phase, switch to GMII (time zero) and the growth was continued for 150 minutes. At time zero, 45, 90 and 150 minutes, samples were taken and visualized in agarose slides. Orange triangles show GFP-LrpC polar at both poles. Yellow triangles show one focus at the cell pole. Blue triangles point to GFP-LrpC aggregates. Green triangles show foci located in the borders of the nucleoid. White bar: 2 μm.

time after shift to GMII	two symmetric foci	one focus at pole per cell	two foci at poles per cell	one focus borders of nucleoid	aggregates	total cells
time 0	26 (5.2%)	2 (0.4%)	1 (0.2%)	0 (0%)	252 (50.6%)	498
45 min	11 (2.1%)	3 (0.6%)	2 (0.4%)	3 (0.6%)	121 (24%)	503
90 min	4 (0.8%)	7 (1.4%)	5 (1%)	4 (0.8%)	46 (9.3%)	495
150 min	4 (0.7%)	37 (7.2%)	7 (1.3%)	15 (2.9%)	23 (4.5%)	510

Table 14: *In vivo* quantification of GFP-LrpC pattern during competence development. Around 500 cells were counted for each time. Out of the parenthesis, number of cells showing distinct pattern of localization, and inside the parenthesis the calculated percentage related to the total cells counted.

The GFP-LrpC fusion was observed till now in a wildtype background. To determine the dependence of GFP-LrpC polar foci on the presence of the competence machinery, the pattern of localization of the fluorescent fusion was studied in the absence of the two main competence regulators: ComK and ComA. ComK is the master regulator of competence, needed for initiation of transformation (van Sinderen et al., 1995). ComA is one of the regulators that activate a gene cascade that is transcribed during competent state (Weinrauch et al., 1989).

GFP-LrpC was visible at the cell poles in the absence of any of these regulators, showing that polar LrpC foci are not dependent on the competence machinery (data not shown). GFP-LrpC foci quantification was performed for wt, *ΔcomK* and *ΔcomA* backgrounds. Strains BS158 (wt background), BS1525 (*ΔcomK* background) and BS1526 (*ΔcomA* background) were grown in GMI at 37°C, shifted to GMII and 150 minutes after this shift foci were quantified (table 15). This table shows that the presence or absence of the two main competence regulators is not affecting the number or the localization of GFP-LrpC foci. This is in accordance with microarray data that show that LrpC expression is not controlled by ComK (Berka et al., 2002) and ComA (Comella and Grossman, 2005).

	one focus at pole per cell	two foci at poles per cell	one focus borders of nucleoid	aggregates	total cells
wt	35 (6.8%)	12 (2.3%)	12 (2.3%)	11 (2.1%)	511
ΔcomK	30 (6.1%)	17 (3.4%)	10 (1.9%)	8 (1.6%)	503
ΔcomA	28 (5.7%)	12 (2.4%)	14 (2.8%)	5 (1%)	495

Table 15: Quantification of GFP-LrpC pattern in *ΔcomK* and *ΔcomA* backgrounds during competence. Around 500 cells were counted for each genetic background. Out of the parenthesis, number of cells showing distinct pattern of localization, and inside the parenthesis the calculated percentage related to the total cells counted. Experiment was performed at the maximum state of competence (150 min after the shifting to the GMII medium).

1.4 Transformation efficiency studies

GFP-LrpC polar foci are brighter and seem to have a dynamic behavior during the competent state of the cell. Furthermore, it has been shown that LrpC is able to anneal two complementary ssDNA (Tapias et al., 2000). Other recombination proteins that were found to localize at the cell poles in competence medium are also involved in DNA annealing. That is the case for the recombination proteins RecO and RecU and the processing protein DprA/Smf. RecO and RecU are able to perform DNA strand annealing (Manfredi et al., 2008). RecO localizes at the cell poles upon the addition of DNA, while RecU seems to dissipate from the pole once DNA is added (Kidane et al., 2009). Smf is able to bind ssDNA and protect it from the action of nucleases, is able to perform strand annealing and it also interacts with RecA (Mortier-Barriere et al., 2007).
Strain BS158 carrying the GFP-LrpC fusion was grown in GMII medium till the moment of maximum competence, and then 150 ng of plasmid DNA (pDG148) or 200 ng of chromosomal DNA (YB886) was added for 30 min at 37ºC and GFP-LrpC foci were quantified. After the addition of DNA, the number of cells showing foci at the poles is 9.3% (plasmid DNA) and 10.1% (chromosomal DNA), showing no difference with the control experiment without DNA, where 9.8% of total cells were showing foci at the poles.
The transformation efficiency of a *lrpC* null mutant, as well as combinations of a *lrpC* mutation with other mutations in DNA annealing proteins involved in transformation was studied. Single mutant *lrpC* shows a half decay in plasmid transformation efficiency when compared to the wildtype strain, while chromosomal efficiency in this mutant is marginally affected (table 16). Single mutants *recU*, *recO* and *smf* are seriously affected in plasmid transformation (around 2% transformants) when compared to the wildtype strain (100%), as it was published before (Kidane et al., 2009; Tadesse and Graumann, 2007).
Double mutants *recO-lrpC*, *recU-lrpC* and *smf-lrpC* show a plasmid transformation defect of 2.3, 9 and 2.4%, very similar to the one of the single mutants *recO*, *recU* and *smf*, respectively.

The almost identical behaviour between single and double mutants is also observed in the case of chromosomal transformation efficiency for the double mutants *recO-lrpC* and *recU-lrpC*. In the case of double mutant *smf-lrpC*, chromosomal transformation is reduced to the half when compared to the single mutant *smf*. This means that in the absence of both proteins, the transformation defect could be synergic.

	Plasmid transformation	Chromosomal transformation
wildtype	100	100
ΔlrpC	49.5	70
ΔrecO	2.4	59.6
ΔrecU	6.7	56
Δsmf	2.8	2.3
ΔrecOΔlrpC	2.3	50.3
ΔrecUΔlrpC	9	55
ΔsmfΔlrpC	2.4	1.3

Table 16: Transformation efficiency assays of *lrpC* mutants. Relative percentages of transformants compared to wildtype strain are showed. Data are normalized to cell viability and entrance of ^{32}P-DNA. Table shows the average of five independent experiments. Standard deviation is around 10%.

Hbsu is an abundant and essential architectural protein that has been shown to be involved in DNA transformation (Fernandez et al., 1997). Its function is to stabilize the cellular chromosome and the *in vivo* localization shows a clear tight link to the nucleoid during exponential phase (Kohler and Marahiel, 1997). Partial mutant *hbsu4755* shows 30% of chromosomal transformation when compared to the wildtype strain (100%). To determine whether a bona-fide architectural protein as Hbsu is recruited to the cell poles during competence, the fluorescent fusion Hbsu-GFP was visualized in competent state. Hbsu-GFP is also localized inside the nucleoid during competent state (fig. 21). This pattern is exactly the same as the one previously described for vegetative growth.

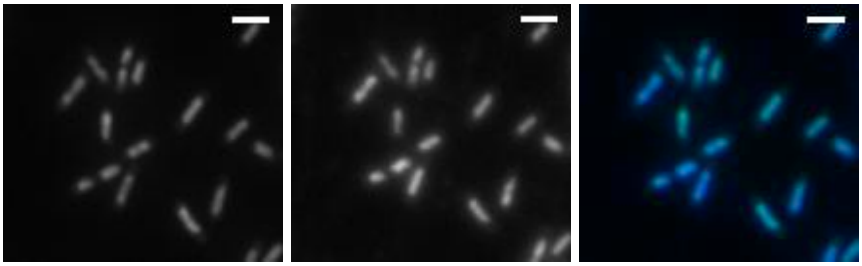

Hbsu-GFP **DAPI** **merge**

Figure 21: Localization of Hbsu-GFP during competence. Strain PK9C8 carrying a Hbsu-GFP fusion was grown in GMI medium at 37ºC until stationary phase, switch to GMII and further incubated for 150 minutes. In this moment, an aliquot of the sample was stained with 1 μg/μl DAPI, mounted on agarose slides and visualized under fluorescence microscopy. White bar: 2 μm.

2. Analysis of the *lrpC-topB* operon

2.1 Analysis of the expression of *lrpC-topB* operon

Between *B.subtilis* genes *lrpC* and *topB*, located in the chromosome region 37°, there are only 67 bp. Theoretical studies from this region have localized two putative promoters in the upstream region of *lrpC* (Beloin et al., 2000), though no putative promoter has been found in the intergenic region between the two genes. One of the aims of the present thesis was to study both genes and to define if they belong to a common operon in which a polycistronic mRNA would lead to the expression of both genes, which remained unknown. For this purpose, RT-PCR experiments were performed, that covered the two possible ways of gene expression: whether *lrpC* and *topB* are expressed separately, leading to two independent mRNAs, or both genes are transcribed under the same promoter conforming a single mRNA. Due to the different length of the mRNAs that could be synthesized it is possible to distinguish between both possibilities. An experiment with different primers was designed for the retrotranscriptase reaction and the following PCR (see material and methods). Figure 22 shows the PCR fragments obtained from the cDNA.

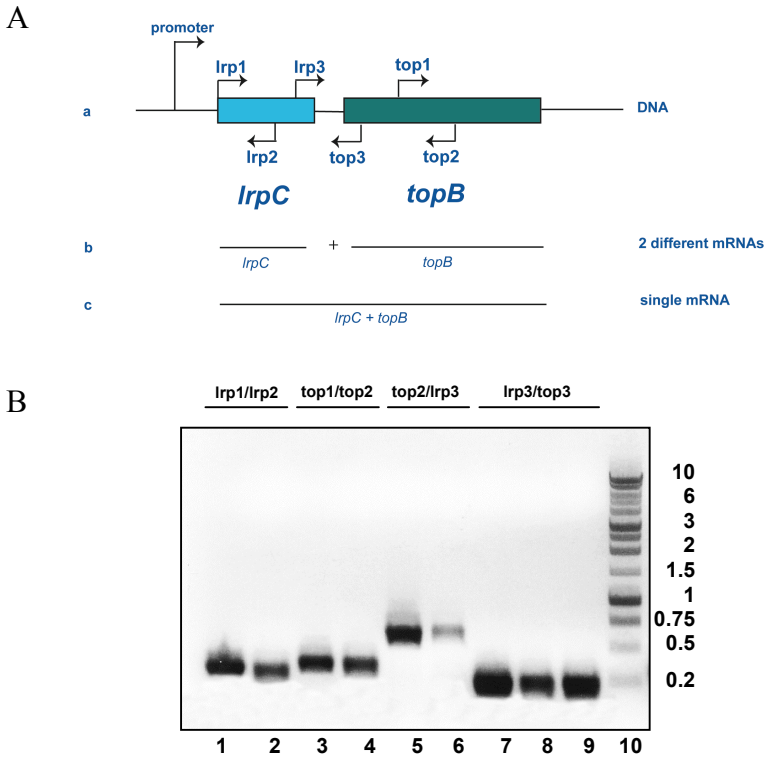

Figure 22: LrpC and Topoisomerase III are expressed under the same promoter. **A:** Design of the RT-PCR experiment showing the chromosomal region and the localization of the primers used for the experiment (a) and the two types of mRNA that could be resulted depending on gene expression under different promoters (b) or under the same promoter (c). **B:** Result of the RT-PCR experiment. Total RNA was extracted from the cell and the complementary cDNA obtained by retrotranscriptase reaction. As a control, chromosomal DNA from *B.subtilis* was used as a template for the PCR (lanes 1, 3 5 and 7). In lanes 2, 4, 6, 8 and 9, the cDNA obtained from the RT reaction was used as a template for the PCR. In the upper part of the figure, pairs of primers used for the RT reaction are indicated. In the right part of the figure it is shown the molecular marker in Kbp.

Total RNA extracted from the cell was treated with DNase to get rid of possible contaminant DNA in the samples. Four different PCRs were done with the cDNA obtained from the retrotranscriptase reaction, to check the gene expression.
Two of them were made with primers binding inside *lrpC* gene (lanes 1 and 2) or inside topB gene (lanes 3 and 4). These two PCR products show that both *lrpC* and *topB* are being transcribed. The other two PCRs were made using couples of primers that amplify a common region between the two genes. Only if the two genes are transcribed in the same mRNA that would cover the intergenic region between the two genes, the PCR product is visible. As this was the case, in lanes 5 and 6 using primers top2 and lrp3 and lanes 7, 8 and 9, using primers lrp3 and top3 show PCR products of the expected size covering partially the two genes plus the intergenic region. By this experiment, it is proved that *lrpC* and *topB* are expressed under the same promoter, located in the upstream region of *lrpC*.

2.2 LrpC and Topo III mediated DNA relaxation

Due to the fact that genes *lrpC* and *topB* are transcribed under the same promoter (this Thesis, fig.22), that LrpC is able to constrain DNA supercoils (Tapias et al., 2000), while Topo III can relax a supercoiled plasmid DNA (fig.32), the effect of LrpC on TopoIII-mediated DNA relaxation was analyzed. Both proteins were put together in the pUC18 relaxation reaction (fig. 23). At 52ºC and pH 9.8, Topo III is able to partially relax supercoiled DNA (fig. 23, lane 2). LrpC alone cannot relax supercoiled DNA alone (fig. 23, lanes 5 and 6). When DNA is preincubated with Topo III for 10 minutes at 52ºC, followed by incubation with LrpC for additional 10 minutes at 52°C, new topoisomers can be seen that are not present when the proteins are incubated separately in the reaction (fig. 23, compare lanes 2 with 3 and 4). When LrpC was preincubated with the DNA, followed by Topo
III addition, this effect could not be seen (data not shown). This experiment suggests that LrpC is promoting DNA relaxation mediated by Topo III.

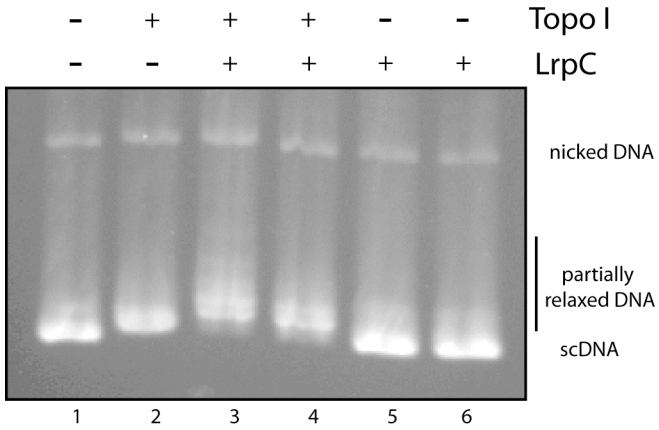

Figure 23: LrpC stimulates Topo III mediated relaxation activity. Superhelical DNA pUC18 (400 ng) was pre-incubated with 90 nM of Topo III in buffer A in 20 µl of final volume at 52ºC for 10 minutes. LrpC (1.5 or 0.3 µM) was added to the samples and incubated for additional 10 minutes at 52ºC. Reaction was deproteinized by adding 2% SDS, 30 mM EDTA and 2 mg/ml proteinase K at 37ºC for 30 minutes. Reaction mixtures were run through 0.8% agarose gels in TBE buffer at 2 V/Cm for 22 hours approximately. Topoisomers were visualized by staining with ethidium bromide. Lane 1: control DNA. Lane 2: 90 nM of Topo III. Lane 3: 90 nM of Topo III and 1.5 µM of LrpC. Lane 4: 90 nM of Topo III and 0.3 µM of LrpC. Lane 5: 1.5 µM of LrpC. Lane 6: 0.3 µM of LrpC.

2.3 *In vitro* LrpC-TopoIII interaction

The next step was to study the possible protein-protein interaction. *In vitro* crosslink experiment using different concentrations of DSS (suberic acid) was performed with purified LrpC and Topo III, and the crosslinked proteins were visualized by western blott with antibodies anti-LrpC in a 12 % SDS-PAGE (fig 24).

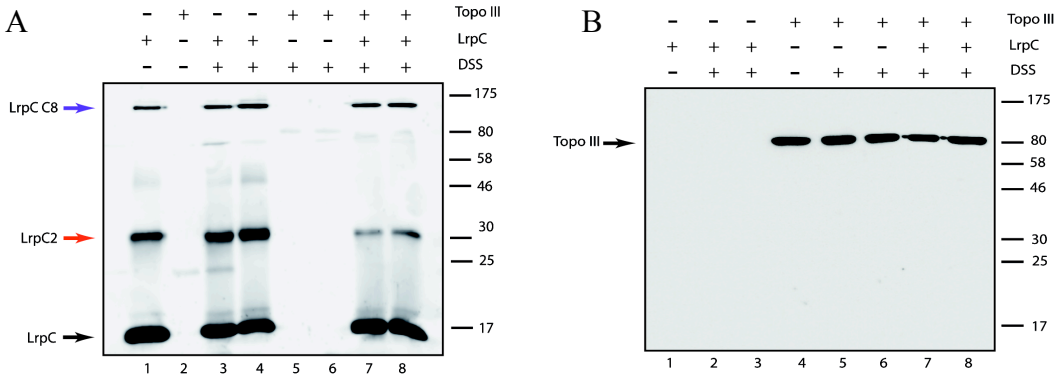

Figure 24: *In vitro* crosslink of purified LrpC and Topo III. LrpC (0.5 µM in octamer) and Topo III (0.5 µM in monomer) were incubated in a buffer containing 50 mM Na-P pH 7.5, 50 mM NaCl and 1 mM $MgCl_2$. After 10 minutes of preincubation at 37ºC, DSS (1 or 0.5 µM) was added to the samples and put at 37ºC for an additional 15 minutes. SDS loading buffer was added and samples run in a 12 % SDS-PAGE, followed by western blott using polyclonal antibodies anti-LrpC (A) or anti-his (B). Lane 1: LrpC control without DSS. Lane 2: Topo III control without DSS. Lane 3: LrpC with 0.5 µM DSS. Lane 4: LrpC with 1 µM DSS. Lane 5: Topo III with 0.5 µM DSS. Lane 6: Topo III with 1 µM DSS Lane 7: LrpC and Topo III in relation with 0.5 µM DSS. Lane 8: LrpC and Topo III with 1 µM DSS. Arrows indicate the position of LrpC monomer (LrpC, black arrow), LrpC dimers (LrpC2, red arrow) and LrpC octamers (LrpC8, purple arrow). The black arrow points to a Topo III monomer. In the right part of both figures, lines indicate the running positions of molecular weight marker in KDa.

Under the conditions tested, dimers (fig. 24A, red arrow) and octamers (fig. 24A, purple arrow) of LrpC can be detected. Together, Topo III and LrpC (in a ratio 1:1 in molecules) do not present any additional band that could correspond to an interaction between both proteins, but the amount of LrpC dimers detected by crosslink is decreased when compared to LrpC alone (fig. 24A, compare lanes 3,4 with 7,8). Under conditions tested, an interaction between LrpC and Topo III could not be detected. The same experiment was also done by western blot developed with antibodies anti-his (fig. 24B), where only Topo III monomer was visible, showing no detectable interaction between both proteins.

3. Characterization of Topoisomerase III

3.1 Phenotype of *topB* single and double mutants

3.1.1 Repair of DNA damage caused by MMS in *topB* mutants

To study the role of *topB* in DNA repair, *in vivo* assays were performed in the presence of DNA damaging agents MMS and H_2O_2. In other *Bacteria* it is known that the lesions provoked by MMS are specifically repaired by BER (Friedberg et al, 2006). When a replication fork encounters a DNA lesion produced by MMS, single strand gaps (SSGs) are formed, and these can be repaired by homologous recombination. In the case of treatment with H_2O_2, the lesions lead to double strand breaks (DSBs) that can be repaired by homologous recombination. Because it is known that *E.coli* Topo III is implied in DNA recombination (Lopez et al., 2005), single mutant *topB* was obtained and exposed to acute doses of MMS (fig. 25). After acute exposition to 10 mM MMS, single mutant *topB* showed a similar phenotype in comparison with the wildtype. The lack of an evident phenotype for *topB* mutant has also been shown for *E.coli topB* (Lopez et al., 2005). To obtain more information about the effect of a *topB* mutation, several double mutants of *topB* with genes implied in the different stages of DNA recombination were obtained: *recF* and *recO* from epistatic group α; *addAB* from β; *ruvA*, *ruvB* and *recU* from ε; *recS*, *recQ*; *recJ* from ζ and *recG* from η. The genes *recF*, *recO*, *addAB*, *recJ*, *recS* and *recQ* are involved in presynaptic stages of DNA recombination, while *ruvA*, *ruvB*, *recG* and *recU* are implicated in late stages of this process. After acute exposition to 10 mM MMS, double mutants *recJtopB* and *addABtopB* slightly recovered from the single mutations *recJ* and *addAB* respectively (fig. 25A). This recovery is more evident in the case of double mutants *recOtopB* and *recFtopB* (fig. 25B), whose single mutations *recO* and *recF* are very sensitive to MMS. RecF and RecO belong to the *recFOR* pathway that has been implicated in the repair of ssDNA gaps, supposed to be the main lesions after MMS treatment. Null mutations in genes *recF* and *recO* have been shown to be extremely sensitive to the killing action of 10 mM MMS (Alonso et al., 1993; Alonso et al., 1988). On the other hand, *recJ* mutation is slightly sensitive to chronic exposure to MMS (Sanchez et al., 2006).
In late stages of DNA recombination (post-synapsis) there are two possible pathways to resolve the recombination intermediate: one in which the helicase complex RuvAB is able to bind to the Holliday Junction (HJ) followed by resolution by the HJ resolvase RecU (Ayora et al., 2004; Carrasco et al., 2004) and another one in which the branch migration translocase RecG would act as an alternative to RuvAB for resolving HJ (Sanchez et al., 2007). In the case of *E.coli* Topo III, it has been proposed that it is acting in late stages of DNA recombination and Topo III from humans is able to dissolve a double HJ (Lopez et al., 2005; Raynard et al., 2006). For defining if TopoIII might be involved in late stages of homologous recombination, double mutants *ruvABtopB*, *recUtopB* and *recGtopB* were obtained. Double mutants *recGtopB* and *ruvABtopB* were almost as sensitive as single mutants *recG* and *ruvAB*, respectively (fig 25D). Mutations in these genes render cells highly sensitive to MMS, as it was published before (Sanchez et al., 2005). However, in both cases, a slight recovery was observed.
In the case of *recUtopB*, a synergic effect was observed: this double mutant seems to be more affected by the addition of MMS in comparison with single mutant *recU* (fig 25E), which was already shown to very sensitive to 10 mM of MMS (Fernandez et al., 1998). This is the only double mutant of *topB* that show this phenotype. This synergic effect could mean that Topo III and RecU might have redundant roles in the cell, so that the absence of both proteins render the cells very sensitive to the DNA damaging agent MMS. Therefore, Topo III may act in late stages of DNA recombination.

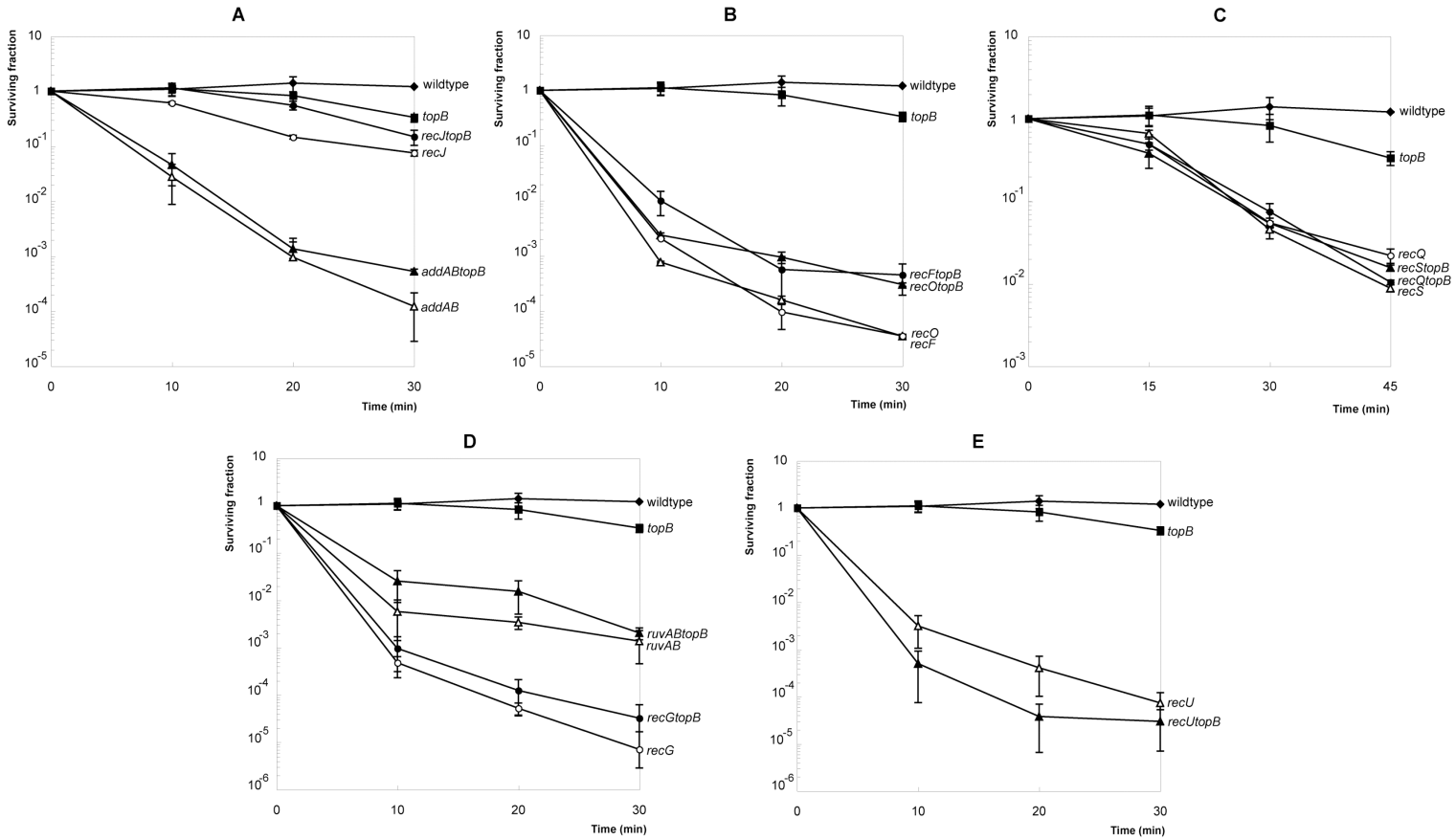

Figure 25: Survival of strains exposed to an acute dose of MMS. Strains were grown in LB media at 37ºC till exponential phase (O.D= 0.4) and exposed to 10 mM MMS for the indicated time. Dilutions of the culture were plated on LB agar and incubated overnight at 37ºC. In A it is shown nucleases RecJ and helicase/nuclease complex AddAB. In B, ge

In *B.subtilis*, there are two recQ-like helicases: RecQ and RecS. Both share homology with *E.coli* RecQ, but whether they perform similar roles in the cell is unknown (Ayora et al., 2011). To define if TopoIII is acting in concert with one of these helicases or not, two double mutants were obtained: *recQtopB* and *recStopB*. In both cases, it seems that Topo III is epistatic with these two helicases (fig 25C), so that Topo III could work in concert with RecQ or RecS.
Double mutant *recUtopB* was the only mutant that showed a synergic effect in presence of MMS. Since *recU* mutants have a defect in segregation with an accumulation of unresolved and linked chromosomes and anucleate cells (Carrasco et al., 2004), nucleoids of double mutant *recUtopB* were analyzed. Cells were analyzed under fluorescence microscopy and defects associated with DNA segregation and/or recombination (anucleate cells, filamented cells without division septum, condensed nucleoids and abnormal positioning of the nucleoid) were quantified.

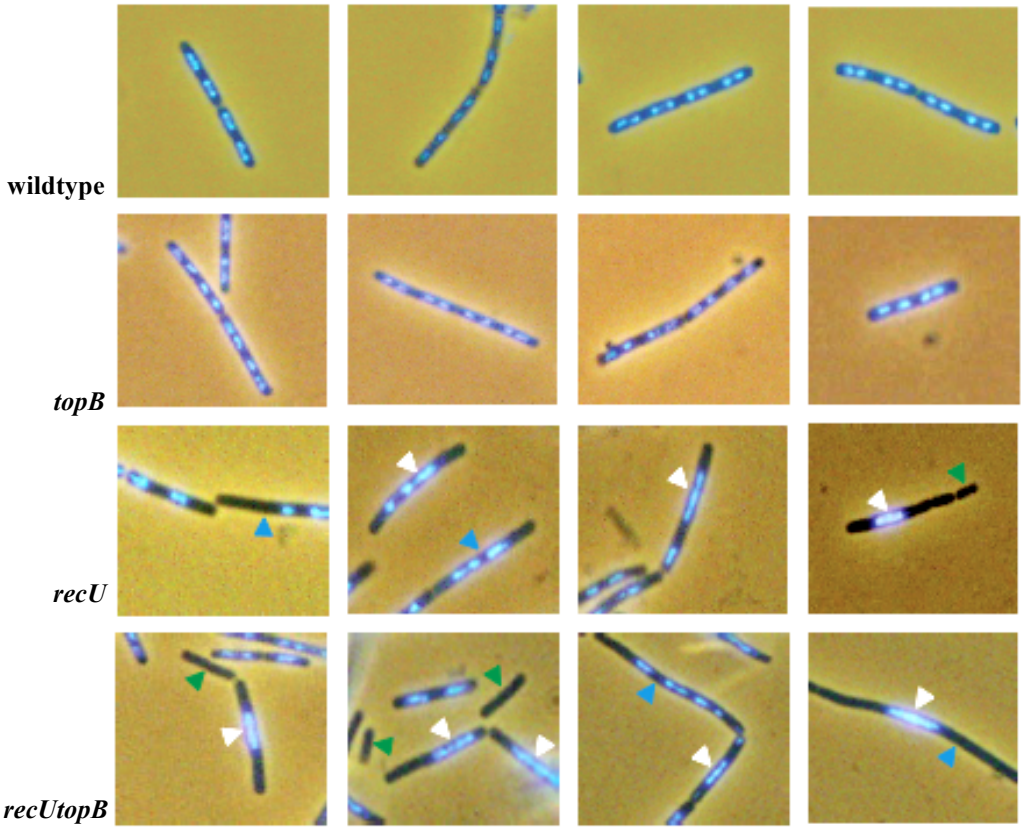

Figure 26: Nucleoid morphology of *topB* and *recUtopB* mutants. Strains were grown in LB medium at 37ºC till exponential phase (0.4), moment in which cells were fixed with 2% of formaldehyde, stained with 1 µg/µl DAPI followed by addition of mountain medium and visualized by fluorescent microscopy. White triangles indicate condensed or misplaced nucleoids. Green triangles indicate anucleate cells. Blue triangles indicate non-septated cells (filaments).

Single mutant *recU* has been previously reported to show 1-3% of anucleate cells (Carrasco et al., 2004). Single mutant *topB* does not show any significant phenotype in comparison with wildtype cells (fig.26). Single mutant recU showed 2.6% of anucleate cells (n≈500) (fig.26). Double mutant *recUtopB* shows a 3-fold increasement in anucleate cells (6.8%) (n≈500). Though this effect is not very accused, it is significant and confirms the genetic data previously shown for MMS survival (fig. 25E), and it suggests that RecU and Topo III act in different pathways for resolution of HJs in the cell.

3.1.2 Repair of DNA damage caused by H_2O_2 in *topB* mutants

Damage caused by H_2O_2 in the DNA includes single and double strand breaks, base modifications, abasic sites and sugar modifications (Friedberg et al, 2006). Single mutant *topB* was exposed to different doses of H_2O_2 to further investigate its role in DNA repair. At high concentrations of H_2O_2, *topB* mutant showed a slight decrease in viability, compared to the wildtype strain (fig.27).
Under the killing action of different concentrations of H_2O_2, double mutants *addABtopB*, *recFtopB* and *recOtopB* show a recovery of cell viability when compared to single mutants *addAB*, *recF* and *recO*, respectively (fig.27 A and B), as it was the case for damage with MMS (fig.26A and B). Under the conditions tested, the sensitivity of mutants *recJ* and *recJtopB* was still too low to be distinguished, so another experiment was done this time changing the concentration of H_2O_2 (fig.28A). In this case, the experiment showed that *recJtopB* is more sensitive to H_2O_2 exposure than single mutant *recJ*.
Double mutant of *topB* with HJ helicase *ruvAB* show almost the same behaviour as single mutant *ruvAB* (fig. 27 C), while double mutant *recGtopB* recovers partially compared to single mutant *recG* (fig.27C). This is the same behaviour as with MMS. Double mutant *recUtopB* shows a synergic effect, because is more sensible to the killing action of H_2O_2 when compared to single mutant *recU* (fig. 27D), the same behaviour as with MMS treatment.
In the case of double mutants with the two recQ-like helicases, *recStopB* was recovering partially compared to single mutant *recS*, while *recQtopB* behaves like *recQ* (fig. 28B). The fact that double mutant *recQtopB* is recovering suggests that *topB* would be epistatic with *recQ*, and though, they could work together.

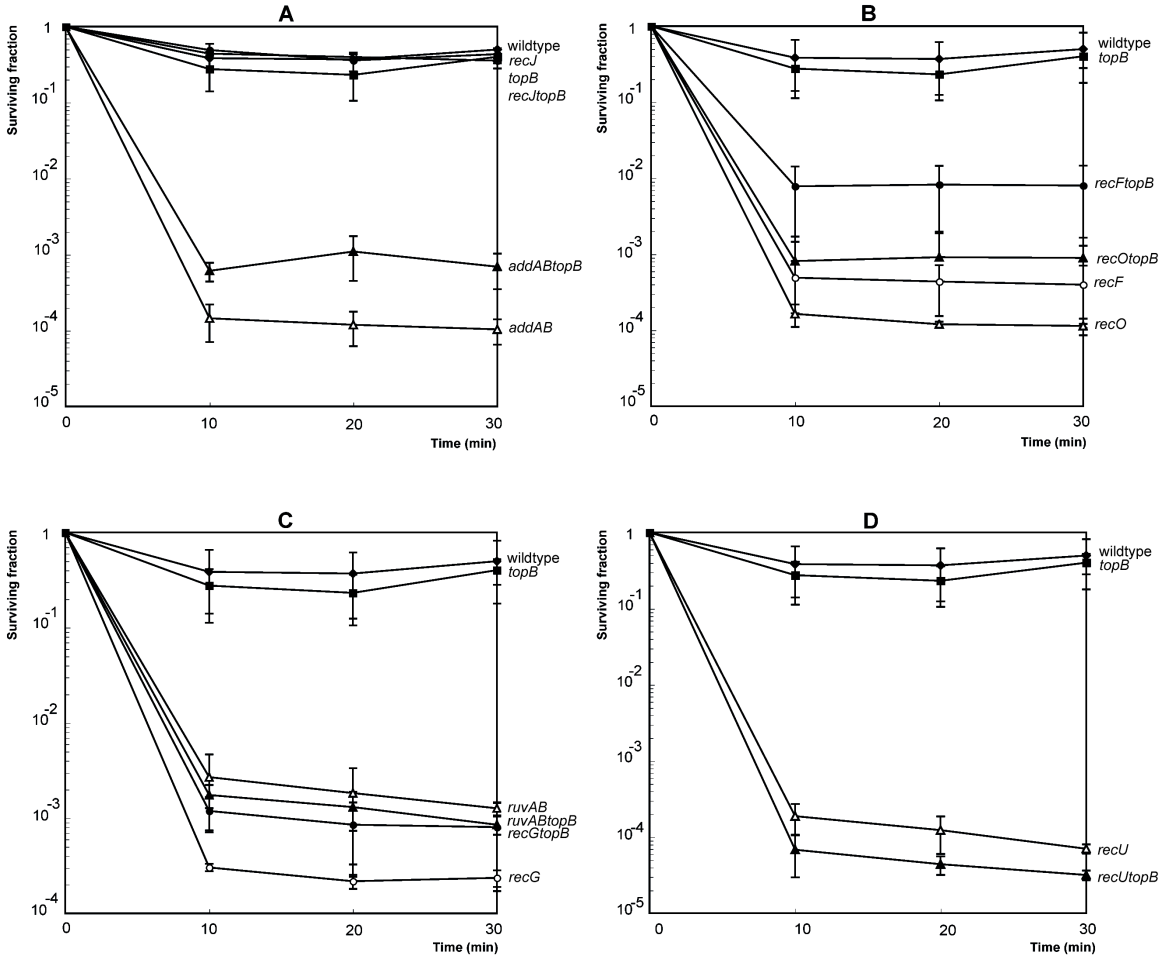

Figure 27: Survival of strains exposed at different times to an acute dose of H_2O_2. Strains were grown in LB media at 37ºC till exponential phase (O.D= 0.4) and exposed to 5 mM of H_2O_2 for the indicated time. Dilutions of the culture were plated on LB agar and incubated overnight at 37ºC. In A it is shown nucleases RecJ and helicase/nuclease complex AddAB. In B, genes belonging to the RecFOR pathway. In C, HJ helicases RuvAB/RecG, and in D, HJ resolvase RecU.

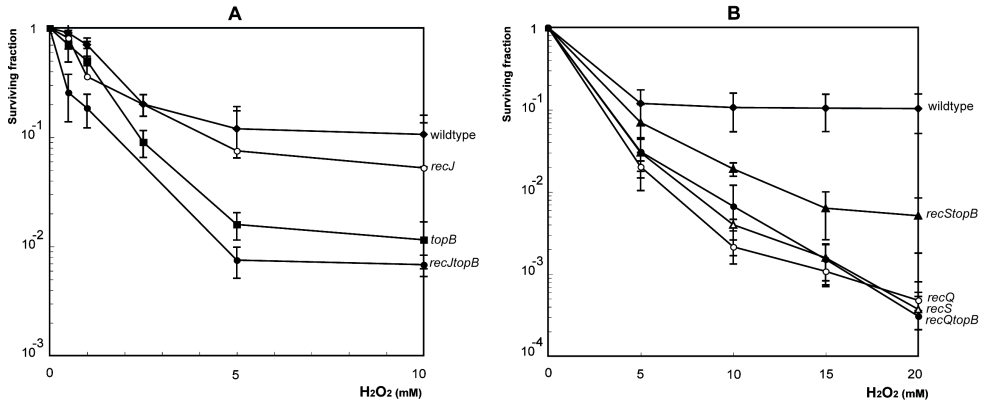

Figure 28: Survival of strains exposed to different doses of H_2O_2. Strains were grown in LB media at 37ºC till exponential phase (O.D= 0.4) and exposed to the indicated concentrations of H_2O_2 for 15 minutes. Dilutions of the culture were plated on LB agar and incubated overnight at 37ºC. In **A** it is shown nuclease RecJ. In **B** helicases RecQ and RecS.

3.2 Transformation efficiency in *topB* null mutant

In *B. subtilis* competent cells, recombination proteins can integrate homologous or partially homologous foreign DNA into the chromosome (chromosomal transformation), or allow the establishment of autonomously replicating molecules (plasmid transformation). The types of recombination intermediates formed by these two types of DNAs are different and the recombination proteins involved in both processes also vary. As an example, chromosomal transformation is a RecA dependent event, whereas plasmid transformation is RecA independent (Kidane et al., 2009). In chromosomal transformation, the incoming ssDNA displaces the identical strand in the duplex of chromosomal DNA forming a D-loop structure. When oligomeric plasmid DNA, is transformed into *B. subtilis* competent cells, the incoming ssDNA is longer than a unit-length plasmid genome. Replication may convert the ssDNA onto dsDNA, and after DNA replication, complementary regions may anneal to generate a circular intermediate that is then converted into a single plasmid monomer

Since Topo III is able to specifically cleave the recombination intermediate known as D-loop (see part 4.7), that is formed after the entrance of chromosomal DNA in the cell, transformation efficiency was studied for single mutant *topB*. Plasmid transformation efficiency was marginally affected, 86% when compared to wildtype (100%). However, chromosomal transformation efficiency was 36. 6% when compared to wildtype (100%), what is suggesting a possible role in chromosomal transformation processes.

3.3 *In vivo* localization of Topo III-YFP

Topoisomerase III is the only non-essential topoisomerase in the cell and its cellular role remains unknown. Other DNA topoisomerases have been localized in the cell by fluorescence microscopy, mainly bound to the DNA. Gyrase is located forming foci inside the nucleoid and colocalizing with replication machinery, Topo I is forming foci that colocalize with SMC and Topo IV is uniformly distributed inside the nucleoid (Tadesse and Graumann, 2006). Localization of Topo III was addressed by creating a C-terminal fusion followed by insertion in the original locus. The recombinant protein showed the correct full length by western blot using antibodies anti-GFP (data not shown).
In order to test the functionality of the fusion, the *topB-yfp* gene was placed in a *ΔrecU* background and the sensitivity of the resultant strain to 10 mM MMS was analyzed. Strain *ΔrecU topB-yfp* was as sensitive to MMS as strain *ΔrecU* alone. Therefore, the fusion was supposed to be functional and further experiments were done.
TopoIII-YFP shows a distinct localization pattern in vegetative growth in comparison with other topoisomerases: it is localized mainly in the cytosol, outside the nucleoid (fig.28, white triangles) and sometimes close to the cell poles (fig.29, blue triangles).

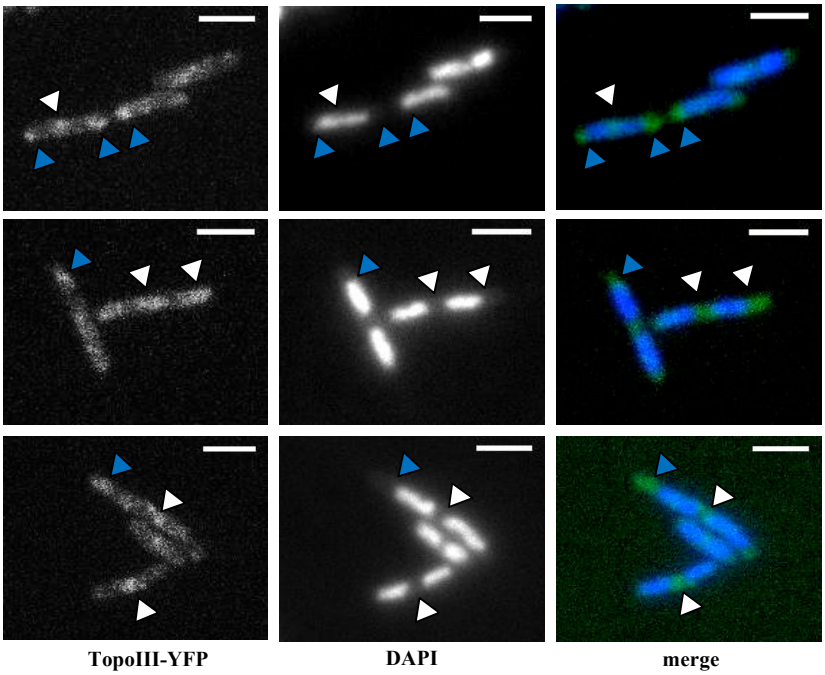

Figure 29: Distribution of Topo III-YFP during vegetative growth. Strain Topo III-YFP was grown in minimal medium S750 at 30ºC till exponential phase (0.4 O.D). Cells were stained with 1 μg/μl DAPI, mounted on agarose slides and visualized under fluorescence microscopy. White triangles show cytosolic localization of the protein. Blue triangles show polar foci. White bar: 2 μm.

Around 30% of the total cells showed a slightly brighter fluorescence in the cytosol (fig. 29, white triangles) and 15% showed polar foci (fig. 29, blue triangles) (n≈220). In 12% of total cells, a slight signal of fluorescence can be seen inside the nucleoid.

In order to understand the role of Topo III in DNA repair and to see if the foci of TopoIII-YFP change by DNA damage, exponential growing cells carrying the Topo III-YFP fusion were exposed to 50 ng/ml of MMC for 2 hours. RecU is recruited to the repair centers upon 90 minutes of exposition to MMC (Sanchez et al., 2005), so if Topo III is acting also at late stages of DNA recombination, a similar behaviour could be expected. After induction with 50 ng/ml MMC (time zero), aliquots from the culture were taken after 1 and 2 hours (fig. 30). Topo III-YFP pattern slightly changed after 1 and 2 hours of induction of damage, so that cells were showing fluorescence all over the cell, that was slightly brighter than the one that is seen at time zero, when the effect of MMC is still not visible (fig. 30, green triangles).

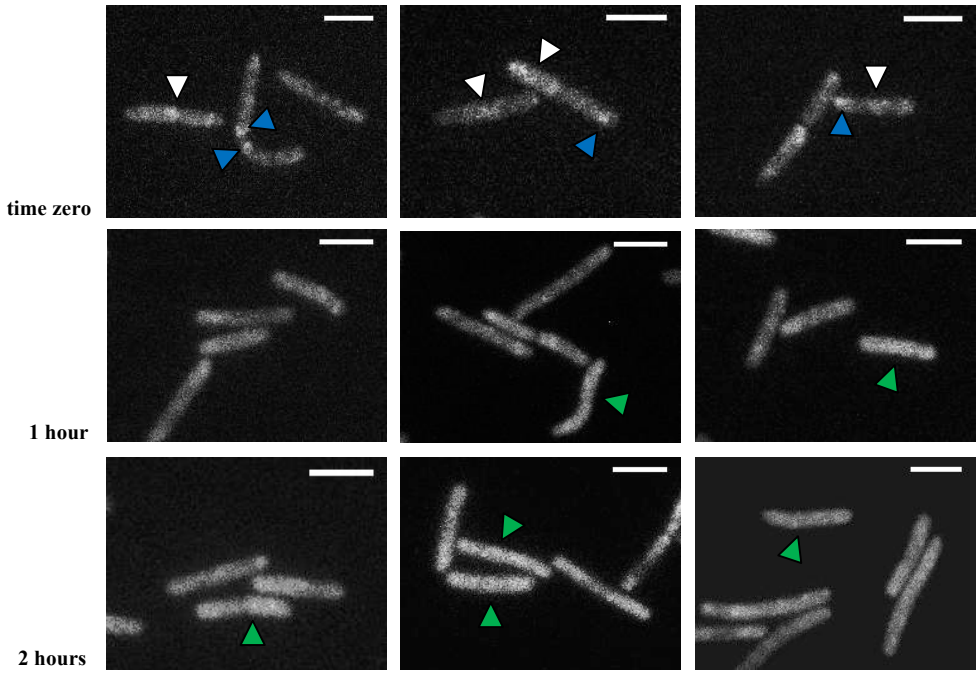

Figure 30: Effect of addition of 50 ng/ml MMC on the localization of TopoIII-YFP. Strain TopoIII-YFP was grown in minimal medium S750 at 30ºC until exponential phase (0.4 O.D.). At this moment, 50 ng/ml MMC was added. Samples were taken at different times, mounted on agarose slides and visualized under fluorescence microscopy. White triangles show TopoIII-YFP cytosolic localization. Blue triangles point to TopoIII-YFP polar localization. Green triangles show cells with TopoIII-YFP fluorescence homogenously distributed. White bar: 2 μm.

4. Characterization of Topoisomerase III

4.1 Purification and native state of *B.subtilis* TopoIII

B.subtilis Topo III, carrying a his-tag in the C-terminus, was purified from a soluble fraction of an *E.coli* cell extract bearing plasmid pTOPhis to near homogeneity (95%). After the purification protocol, a homogeneous protein of 80 Kda was observed under SDS-PAGE (fig.31B), that corresponded to the expected molecular weight deduced from the protein sequence. As it was the first time that this enzyme was purified, Topo III was subjected to gel filtration by FPLC to determine the oligomerization state. Using a Superdex 12 10/300 GL, 0.14 mg of soluble Topo III in 250 µl of a buffer containing 100 mM NaCl were injected to the column. The protein eluted in a volume that correspond to the size of a monomer of around 80 KDa (fig.31A). Topo III from *B.subtilis* is a monomer in solution, as well as its counterpart in *E.coli* (Mondragon and DiGate, 1999).

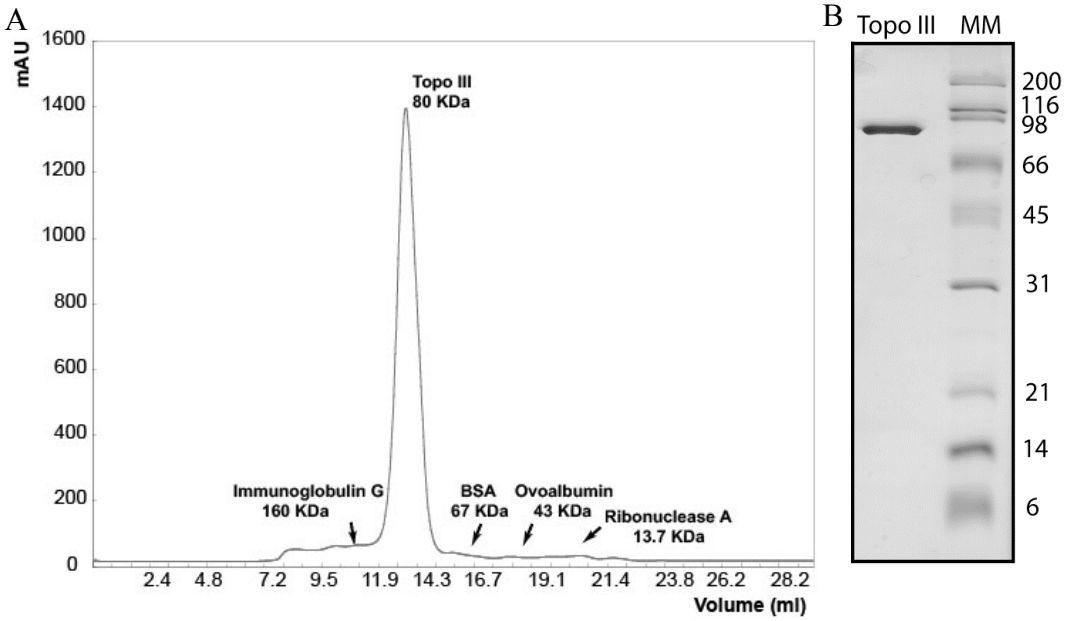

Figure 31: Determination of the Topo III native state by gel filtration chromatography. **A:** Superose 12 10/300 GL column was used and the chromatography was carried out in buffer 50 mM Tris-HCL, 100 mM NaCl and 5% glyzerol, at a flow rate of 0.3 ml/min. Around 0.14 mg of pure Topo III in a final volume of 25 µl were injected to the column and the O.D. at 280 nm was measured. Peak shows a major protein detected at the expected volume of a monomer of 80 KDa, between 11 and 14 ml. The determined elution volumes for different proteins are shown with arrows **B:** 15% SDS-PAGE showing 1.5 µg of pure Topo III obtained after purification protocol.

4.2 DNA Relaxation activity of TopoIII

Type IA topoisomerases are able to relax negatively supercoiled DNA. It was published that the homolog of *B.cereus* Topo IIIβ is able to partially relax a supercoiled plasmid, with a pH of 10 and at 52ºC (Li et al., 2006). As stated before, *B.subtilis* TopoIII shows 64% of sequence identity with *B.cereus* Topo IIIβ. To prove that Topo III from *B.subtilis* is a bona-fide topoisomerase, a superhelical DNA relaxation assay was performed. The same conditions that were used for *B.cereus* were assayed here.

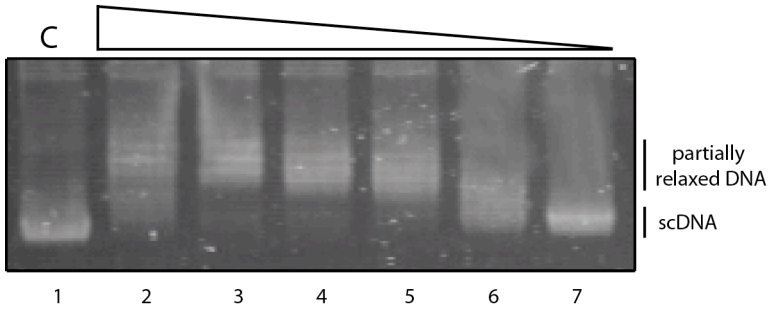

Figure 32: Topo III is able to partially relax supercoiled DNA. Superhelical DNA pUC18 (5 nM) was incubated at 52ºC for 10 minutes with increasing amounts of Topo III with buffer A. Lane 1: control without protein. Lanes 2-7: decreasing amounts of Topo III (80, 40, 20, 10, 5 and 2.5 nM). Reactions were deproteinized by incubating with 2% SDS, 30 mM EDTA and 2 mg/ml proteinase K at 37ºC for 20 minutes. Samples were run through 1% agarose gels in TBE buffer at 2 V/Cm for 22 hours approximately at room temperature. Topoisomers were visualized by staining with ethidium bromide. scDNA: supercoiled DNA.

Topo III is able to partially relax a supercoiled DNA (fig.32), showing its maximum activity at 40 nM (fig.32, lane 3).
When the relaxation reaction is performed at 37ºC or in pH 7.5, the protein is not able to modify the DNA (data not shown). These characteristic features are shared with its homolog in *B.cereus* Topo IIIβ, as well as the fact that both are only able to relax partially the DNA (Li et al., 2006). The homolog in *E.coli*, Topo III, also shows an optimum activity at 52ºC and it is relaxing DNA in a highly efficient way (DiGate and Marians, 1988). These results confirm that the his-tag used for the purification of the protein is not affecting the activity.
It is known that *B.subtilis* Topo III and *B.cereus* Topo IIIβ sequences contain at least two putative zinc finger domains in the C-terminal (Li et al., 2006). For this reason, a superhelical relaxation assay was also performed in the presence of 25 μM $ZnCl_2$, showing no difference in the relaxation pattern (data not shown).

In *E.coli*, Topo III and SSB physically interact (Suski and Marians, 2008). To learn about the possible interaction between these two proteins in *B.subtilis*, *in vitro* crosslink using DSS was performed (fig.33). The experiment was revealed by western blot with antibodies anti-G36P (fig. 33A), a *B. subtilis* SPP1-phage homolog of SsbA, that cross react with SsbA, or with anti-his (fig.33B), that recognize Topo III

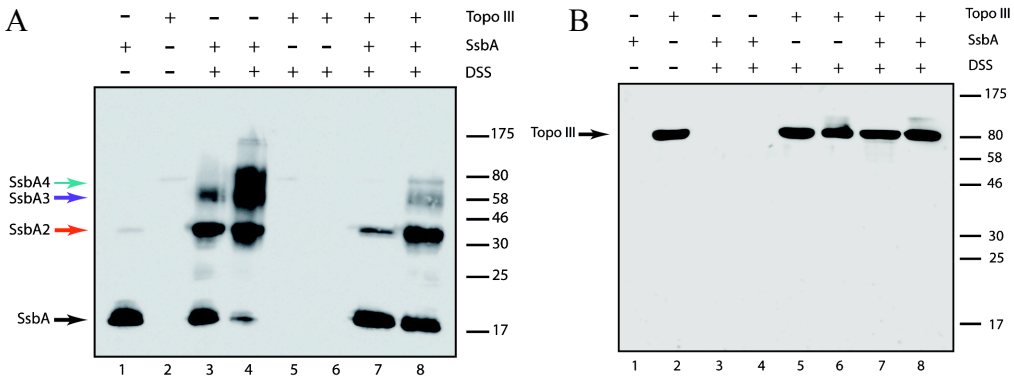

Figure 33: *In vitro* crosslink of SsbA and Topo III. SsbA (0.25 μM in tetramer) and Topo III (0.25 μM in monomer) were incubated in a buffer containing 50 mM Na-P pH 7.5, 50 mM NaCl, 1 mM $MgCl_2$. After 10 minutes of preincubation at 37ºC, DSS (0.1 or 0.5 mM) was added to the samples and put at 37ºC for an additional 15 minutes. SDS loading buffer was added and samples run in a 12 % SDS-PAGE, followed by western blot with revealed with antibodies anti-G36P (A) or anti-his (B). **A:** Lane 1: SsbA control without DSS. Lane 2: Topo III control without DSS. Lane 3: SsbA with 0.1 mM DSS. Lane 4: SsbA with 0.5 mM DSS. Lane 5: Topo III with 0.1 mM DSS. Lane 6: Topo III with 0.5 mM DSS. Lane 7: SsbA and Topo III in relation 1:1 with 0.1 mM DSS. Lane 8: SsbA and Topo III in relation 1:1 with 0.5 mM DSS. In the left part of the figure, arrows indicate the position of SsbA monomer (SsbA, black arrow), SsbA dimers (SsbA2, red arrow), possible SsbA trimers (SsbA3, purple arrow) and SsbA tetramer (SsbA4, green arrow). **B:** Lane 1: SsbA control without DSS. Lane 2: SsbA with 0.1 mM DSS. Lane 3: SsbA with 0.5 mM DSS. Lane 4: Topo III control without DSS. Lane 5: Topo III with 0.1 mM DSS. Lane 6: Topo III with 0.5 mM DSS. Lane 7: SsbA and Topo III in relation 1:1 with 0.1 mM DSS. Lane 8: SsbA and Topo III in relation 1:1 with 0.5 mM DSS. In the right part of each figure, lines indicate the running positions of molecular weight marker in Kda.

In the presence of DSS, dimers, trimers and tetramers of SsbA can be detected (fig. 33, red, purple and blue arrow). In the presence of Topo III, SsbA forms the same oligomers as in the absence, but there is a decrease in the formation of trimers and tetramers (fig.33, compare lanes 3,4 with 7,8). Under the conditions tested, no interaction could be detected for SsbA and Topo III. The same experiment performed with antibodies anti-his did not detect any further interaction (fig. 33B).

4.3 Binding to DNA

In this work, it has been shown genetic evidence for a role of *B.subtilis* Topo III in DNA repair mediated by recombination, and that Topo III could act as an alternative pathway for HJ resolution. Therefore, the ability of the enzyme to bind different DNA substrates representing different recombination intermediates was tested. As shown in figure 34, Topo III is able to bind to different substrates: four way junction or HJ, consisting of a cruciform structure resembling the main intermediate in DNA recombination; 3-branched structure, which resembles a D-loop, and flayed substrate, that mimics an unreplicated fork. Topo III forms stable complexes with the three γ-^{32}P 5´-labelled recombination intermediates (fig.34), in the presence of 1 mM $MgCl_2$.
Apparent binding constants are in the range of 14-23 nM (table 17). In the presence of 1mM EDTA, Topo III shows a decay in binding affinity for the HJ, 3-branched and flayed DNA substrate (table 17). In the case of binding to the HJ, there is a 6-fold reduction for the binding in the presence of EDTA. In all three cases of binding, TopoIII-DNA complexes were high molecular species that could not be able to enter into the gel (fig.34). Treatment of these complexes with different amounts of detergent did not solubilise these complexes (data not shown).

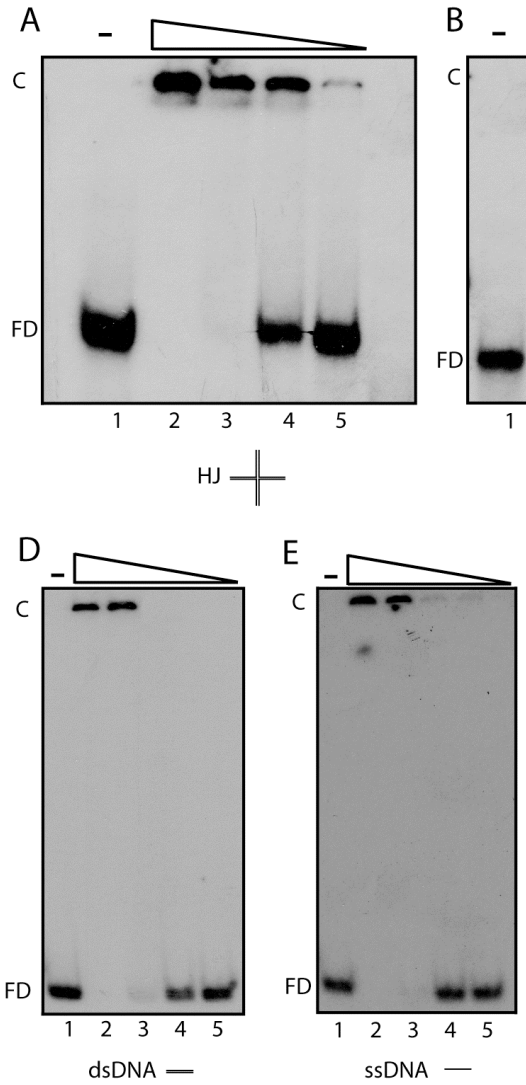

Kapp in 1mM $MgCl_2$ (in nM)		Kapp in 1mM EDTA (in nM)	
HJ	14.5	HJ	86.6
3-branched	13.7	3-branched	46.6
flayed	23.3	flayed	88.6
dsDNA	82.3	dsDNA	270
ssDNA	81.6	ssDNA	270

Table 17: Apparent binding constants of TopoIII to different DNAs

Figure 34: Topo III binding specificity. The indicated substrated labeled at the 5´end were incubated with increasing amounts of Topo III (range of 6-240 nM) in buffer B in a final volume of 20 µl. Reactions were incubated at 37ºC for 15 minutes. Loading buffer was added to the samples. Formation of protein-DNA complexes was analyzed in non-denaturing PAGE 6% in buffer TAE 1X. Gels were dried and revealed by autoradiography. **Table 17** shows apparent constant of binding for each substrate. The values obtained are an average of at least 3 independent experiments. In panels A, B and C, Topo III concentration is as follows: 60 (lane 2), 30 (lane 3), 15 (lane 4) and 7.5 nM (lane 5). In panels D and E, Topo III concentration is: 240 (lane 2), 120 (lane 3), 60 (lane 4) and 30 nM (lane 5). Lane 1 from every gel is control free DNA (FD). Complexes formed are termed by C in every gel.

To define if Topo III preferentially binds recombination intermediates, binding to ssDNA (poly-dT of 40 nt) and dsDNA (60 nt) was compared. The substrate poly-dT is a bona-fide ssDNA oligonucleotide that does not form any secondary internal structure. Binding of Topo III to ssDNA and dsDNA showed a 6-fold decay in binding specificity when compared to the HJ (table 17).
Unexpectedly, *B.subtilis* Topo III is binding to ssDNA in a similar way than to dsDNA (table 17). In both cases, protein-DNA complexes are very similar and their high molecular weight does not allow them to enter into the gel (fig.34).

Comparison of the apparent binding constants obtained with the different recombination intermediates and with ssDNA and dsDNA suggests that Topo III is binding at least 6-fold more efficiently to these recombination intermediates.

4.4 Resolution of the Holliday Junction

One main intermediate of DNA homologous recombination is the Holliday Junction (HJ, fig.9). This intermediate appears when a DSB is formed, which can be repaired by homologous recombination. The HJ is processed by the helicase complex RuvAB and by the resolvase RecU. *B.subtilis* RecU is the homolog for *E.coli* RuvC resolvase, and it has been shown to be able to symmetrically cleave the HJ DNA in the presence of 10 mM $MgCl_2$ (Ayora et al., 2004). Some homologs of *B.subtilis* Topo III are able to cleave recombination intermediates: in *Drosophila*, Topo IIIβ cleaves plasmids carrying a synthetic D-loop (Wilson-Sali and Hsieh, 2002). In eukaryotes, the couple helicase BLM-Topo IIIα can dissolve a double Holliday Junction (Wu and Hickson, 2003). With all these antecedents, and taking into account the specific preference of Topo III for the HJ (table 17), Topo III mediated HJ-cleavage was performed in the presence of 10 mM $MgCl_2$ (fig.35). As a control, bona-fide *B.subtilis* RecU resolvase was used. Each strand of the HJ was labelled for trying to find a cleavage pattern for Topo III. Topo III is not able to cleave the HJ alone in any of the strands (fig.35 lanes 2, 4, 6 and 8), as it is the case of RecU (fig.35, lane 9), which can cut symmetrically this structure, releasing the labelled oligonucleotide of half size (40 nt). Similar results were obtained in other several conditions, like incubating with 1 mM $MgCl_2$, with less concentration of Topo III, or in the conditions of relaxation activity (1 mM $MgCl_2$, pH 9.8, 52ºC) (data not shown). These results indicate that Topo III might need an accessory protein for developing this function, or that resolution of the HJ cannot be performed by Topo III.

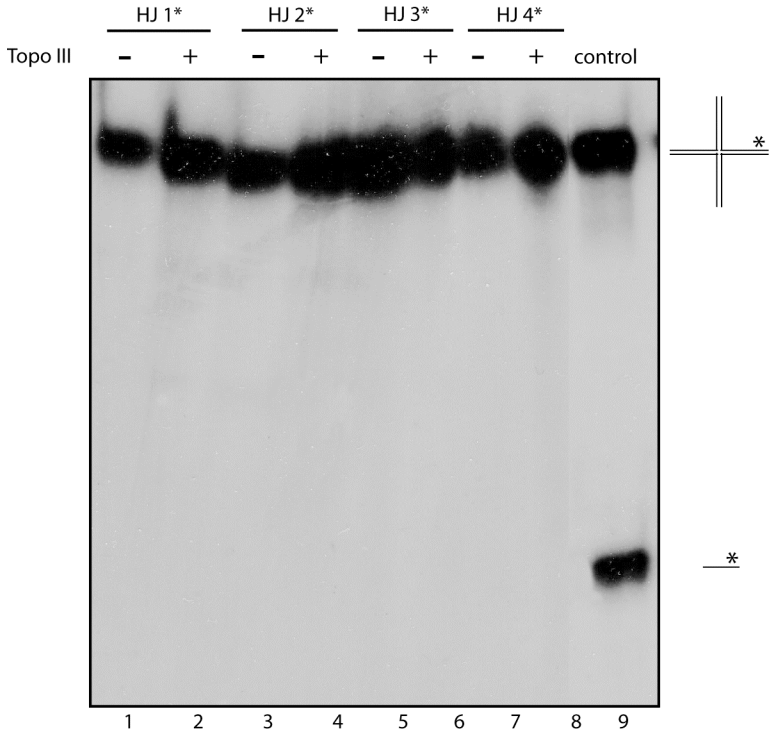

Figure 35: Topo III-mediated cleavage of the HJ. Holliday Junction J3 structure labeled in one arm at the 5´end using [γ^{32}P]-ATP was incubated with 400 nM of Topo III in buffer C in a final volume of 10 µl at 37ºC for 15 minutes. An equal volume of loading buffer containing 90% formamide and 25 mM EDTA was added to the samples and incubated at 95ºC for 5 minutes. Samples were immediately stored on ice and loaded into a 15% PAGE denaturing gel containing 7.6 M urea. Gel was revealed by autoradiography. As a cleavage control, *B.subtilis* resolvase RecU (100 nM) was incubated with HJ labeled in oligonucleotide J3.4 in buffer C in a final volume of 10 µl at 37ºC for 10 minutes. Drawings indicate the substrate (HJ structure) and the resultant product cleavage (ssDNA) labeled in one of the strands.

4.5 TopoIII-mediated D-loop cleavage

The structure so called "D-loop" resembles a synapsis recombination intermediate, in which one of the dsDNA molecules is invaded by one strand of another DNA molecule, to initiate recombination. *In vivo* results obtained in the transformation assays showed that Topo III may act on these three-stranded DNA recombination intermediates (part 3.2 of results). Moreover, the binding analysis were showing also a preference in binding for the three-stranded recombination intermediate and the flayed DNA, that both represent a part of the D-loop structure. For all these reasons, the ability of TopoIII to cleave D-loops and other recombination intermediates resembling a D-loop was studied. These D-loop derivatives are formed when the invading DNA molecule shows one of the ends processed to ssDNA, having the other end as dsDNA (recessed D-loop, denoted as RC-Dloop in figure 36) or when replication has already started in the D-loop (replicated D-loop or r-Dloop). As a control, a HJ based on these substrates was also used, as well as the ssDNA oligonucleotide alone.
The substrates were constructed by annealing the different oligonucleotides as described in material and methods and further used without purification. The cleavage reaction was carried out at pH 9.8, in which Topo III shows its relaxase activity. When oligonucleotide 19M is labelled

(invading strand), Topo III shows two cleavage sites in a ssDNA molecule (fig. 36A, lane 10, products P1 and P2), being P2 the preferential cut. Topo III slightly cleaves all the substrates at P1, except in the D-loop (fig.36A, lanes 2, 4, 6, 8 and 10),but since this cleavage site is also seen in the reaction control where only the labelled oligo 19M is detected, it is supposed that the cleavages observed would correspond to cleavage of parts of the structure that have been disassembled or not properly annealed, so that the cleavage is on ssDNA but not on dsDNA. The same can be attributed in cleave at position P2, but here there is a strong product P2 when the D-loop structure is incubated with TopoIII (fig.36A, lane 8). The cleavage product P2 is also the most efficient when compared to the intensities of other cleavage products with the other structures (fig. 36A, compare lanes 2, 4, 6 and 10 with 8).
When oligonucleotide 17M is labelled (displaced strand), Topo III is only cleaving when this oligo is ssDNA, showing no cleavage products in HJ or r-Dloop (fig. 36B, lanes 2 and 6). The cleavage in ssDNA is used as a control (fig.36B, lane 10), showing that Topo III is clearly making different cleavages in the D-loop and RC-Dloop structures, because when oligo 17 is just as ssDNA (fig.36B, control lanes 9 and 10) other products are observed. When TopoIII is incubated with the RC-Dloop and D-loop structures, which have this part of the oligo as ssDNA but clearly forming part of a D-loop, three major products P3, P4 and P5 are observed (fig.36B, lanes 4 and 8).

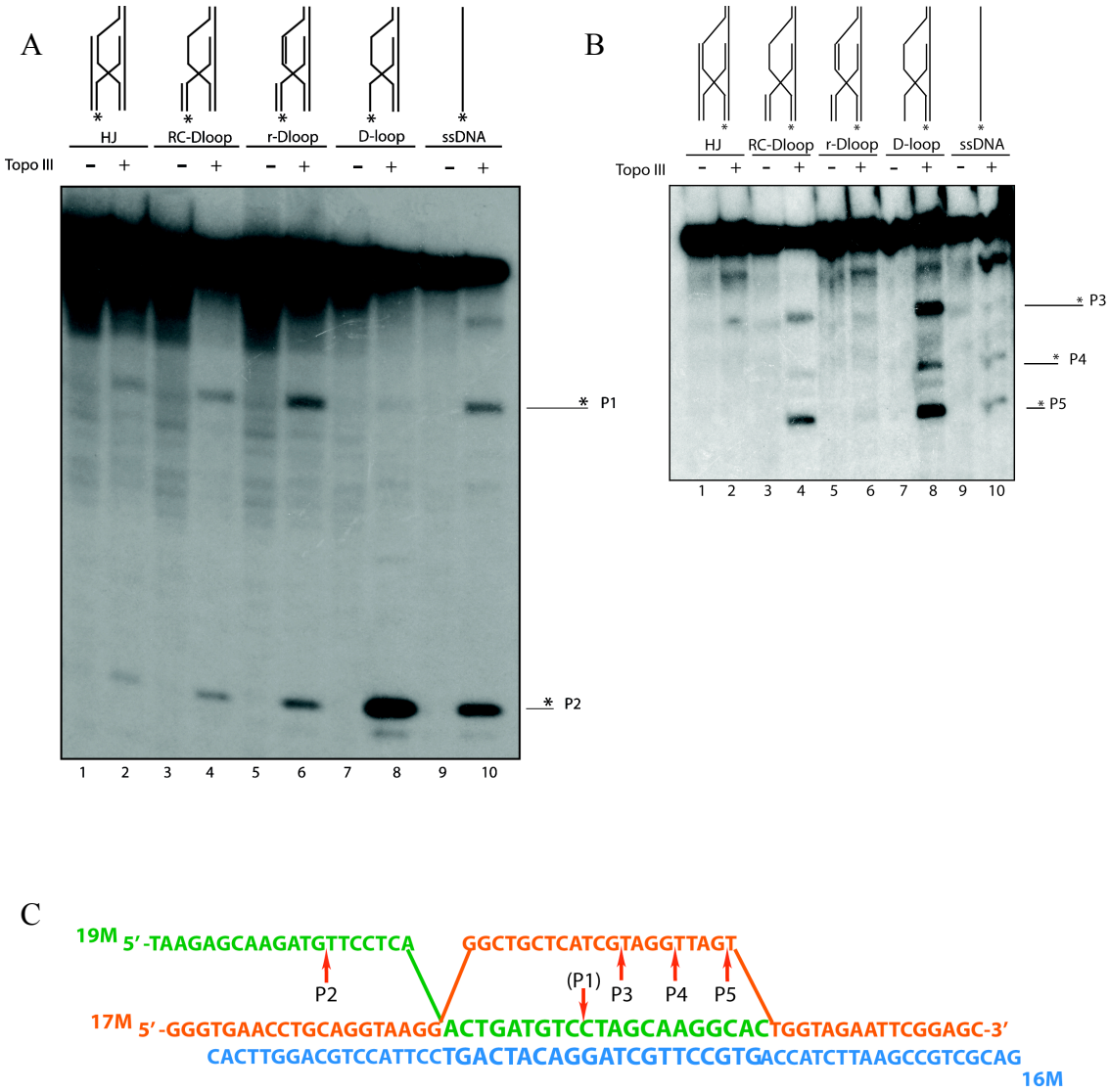

Figure 36: Topo III-mediated cleavage of the D-loop intermediate. Different constructions resembling synapsis intermediates labeled in one arm at the 5´end of oligonucleotide 19, that is the invading strand (**A**) or 17 oligonucleotide, the displaced strand (**B**) using [γ^{32}P]-ATP were incubated with 90 nM of Topo III in buffer F in a final volume of 10 µl at 37ºC for 30 minutes. An equal volume of loading buffer containing 90% formamide and 25 mM EDTA was added to the samples and incubated at 95ºC for 5 minutes. Samples were immediately stored on ice and loaded into a 15% PAGE denaturing gel containing 7.6 M urea. Gel was revealed by autoradiography. Asterisk indicates the [γ^{32}P]-ATP labeling of oligos in the 5´end. Drawings indicate the different substrates labeled in one of the oligos and the principal cleavage products, P1 and P2 (in A) or P3, P4 and P5 (in B) are highlighted. **C**: schematic representation of the cleavage sites of Topo III. Each oligonucleotide shows a different color. Oligo 19M (green) is the invading strand of the D-loop that is formed when it is invading the other DNA molecule and displacing one of the strands (oligo 17M, orange). When invading strand is labeled (A), there is one major cleavage site P2, detected in the reactions were TopoIII is incubated with the d-loop while when displacing strand is labeled (B), three major products are formed, P3, P4 and P5, not detected in the controls (HJ, RC-Dloop or ssDNA), all of them represented as red arrows.

DISCUSSION

1. *In vivo* role of *B.subtilis* LrpC

1.1 Implications in global gene expression: LrpC as a local transcriptional regulator

Some member of the Lrp/AsnC family, to which *B.subtilis* LrpC belongs, have been shown to respond to nutritional changes in the environment, as *E.coli* Lrp, that controls the transition from feast (optimal nutritional conditions) to famine (starvation conditions) (Calvo and Matthews, 1994). LrpC belongs to this family due to the resemblance of its structure to the rest of members of the family. Till now, only *E.coli* Lrp has been proved to be a global regulator (reviewed in Kawashima et al., 2008). In *Haemophilus influenzae* the Lrp-like protein LrfB has been shown to be a local transcriptional regulator, even though it shares 75% of sequence identity with *E.coli* Lrp (Friedberg et al., 2001). In this work, the authors show that even sharing this high homology with *E.coli* Lrp, LrfB does not show a global regulatory role. LrfB is present in a low amount in the cell, which suggests a local regulatory role. In the case of *B.subtilis* LrpC, it shares 34% of sequence identity with *E.coli* Lrp. In order to observe if *B.subtilis* LrpC could be or not a global regulator, first a quantification of LrpC amount in the cell was performed (fig. 13). Experimental data show that LrpC levels increase at the end of exponential phase, while the cell enters in starvation conditions, showing a maximum level of 1300 octamers/cell (fig.13). When these conditions are exacerbated (early stationary phase) LrpC shows a 4-fold decay, which is slightly recovered in late stationary phase (fig. 13). A explanation for this fluctuation is that LrpC is somehow specifically needed at the end of exponential phase (when the amount of protein reaches its maximum). It could be that LrpC has a specific role during this stage of growth. In *B.subtilis*, at an O.D of 0.8 in minimal medium, LrpC shows around 1300 octamers/cell, which is almost the double amount when compared to *E.coli* Lrp, that shows around 750 octamers/cell in minimal medium at 0.9 O.D (Willins et al., 1991). The fact that LrpC is so abundant during this moment of growth favours the idea that LrpC could be a global regulator in *B.subtilis*.

E.coli Lrp has been studied deeply and it is known to be a bona-fide transcriptional regulator of around 10% of the genome, and its binding to DNA is modulated by leucine (Cho et al., 2008; Tani et al., 2002). LrpC and its homolog in *E.coli* share a general overall structure of an octamer. They are both DNA bending proteins (Tapias et al., 2000; Wang and Calvo, 1993). Nevertheless, the effector binding pocket that is conformed in the C-terminus, located in the interior of the protein in the overall structure is not big enough to place any effector aminoacid in the case of LrpC, while in the case of Lrp the binding to leucine is possible. Taken into account these previous data, microarray experiments in LB medium were performed in the case of LrpC (tables 8-11). The number of genes whose expression is modulated by LrpC is very low, confirming that LrpC is not a global regulator in *B.subtilis*. In a closer look to the genes downregulated by LrpC at the end of exponential phase, most of them are implicated in general metabolism (table 8). Among these genes are *purH*, *purL* and *purS*, part of the purine biosynthesis operon and *mtlA* and *mtlD*, implicated in mannitol metabolism. In these microarrays experiments it was also found that genes *ilvB* and *ilvD*, part of the *ilvH* operon, are downregulated by LrpC. Interestingly, it was found that LrpC is downregulating KipI, the inhibitor of KinA. KinA is the major sense kinase of sporulation (Burbulys et al., 1991). In conditions of nutrient deprivation, a still unknown extracellular signal triggers the autophosphorilation of KinA (Lee et al., 2008). This activates a cascade of phosphorilated proteins that in the end will activate Spo0A, the master transcriptional regulator of sporulation (Hoch, 1993). The fact that LrpC is somehow indirectly influencing the entrance in sporulation by regulating KipI is in accordance with the previous observations that a null mutant *lrpC* enters earlier in sporulation (Beloin et al., 1997).

Among the genes upregulated by LrpC at the end of exponential phase is its own gene *lrpC* (table 9). This confirms that LrpC is autoregulating its own gene in a weak positive manner, what was proved before by the *lrpC-lacZ* transcriptional fusion (Beloin et al., 2000). In stationary phase it was found that LrpC regulates genes implicated in metabolism as well (tables 10 and 11). The activation of gene *topB*, which is under the same promoter and downstream of the *lrpC* gene could not be detected, due to the fact that microarrays were performed in a null mutant *lrpC* strain. This strain was obtained by replacement of the *lrpC* gene by the Cm cassette, which has its own promoter. Therefor, *topB* gene is not under the control of *lrpC* promoter anymore, so the presence or absence of LrpC protein is not influencing its regulation.

Most of the genes regulated by LrpC are metabolic genes, which opens the question if this protein acts as a local regulator acting as a specific activator/repressor of just some genes. Up to now, in *B.subtilis* two global regulators have been described: CodY and AbrB. CodY is a global regulator that responds to aminoacid availability (Molle et al., 2003) that acts as a transcriptional repressor in response to high cellular levels of GTP (Ratnayake-Lecamwasam et al., 2001). When GTP levels decrease, occurring in the transition from exponential to stationary phase, CodY loses its repression activity, allowing transcription of its target genes. CodY is able to perform its function by direct interaction with branched-chain amino acids. This type of aminoacid increases the affinity of CodY for the promoters of the target genes tested (Shivers and Sonenshein, 2004).
AbrB is considered a transition-state regulator that controls more than 100 genes (Chumsakul et al.; Strauch, 1993). Genes controlled by this regulator comprise a variety of metabolic and physiological processes. AbrB has been show to be one of the regulators of many genes implicated in the onset of sporulation (Strauch et al., 1990). AbrB is also responsible for controlling the cellular decision to develop sporulation or competence in stress conditions (Hahn et al., 1995). In *B.subtilis* there are 6 homologs of LrpC and none of them have been described as global regulators (see Introduction, part 1.1). Probably in Gram-positives, or at least in Firmicutes, global regulators are other family of proteins distinct than this one.

Previous studies also show that LrpC is quite different from the rest of the other characterized members of Lrp/AsnC family. LrpC activity is not influenced by the presence of leucine (Beloin et al., 2000; Tapias et al., 2000). As a DNA bending and DNA annealing protein, it may has a role in DNA recombination (Lopez-Torrejon et al., 2006), but not in global gene transcription (present Thesis). Results obtained in this Thesis suggest a local regulatory role for LrpC, as it is the case for the Lrp-like LrfB of *H.influenzae* (Friedberg et al., 2001), even though it shows a high abundance in the cell.

1.2 Role in vegetative growth: LrpC as a indicator of changing in cellular processes

Discarding the role of LrpC in global gene expression, the *in vivo* localization of GFP-LrpC during vegetative role was addressed, in order to obtain a hint of the possible role proposed as an architectural protein in the cell (figs. 15 and 16). However, in contrast to well known architectural proteins as Hbsu, LrpC is not just decorating the full nucleoid (Kohler and Marahiel, 1997). But during exponential phase, LrpC is mainly visible as two symmetric foci located in the borders of the nucleoid, and in very low amount of cells as one single focus or forming aggregates coincident with the nucleoid (table 12). Remarkably, LrpC foci are mainly located at the borders of the nucleoid (fig. 15 and 16). The origins of replication are located as well in the borders of the nucleoid (Glaser et al., 1997; Lin et al., 1997), and also SMC shows this distinct pattern (Britton et al., 1998). During stationary phase, when replication is not active, the percentage of cells showing

two foci per nucleoid is lowered (figure 16, table 12). 32.5% of total cells are showing one foci close to the cell pole, what opens the question of another role for LrpC at the pole.
LrpC could act as an architectural protein as SMC, due to several reasons: a) the localization pattern in vegetative growth during exponential phase is similar to that of SMC (Britton et al., 1998), b) LrpC is able to do wrapping onto a DNA molecule *in vitro* by constraining a DNA molecule to compact it (Tapias et al., 2000) and SMC is able to compact the nucleoid (Britton et al., 1998) and c) the null mutant *lrpC* shows an increased lag-phase in vegetative growth (Beloin et al., 1997), which could mean that in the absence of this protein DNA replication needs to reorganize before starting.
Architectural proteins as SMC have been proposed to have a role in DNA replication. It was recently showed that SMC could be recruited to the origins of replication in *B.subtilis* (Gruber and Errington, 2009) . In this model, SMC would be recruited to a large region around the origin of replication. Segregation protein Spo0J is required for this recruitment. At the same time that Spo0J is recruiting SMC, it is also responsible for the dimerization of Soj protein. Soj is a ParA-homolog that is implicated in initiation of sporulation (Ireton et al., 1994) and chromosome segregation (Lin and Grossman, 1998). In the dimeric conformation, Soj is able to activate DnaA, which will lately bind to *oriC* and start replication. Due to the specific localization of LrpC during exponential phase, similar to SMC, and taking into account that both are architectural proteins, it would be possible that LrpC could act together with SMC. LrpC is able to perform DNA bending and condense the DNA (Tapias et al., 2000). It also cooperates with Hbsu in the bending of DNA (Tapias et al., 2000), so one possibility could be that by bending the DNA at the origin of replication, LrpC could recruit or work together with SMC in the same way it has been shown *in vitro* with Hbsu. Data obtained in the present Thesis suggest that LrpC does not interact with SMC: localization of SMC-YFP does not change in the absence of LrpC, and bimolecular fluorescence microscopy revealed no fluorescent signal (data not shown).

Focussing on the *in vivo* microscopy, LrpC is very often placed in the borders of the nucleoid in a high percentage of cells, in different moments of growth and media conditions (fig. 15, 16 and 18). This special pattern is not only observed for proteins associated with the origin of replication (as SMC), but also for the so called “transcription foci” (TFs), located generally in the borders of the nucleoid, but still inside the bulk of DNA (fig.37). These TFs reflect the cellular localization of RNAP in *B.subtlis* (Lewis et al., 2000). TFs show 2 foci per nucleoid in minimal medium and 4 per nucleoid in rich medium, where transcription is more active (Lewis et al., 2000), while LrpC foci are always 2 per nucleoid in minimal medium. This favours once more the idea of LrpC as a local regulator that could perform its function in some of the TFs during vegetative growth. During exponential phase, when transcription is active, there is stable RNA synthesis, RNAP is recruited to the TFs, the nucleoid is condensed and at the border of the nucleoids DNA loops are formed that interact each other (fig.38, down part, green dots). In stationary phase, when there is no active transcription, RNAP is dispersed through the nucleoid, which is decondensed (fig. 38, upper part) (Jin and Cabrera, 2006). LrpC is forming foci at the borders of the nucleoid during active transcription (exponential phase, fig. 15), so in these places it could bind curved DNA. Preferential binding to curved DNA has been demonstrated *in vitro* (Lopez-Torrejon et al., 2006; Tapias et al., 2000). It has also been shown that LrpC is able to do bridging between DNA molecules, what would explain the presence in the DNA loops, favouring them to interact (Lopez-Torrejon et al., 2006). During stationary phase, when transcription is not active anymore and DNA loops are fewer, LrpC starts to be recruited closer to the cell poles (fig.16 and 18), or through the entire nucleoid (fig.20). At low cellular growth rate in a starvation medium, as competence medium, DNA is decondensed and it shows fewer loop domains (Jin and Cabrera, 2006). If DNA looses its curvature and there are fewer loops, it makes sense that LrpC would be dispersed through the nucleoid, that is in fact what is visible (fig.20).

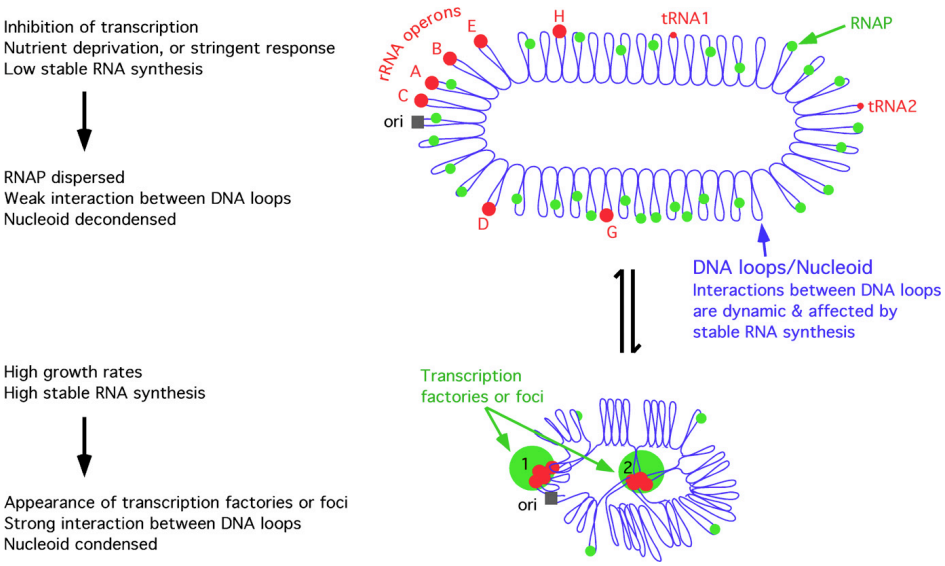

Figure 37: Model linking stable RNA synthesis, RNAP distribution and the dynamic structure of the nucleoid in *E.coli*. The *E. coli* chromosome is represented as blue lines folded in loops, the *ori* of replication as a black square, the seven rRNA operons as large red circles with letters, and two representative tRNA operons as small red circles. The RNAP molecules are represented as small green circles. For simplicity, only two putative transcription factories/foci, which make the nucleoid more compact by pulling divergent stable RNA operons into proximity, are indicated here (bottom part of the diagram, large green circleslabeled 1 and 2. Figure adapted from Jin and Cabrera 2006.

GFP-LrpC forms aggregates, which are coincident with the nucleoid (fig.15, table 12). The number of cells showing this pattern is 7% in exponential phase, in contrast to 55% of total cells that show discrete LrpC foci (fig.15). This pattern has also been shown for a bona-fide architectural protein in *B.subtilis* Hbsu, though this protein shows this localization pattern in almost every cell (Kohler and Marahiel, 1997). LrpC could be an architectural protein, but acting only locally in the DNA and not in a global manner as Hbsu. The total amount of Hbsu in the cell during vegetative growth is much higher than that of LrpC. In minimal medium at 37ºC and 0.9 O.D, there are 25000 dimers/cell of Hbsu (Ross and Setlow, 2000), while in the very same conditions the amount of LrpC is 5200 dimers/cell (1300 octamers/cell, fig. 13). This high difference confirms that Hbsu is the main architectural protein and that LrpC could be performing this function only at certain parts of the genome, which is also enforced by that fact that LrpC localizes as distinct foci (fig. 15 and 16) while Hbsu decorates the nucleoid (Kohler and Marahiel, 1997). In *E.coli*, architectural proteins show two distinct patterns. The major architectural proteins (HU, H-NS) are distributed uniformly within the entire nucleoid, while the ones that have a regulatory role (SeqA, Fis) localize in the DNA, but forming foci (Azam et al., 2000). All these findings reinforce the idea of LrpC, by binding at the curved regions of the borders of the nucleoid, could act as a local transcriptional regulator.

The implication of LrpC in DNA repair was also addressed by treatment with MMC (fig.17, table 13). LrpC is not recruited to the RCs after induction of DNA damage, but the pattern of foci changed from almost 70 % of cells showing foci to only 30%, from which a half of cells was showing one focus per cell and the other half two foci per cell (table 13). Addition of MMC leads to a replication stop to repair the damage, so when replication is not active anymore cells showing LrpC foci decrease extensively. Once more, LrpC shows an alteration of localization pattern due to a change in growing conditions. Under DNA damage by MMC, nucleoid structure is also affected.

It has been shown that the absence of replication proteins in these conditions provokes chromosome breakages that are observed in the absence of some recombination mutants (Grompone et al., 2002). It could be that by MMC treatment the nucleoid structure is disrupted by these breaks and this will cause the loss of LrpC foci.

1.3 New role for LrpC in DNA transformation

As already mentioned, localization of GFP-LrpC in competence medium at time zero (beginning of stationary phase) shows a complete different pattern as the one observed in stationary phase in vegetative growth (compare tables 12 and 14). The percentage of cells showing fluorescence with a tight link to the nucleoid without specific foci is higher (50%) than in normal stationary vegetative growth (1%).
Another pattern of localization is observed in competence, as polar foci with a higher fluorescence intensity than the polar foci observed for vegetative growth in stationary phase (fig. 16). Western blott analysis of the GFP-LrpC fusion showed that the amount of protein in this special competent medium is even lower as the one for LB medium (fig.19), so polar localization of LrpC is not due to an artifact caused by an excess of protein.
One possible explanation for this polar localization of LrpC could be that, as in the end of stationary phase there is no active transcription, so that LrpC could not act as a local regulator, and though could be sent to the cell poles as a storage center. The weak point of this possibility is that, as LrpC is a DNA binding protein, it is striking that LrpC is not localizing in the nucleoid anymore. This is also happening for another DNA binding protein, SMC, which is associated with the chromosome but is also present in discrete foci near the poles of the cell (Graumann et al., 1998).

The other possibility that came out more probable is that LrpC is recruited to the cell poles by an unknown mechanism to perform its function at this place, taking into account its DNA annealing activity. The confirmation of this idea arrived when a time lapse experiment was done (fig. 20). At time zero, and before the cell is competent, half of the population is forming the aggregates that were seen before during vegetative growth (fig. 20, table 14). In competent medium the percentage of cells showing this pattern is higher (50% compared to 7% in exponential phase of vegetative growth). As the cell enters in competent state, GFP-LrpC clearly starts to be recruited at the cell poles (fig.20) pointing to a very specific role in this moment of growth. Formation of GFP-LrpC polar foci is independent on ComK or ComA. Such an independence of ComK has also been observed for some *rec* proteins involved in competence that localize at the cell poles, like RecN (Kidane and Graumann, 2005). As RecN, LrpC could also have a small role and yet undefined in competence in *B.subtilis*. However, the polar localization of other recombination proteins is dependent on the formation of the DNA uptake machinery. In the absence of ComK, GFP-RecA is not able to localize at the cell poles (Kidane and Graumann, 2005). Polar localization of RecO-YFP and RecU-YFP fusions are also ComK-dependent (Kidane et al., 2009)

LrpC polar foci are present in around 10% of total cells (table 14). Taking into account that in the studied genetic background the percentage of cells developing competence is 8-10%, it is reasonable that LrpC could be located near the DNA uptake machinery as well.
The majority of the polar LrpC foci are located at one cell pole (table 14). During competence, DNA uptake machinery in *B.subtilis* is also located mainly at one cell pole. A fusion ComGA-GFP showed the majority of foci located at one cell pole (Hahn et al., 2005). For this reasons, an attempt to colocalize YFP-LrpC and ComGA-CFP was done. The fusion constructed for this purpose, YFP-LrpC resulted to be non functional and did not show any detectable foci (data not shown).

In the absence of this data and taking into account the polar localization, a role in DNA transformation was obtained by analyzing the yield of transformants of a null mutant *lrpC* strain after plasmid or chromosomal transformation, and comparing it with the wildtype strain. Null mutant lrpC shows a half decay of plasmid transformation efficiency (table 16) when compared to the wildtype strain. The loss of LrpC in the cell does not cause a big effect in plasmid transformation, as happens with RecU or RecO, which are also *in vitro* DNA annealing proteins (table 16). Chromosomal transformation in this mutant is almost not affected. In this point, it differs from what is been published for *hbsu4755* partial mutant, that is affected in chromosomal transformation in 30% of the total (Fernandez et al., 1997). However, the double mutant *smf-lrpC* has an additive effect in chromosomal transformation when compared to each single mutant separately (table 16), so at least during this type of transformation, LrpC is acting in an alternative pathway to the one performed by Smf.

During competence, LrpC is not showing a dynamic behavior at the cell pole upon the addition of DNA. GFP-LrpC foci pattern is not changing after the addition of plasmid or chromosomal DNA, when compared to the control without any DNA (see results, part 1.4). On the contrary, upon addition of DNA, RecO is recruited to the cell poles and RecU dissipates from there (Kidane et al., 2009), so probably LrpC function at the pole is different from the one performed by RecO and RecU during competence.

2. The *lrpC-topB* operon: gene expression and protein interaction study. LrpC and TopoIII as indirect interactive partners in DNA transactions.

In the present Thesis it has been demonstrated that LrpC and TopoIII are transcribed under the same promoter (fig. 22). Taking into account that both are DNA binding proteins and that they both change the topology of the DNA, they could help each other or one could somehow influence the other activity. For this purpose, TopoIII-mediated DNA relaxation was performed in the presence of LrpC (fig. 24). Interestingly, LrpC slightly promotes the relaxation activity of TopoIII, showing DNA topoisomers with a higher extent of relaxation than compared to each protein separately. This could mean that LrpC is helping TopoIII to perform its function. It is important to notice that only when TopoIII is preincubated with the substrate, followed by LrpC addition, this increase in relaxation activity is seen. TopoIII needs partially melted DNA (with ssDNA regions) and LrpC bends the DNA, opening it, what can help TopoIII to perform its function. On the other hand, it has been described that LrpC can introduce negative supercoils to a DNA that has been previously relaxed by Topo I, that is from the same family as TopoIII (Tapias et al., 2000) A direct protein-protein interaction via crosslinker assays was also performed (fig. 23). Under the conditions tested, no interaction between these proteins was detected.

3. *In vivo* role of *B.subtilis* TopoIII

In the beginning of this study, it was only known that *B.cereus topB* gene is not able to complement his homolog *E.coli topB in vivo* (Li et al., 2006). For starting to analyze of the *in vivo* role of this enzyme, drug survival assays were performed with *B. subtilis*, because the genetics of DNA repair by recombination has been extensively studied in this bacterium using MMS or MMC, both chemical compounds that damage the DNA. This damage can be repaired by homologous recombination processes, so it was used as a first approach to study the role of *topB* in DNA recombination.

Under DNA damage caused by MMS, the lack of *topB* gene did not cause any visible change in phenotype when compared to the wildtype strain under the conditions tested (fig. 25). This does not mean that *topB* is not implied in DNA recombination, because other bona-fide recombination genes as *recJ* do not show a high change in cell viability when compared to the wildtype strain (fig. 25A). In fact, double mutants of *topB* with nucleases *addAB* and *recJ* are more resistant to MMS damage than single mutations *addAB* and *recJ* and double mutants of *topB* with the *recFOR* pathway also show a higher resistance to MMS than the single mutants separately. In the last case, the evidence is higher at 30 minutes of exposure to MMS (fig. 25B), when the viability of double mutants is ten times higher. This behaviour of mutants *addABtopB*, *recFtopB* and *recOtopB* is also confirmed after damage by H_2O_2 (fig. 27A and B). Taking all these data together, it seems that *topB* could have an antirecombinase behaviour. Presynaptic proteins AddAB, RecJ and RecFOR work in concert and help RecA to act. When these proteins are not present, RecA is may not able to perform its function, if TopoIII is somehow causing a toxic intermediate or destroying some substrate, so that when TopoIII is also not present, double mutants are more resistant to DNA damage. Biochemical data obtained from this Thesis also support this idea, because TopoIII is able to cleave the D-loop that is formed during synapsis (fig.36).

Double mutant *recUtopB* is the only one that shows a synergic effect: its drug sensitivity is higher than the one of each single mutant separately, though this is only evident after damage by MMS (fig. 25E). This synergic effect has been also observed in *E.coli*. In this bacterium, *recU* homolog is *ruvC*. Double mutant *ruvCtopB* has been shown to be 10-fold more sensitive to UV light than single mutant *ruvC* (Lopez et al., 2005). In the case of *B.subtilis*, the synergic effect is slight under MMS killing action, but is more evident when microscopy analysis of nucleoids is performed. Double mutant *recUtopB* shows almost 3 times more cells with typical nucleoid morphology associated to a defect in DNA segregation or recombination, when compared to single mutant *recU* (fig. 26). Together, MMS results and nucleoid morphology analysis point to another role for TopoIII in the last stages of DNA recombination.

Interaction between RecQ-like helicases and topoisomerases has been studied, suggesting a common role in the dissolution of recombination intermediates (see Introduction). In the experiments performed in this Thesis, double mutant *recQtopB* shows the same sensitivity to MMS and H_2O_2 as single mutant *recQ* (fig.25 and 28B). Double mutant *recStopB*, on the contrary, is partially recovering its phenotype in the presence of H_2O_2 (fig.28B), while in MMS it shows the same behaviour as single mutante *recS* (fig.25). These results could mean that TopoIII and RecQ, but not RecS, could be epistatic. If this is true, RecQ and RecS should show the same behavior when these mutations are combined with mutations in other *rec* genes as the ones described before for *topB* mutations. Double mutant *recSrecU*, that is synergic in comparison with single mutant *recU* under MMS damage (Fernandez et al., 1998). Double mutants *addABrecS*, *recFrecS* and *recJrecS* are all more sensitive in comparison with single mutants *addAB*, *recF* and *recJ*, respectively (Sanchez et al., 2006). On the other hand, *recQ* is also more sensitive when combined with mutations *recJ* and *addAB* (Sanchez et al., 2006). Genetic analysis is showing that RecQ, RecS and TopoIII are not located in the same pathway.

In rich medium at 30ºC, RecS localizes in a regular pattern of discrete foci located inside the nucleoid, coincident with the replication fork, and only in the presence of SSB (Costes et al., 2010). RecQ localizes as well in discrete foci in the nucleoid, in a SSB dependent manner, and this foci are colocalizing with the replication factory (Lecointe et al., 2007). In an attempt to shed more light in this aspect, a fluorescent fusion TopoIII-YFP was visualized in the cell (fig. 28). However, localization of TopoIII differs from the one showed for RecQ and RecS. TopoIII is located in the spaces where DNA is not present, and that could be contradictory with the fact that it is a DNA binding protein (see below). Probably, TopoIII is making transient contacts with the DNA in the nucleoid and being released from the substrate rather fast, so that after performing its function it is somehow moved to the cytosol. That could explain why the main fluorescence of the protein is located outside the nucleoid. Taking into account that TopoIII is not the main cellular topoisomerase/relaxase, and that it is a non-essential protein, it would not be surprising to find that it has a small cellular role in DNA transactions. After performing its function, it might be transported to the cell poles for being degraded, what would explain the polar localization pattern.
Another result that suggests that TopoIII could have another role, and at least in some cases perform its activity independently from RecQ or RecS comes from the TopoIII-SSB interaction experiment. We were not able to detect any interaction between them (fig.33). In *E.coli*, it has been show that RecQ and TopoIII work in concert in the resolution of converging replication forks by interacting with SSB (Suski and Marians, 2008). RecQ and RecS are directly interacting with SSB-TAP-tag protein (Costes et al., 2010), while in these proteomics experiments, no TopoIII-SSB interaction could be detected (Costes et al., 2010) and also SSB, RecQ and RecS were not copurifying in a TopoIII-TAP-tag fusion (data not shown). Genetic and microscopy analysis are not favouring a common role for TopoIII with the helicases RecQ or RecS in the cell.

4. Biochemical features of Topoisomerase III

In the present Thesis, Topoisomerase III from *B.subtilis* has been purified and characterized for the first time. As expected from a member of the family of topoisomerases type IA, it is a relaxase (fig.32), though the conditions in which it performs this reaction are quite unique: 52ºC and pH 9.8, as its counterpart in *B.cereus* (Li et al., 2005). The high temperature and pH is probably promoting the unwind of duplex DNA and thereby facilitating TopoIII to act in the substrate. In this task, *B.subtilis* TopoIII is not quite efficient: supercoiled DNA is only partially relaxed (fig.32), but never reaching the totally relaxed forms that are visible for a other topoisomerases, as *E.coli* TopoIII, that is very efficient at this task *in vitro* (DiGate and Marians, 1988). TopoIII from *E.coli*, in concert with RecQ, is also able to promote *in vitro* decatenation of two daughter chromosomes (Nurse et al., 2003). *In vivo* assays suggest a possible decatenation role of daughter molecules in *E.coli* (Nurse et al., 2003). It is not yet known if TopoIII in *B.subtilis* is also performing this function in the cell, but nucleoid morphology of double mutant *recUtopB*, that shows a greater defect in chromosome segregtion compare to single mutant *recU* (fig.26) suggest that it is possible.

The homologs of *B.subtilis* TopoIII are *E.coli* TopoIII, which shares 33% of sequence identity, and *B.cereus* TopoIIIβ, with shares 64% sequence identity. Alignment of the 3 sequences shows that TopoIII from *E.coli* is shorter and the C-terminal is quite different.

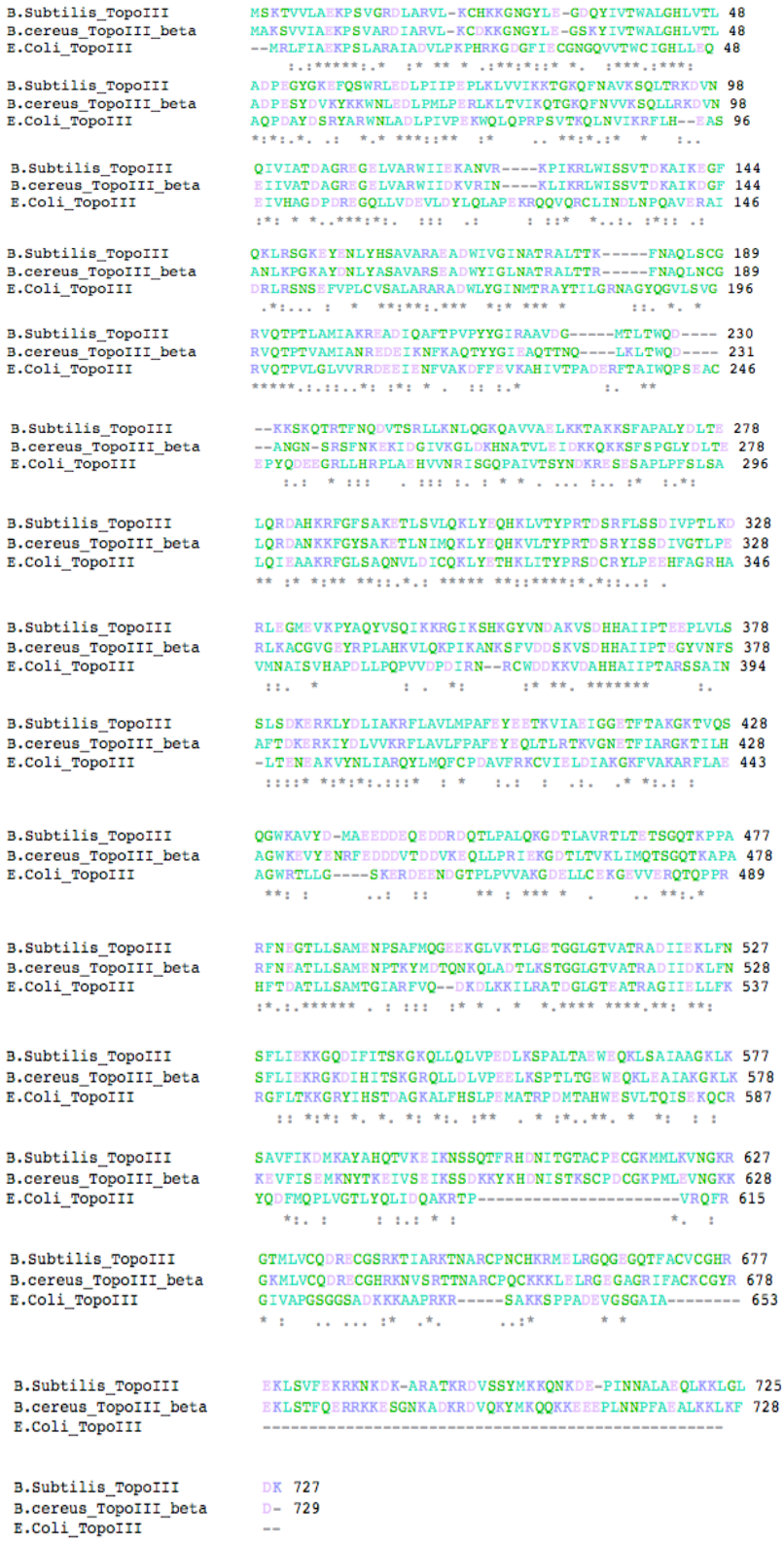

Figure 38: Sequence alignment of *E.coli* TopoIII, *B.cereus* TopoIIIβ and *B.subtilis* TopoIII. Asterisk indicates conserved residues. Two points indicates conserved amino acids and one point indicates no similarity. Apolar amino acids are shown in cyan. Basic amino acids are shown in purple. Acid amino acids are shown in pink. Polar amino acids are shown in green. The alignment was made with ClustalW software.

The main difference between the polypeptide sequence of TopoIII from *E.coli* and from *B.subtilis* and *B.cereus* is that the C-terminal of the last ones shows two putative zinc finger domains. Taking into account the poor relaxase activity of *B.subtilis* Topo III (fig.32), the same assay was done in the presence of 25 μM $ZnCl_2$, but it did not show any effect in the relaxation reaction (data not shown). In *E.coli*, the C-terminal region is not containing zinc finger, and it is implicated in the DNA binding but not in DNA cleavage site specificity (Zhang and DiGate, 1994). Interaction region with SSB is yet unknown

The fact that TopoIII is not very efficient in the relaxation of a supercoiled plasmid *in vitro* suggests that it probably needs an accessory protein to help in this reaction *in vivo*, as in the case detected for LrpC (see above). Another hypothesis is that its substrate *in vivo* is not a supercoiled DNA, but rather another type of structure. In fact, *in vitro* assays have shown here that TopoIII is able to bind to HR intermediates (fig. 34, table 17). Binding of this type of topoisomerases to ssDNA has also been shown for other type I topoisomerases. *E.coli* TopoIII and Topo I and *B.cereus* TopoIIIα and Topo I show binding to ssDNA in the present of 1 mM $MgCl_2$, with binding apparent constants (Kapp) of around 500-600 nM (Li et al., 2005). *B.subtilis* TopoIII shows in the same conditions a Kapp of around 80 nM (table 17), while it binds to the HJ with a Kapp of 14 nM (table 17). Human TopoIIIα binds to the HJ in the presence of 4 mM $MgCl_2$ with a Kapp of around 5 nM (Wu et al., 2006). The fact that TopoIII binds three to six times better for the HJ and other recombination intermediates than to random ssDNA or dsDNA substrate is a strong argument in favour of a DNA recombination *in vivo* role. Even though TopoIII alone is not able to cleave the HJ (fig. 35), it could still perform this reaction in the presence of a RecQ-like helicase, as it was pusblished before (Wu and Hickson, 2003). In this aspect, further experiments are needed to confirm the role of TopoIII in DNA dissolution.

On the other hand, TopoIII is able to preferentially cleave a bona-fide D-loop, with a higher efficiency when compared to other D-loop-resembling structures and to ssDNA (fig. 36). This type of cleavage has been shown for the homolog in Drosophila TopoIIIβ, that is able to cleave plasmid based D-loops and R-loops (Wilson-Sali and Hsieh, 2002). This is the only *in vitro* evidence for now of a possible role of TopoIII in synapsis, when the recombination intermediate is formed. However, it seems that the type of cleavage that TopoIII is performing in this D-loop is looking like a degradation product more than a resolution product (fig.36). This type of cleavage is in accordance with the antirecombinase role proposed in this Thesis. A resolution product of a recombination intermediate should be symmetric, as it is the case for the *B.subtilis* resolvase RecU (Ayora et al., 2004). On the other hand, the transformation assays of null mutant *topB* show that chromosomal efficiency is affected, around 36.6% when compared to the wildtype (part 3.2). During chromosomal transformation, the main player is RecA. Null mutant *recA* shows a very low chromosomal transformation efficiency (Fernandez et al., 2000). The most affected strains, after a *recA* null mutant are *recS* and *recU*, that show a chromosomal transformation efficiency of around 28 and 33% (Fernandez et al., 2000). This means that TopoIII could have an important role in chromosomal transformation *in vivo*. However, *in vivo*, if TopoIII is acting in chromosomal transformation, it should have a resolution activity and not a degradation activity, as the one observed *in vitro*. It could be that, *in vivo* in the cell context, where there is superhelicity, this is affecting TopoIII cleavage or this protein needs an accessory protein that helps by unwinding the substrate, that could be RecQ or RecS. Further experiments with the purified RecQ or RecS would help to understand this function.

CONCLUSIONS

The conclusions obtained from the present work are the followings:

1. LrpC intracellular levels do not show a variation between rich and minimal medium, but between different growth phases, having a maximum of expression in the end of exponential phase. LrpC cannot be considered as a global regulator in *B.subtilis*, due to the small amount of genes whose expression is affected in the absence or presence of this protein.

2. *In vivo* localization of GFP-LrpC in vegetative growth shows two principal patterns of localization, as discrete foci or associated to the nucleoid, that vary depending on the type of media. In exponential phase in minimal medium, GFP-LrpC shows two symmetric foci coincident with the nucleoid or one asymmetric focus in the borders of the nucleoid. This foci pattern is located closer to the cell poles in stationary phase. In competence medium, GFP-LrpC is mainly located at the cell poles.

3. After induction of DNA damage by MMC, GFP-LrpC is not recruited to the RCs. *In vivo* localization of GFP-LrpC in competent state defines a new localization at the cell pole for an architectural protein in *Bacteria*. This new role in DNA competence process is confirmed by transformation efficiency studies of mutant *lrpC*, which shows a half decay of plasmid transformation efficiency compared with the wildtype strain.

4. *B.subtilis* genes *lrpC* and *topB* conform an operon and therefore are transcribed under the same promoter. LrpC promotes DNA relaxation activity of Topo III, though it was not possible to detect any *in vitro* interaction between purified proteins LrpC and Topo III.

5. *B.subtilis* null mutant *topB* shows a very similar phenotype in cell and nucleoid morphology when compared to the wildtype strain. Double mutant *recUtopB* shows a 3-fold increase in anucleate cells when compare to single mutant *recU*.

6. After DNA damage by MMS or H_2O_2, cell viability of null mutant *topB* is very similar to the wildtype strain. Double mutants of *topB* with presynaptic genes *addAB*, *recJ*, *recO* and *recF* recover the defect when compare to the single mutants *addAB*, *recJ*, *recO* and *recF*, respectively. Double mutant *recUtopB* shows a synergic phenotype when compared to single mutant *recU*. TopoIII is implicated in DNA repair by homologous recombination and could have an anti-recombinase role in the cell. Genetic analysis suggest that RecQ and Topo III could be epistatic, while RecS and TopoIII would only be epistatic after damage caused by MMS.

7. *In vivo* localization of TopoIII-YFP shows a preference for cytosolic spaces, contrary to RecQ and RecS, that localize in the nucleoid. After induction of DNA damage by MMC, TopoIII-YFP is not recruited to the RCs.

8. *B.subtilis* Topo III is a monomer in solution of around 80 Kda. Topo III is a DNA relaxase that shows its activity at 52ºC and pH of 9.8.

9. Topo III shows a binding preference *in vitro* for recombination intermediates of 6-fold when compared to ssDNA and dsDNA in the presence of divalent cations as Mg^{2+}. Presence of EDTA decreases the binding affinity of Topo III for these substrates. Topo III is not able to cleave the HJ *in vitro* under the conditions tested.

10. TopoIII is able to specifically cleave the D-loop, a DNA intermediate that is formed during synapsis. Null mutant *topB* shows a defect in DNA chromosomal transformation that ensures the hypothesis of a possible D-loop cleavage *in vivo*.

BIBLIOGRAPHY

Aggarwal, M. & R. M. Brosh, (2009) WRN helicase defective in the premature aging disorder Werner syndrome genetically interacts with topoisomerase 3 and restores the top3 slow growth phenotype of sgs1 top3. *Aging (Albany NY)* **1**: 219-233.

Alonso, J. C., C. Gutierrez & F. Rojo, (1995a) The role of chromatin-associated protein Hbsu in beta-mediated DNA recombination is to facilitate the joining of distant recombination sites. *Mol Microbiol* **18**: 471-478.

Alonso, J. C., A. C. Stiege & G. Luder, (1993) Genetic recombination in Bacillus subtilis 168: effect of recN, recF, recH and addAB mutations on DNA repair and recombination. *Mol Gen Genet* **239**: 129-136.

Alonso, J. C., R. H. Tailor & G. Luder, (1988) Characterization of recombination-deficient mutants of Bacillus subtilis. *J Bacteriol* **170**: 3001-3007.

Alonso, J. C., F. Weise & F. Rojo, (1995b) The Bacillus subtilis histone-like protein Hbsu is required for DNA resolution and DNA inversion mediated by the beta recombinase of plasmid pSM19035. *J Biol Chem* **270**: 2938-2945.

Arwert, F. & G. Venema, (1973) Transformation in Bacillus subtilis. Fate of newly introduced transforming DNA. *Mol Gen Genet* **123**: 185-198.

Ayora, S., B. Carrasco, P. P. Cardenas, C. E. Cesar, C. Canas, T. Yadav, C. Marchisone & J. C. Alonso, (2011) Double-strand break repair in bacteria: a view from Bacillus subtilis. *FEMS Microbiol Rev*.

Ayora, S., B. Carrasco, E. Doncel, R. Lurz & J. C. Alonso, (2004) Bacillus subtilis RecU protein cleaves Holliday junctions and anneals single-stranded DNA. *Proc Natl Acad Sci U S A* **101**: 452-457.

Ayora, S., F. Rojo, N. Ogasawara, S. Nakai & J. C. Alonso, (1996) The Mfd protein of Bacillus subtilis 168 is involved in both transcription-coupled DNA repair and DNA recombination. *J Mol Biol* **256**: 301-318.

Azam, T. A., S. Hiraga & A. Ishihama, (2000) Two types of localization of the DNA-binding proteins within the Escherichia coli nucleoid. *Genes Cells* **5**: 613-626.

Belitsky, B. R., M. C. Gustafsson, A. L. Sonenshein & C. Von Wachenfeldt, (1997) An lrp-like gene of Bacillus subtilis involved in branched-chain amino acid transport. *J Bacteriol* **179**: 5448-5457.

Beloin, C., S. Ayora, R. Exley, L. Hirschbein, N. Ogasawara, Y. Kasahara, J. C. Alonso & F. L. Hegarat, (1997) Characterization of an lrp-like (lrpC) gene from Bacillus subtilis. *Mol Gen Genet* **256**: 63-71.

Beloin, C., R. Exley, A. L. Mahe, M. Zouine, S. Cubasch & F. Le Hegarat, (2000) Characterization of LrpC DNA-binding properties and regulation of Bacillus subtilis lrpC gene expression. *J Bacteriol* **182**: 4414-4424.

Beloin, C., J. Jeusset, B. Revet, G. Mirambeau, F. Le Hegarat & E. Le Cam, (2003) Contribution of DNA conformation and topology in right-handed DNA wrapping by the Bacillus subtilis LrpC protein. *J Biol Chem* **278**: 5333-5342.

Berka, R. M., J. Hahn, M. Albano, I. Draskovic, M. Persuh, X. Cui, A. Sloma, W. Widner & D. Dubnau, (2002) Microarray analysis of the Bacillus subtilis K-state: genome-wide expression changes dependent on ComK. *Mol Microbiol* **43**: 1331-1345.

Bernstein, K. A., S. Gangloff & R. Rothstein, (2010) The RecQ DNA helicases in DNA repair. *Annu Rev Genet* **44**: 393-417.

Birnboim, H. C. & J. Doly, (1979) A rapid alkaline extraction procedure for screening recombinant plasmid DNA. *Nucleic Acids Res* **7**: 1513-1523.

Brinkman, A. B., I. Dahlke, J. E. Tuininga, T. Lammers, V. Dumay, E. de Heus, J. H. Lebbink, M. Thomm, W. M. de Vos & J. van Der Oost, (2000) An Lrp-like transcriptional regulator from the archaeon Pyrococcus furiosus is negatively autoregulated. *J Biol Chem* **275**: 38160-38169.

Britton, R. A., D. C. Lin & A. D. Grossman, (1998) Characterization of a prokaryotic SMC protein involved in chromosome partitioning. *Genes Dev* **12**: 1254-1259.

Burbulys, D., K. A. Trach & J. A. Hoch, (1991) Initiation of sporulation in B. subtilis is controlled by a multicomponent phosphorelay. *Cell* **64**: 545-552.

Calvo, J. M. & R. G. Matthews, (1994) The leucine-responsive regulatory protein, a global regulator of metabolism in Escherichia coli. *Microbiol Rev* **58**: 466-490.

Carrasco, B., M. C. Cozar, R. Lurz, J. C. Alonso & S. Ayora, (2004) Genetic recombination in Bacillus subtilis 168: contribution of Holliday junction processing functions in chromosome segregation. *J Bacteriol* **186**: 5557-5566.

Chen, I., P. J. Christie & D. Dubnau, (2005) The ins and outs of DNA transfer in bacteria. *Science* **310**: 1456-1460.

Chen, S. & J. M. Calvo, (2002) Leucine-induced dissociation of Escherichia coli Lrp hexadecamers to octamers. *J Mol Biol* **318**: 1031-1042.

Chen, S., Z. Hao, E. Bieniek & J. M. Calvo, (2001) Modulation of Lrp action in Escherichia coli by leucine: effects on non-specific binding of Lrp to DNA. *J Mol Biol* **314**: 1067-1075.

Chester, N., F. Kuo, C. Kozak, C. D. O'Hara & P. Leder, (1998) Stage-specific apoptosis, developmental delay, and embryonic lethality in mice homozygous for a targeted disruption in the murine Bloom's syndrome gene. *Genes Dev* **12**: 3382-3393.

Cho, B. K., C. L. Barrett, E. M. Knight, Y. S. Park & B. O. Palsson, (2008) Genome-scale reconstruction of the Lrp regulatory network in Escherichia coli. *Proc Natl Acad Sci U S A* **105**: 19462-19467.

Chumsakul, O., H. Takahashi, T. Oshima, T. Hishimoto, S. Kanaya, N. Ogasawara & S. Ishikawa, Genome-wide binding profiles of the Bacillus subtilis transition state regulator AbrB and its homolog Abh reveals their interactive role in transcriptional regulation. *Nucleic Acids Res* **39**: 414-428.

Comella, N. & A. D. Grossman, (2005) Conservation of genes and processes controlled by the quorum response in bacteria: characterization of genes controlled by the quorum-sensing transcription factor ComA in Bacillus subtilis. *Mol Microbiol* **57**: 1159-1174.

Costes, A., F. Lecointe, S. McGovern, S. Quevillon-Cheruel & P. Polard, (2010) The C-terminal domain of the bacterial SSB protein acts as a DNA maintenance hub at active chromosome replication forks. *PLoS Genet* **6**: e1001238.

Cui, Y., Q. Wang, G. D. Stormo & J. M. Calvo, (1995) A consensus sequence for binding of Lrp to DNA. *J Bacteriol* **177**: 4872-4880.

Dartois, V., J. Liu & J. A. Hoch, (1997) Alterations in the flow of one-carbon units affect KinB-dependent sporulation in Bacillus subtilis. *Mol Microbiol* **25**: 39-51.

Davidoff-Abelson, R. & D. Dubnau, (1971) Fate of transforming DNA after uptake by competent Bacillus subtilis: failure of donor DNA to replicate in a recombination-deficient recipient. *Proc Natl Acad Sci U S A* **68**: 1070-1074.

Davidoff-Abelson, R. & D. Dubnau, (1973) Kinetic analysis of the products of donor deoxyribonucleate in transformed cells of Bacillus subtilis. *J Bacteriol* **116**: 154-162.

de Wind, N., M. de Jong, M. Meijer & A. R. Stuitje, (1985) Site-directed mutagenesis of the Escherichia coli chromosome near oriC: identification and characterization of asnC, a regulatory element in E. coli asparagine metabolism. *Nucleic Acids Res* **13**: 8797-8811.

Depew, R. E., L. F. Liu & J. C. Wang, (1978) Interaction between DNA and Escherichia coli protein omega. Formation of a complex between single-stranded DNA and omega protein. *J Biol Chem* **253**: 511-518.

DiGate, R. J. & K. J. Marians, (1988) Identification of a potent decatenating enzyme from Escherichia coli. *J Biol Chem* **263**: 13366-13373.

Dillon, S. C. & C. J. Dorman, (2010) Bacterial nucleoid-associated proteins, nucleoid structure and gene expression. *Nat Rev Microbiol* **8**: 185-195.

Dubnau, D., (1999) DNA uptake in bacteria. *Annu Rev Microbiol* **53**: 217-244.

Dubnau, D. & C. Cirigliano, (1972a) Fate of transforming deoxyribonucleic acid after uptake by competent Bacillus subtilis: size and distribution of the integrated donor segments. *J Bacteriol* **111**: 488-494.

Dubnau, D. & C. Cirigliano, (1972b) Fate of transforming DNA following uptake by competent Bacillus subtilis. IV. The endwise attachment and uptake of transforming DNA. *J Mol Biol* **64**: 31-46.

Dubnau, D. & C. Cirigliano, (1973) Fate of transforming DNA following uptake by competent Bacillus subtilis. VI. Non-covalent association of donor and recipient DNA. *Mol Gen Genet* **120**: 101-106.

Dubnau, D. & M. Roggiani, (1990) Growth medium-independent genetic competence mutants of Bacillus subtilis. *J Bacteriol* **172**: 4048-4055.

Ernsting, B. R., M. R. Atkinson, A. J. Ninfa & R. G. Matthews, (1992) Characterization of the regulon controlled by the leucine-responsive regulatory protein in Escherichia coli. *J Bacteriol* **174**: 1109-1118.

Fawcett, P., P. Eichenberger, R. Losick & P. Youngman, (2000) The transcriptional profile of early to middle sporulation in Bacillus subtilis. *Proc Natl Acad Sci U S A* **97**: 8063-8068.

Fernandez, S., S. Ayora & J. C. Alonso, (2000) Bacillus subtilis homologous recombination: genes and products. *Res Microbiol* **151**: 481-486.

Fernandez, S., F. Rojo & J. C. Alonso, (1997) The Bacillus subtilis chromatin-associated protein Hbsu is involved in DNA repair and recombination. *Mol Microbiol* **23**: 1169-1179.

Fernandez, S., A. Sorokin & J. C. Alonso, (1998) Genetic recombination in Bacillus subtilis 168: effects of recU and recS mutations on DNA repair and homologous recombination. *J Bacteriol* **180**: 3405-3409.

Fisher, S. H., (1999) Regulation of nitrogen metabolism in Bacillus subtilis: vive la difference! *Mol Microbiol* **32**: 223-232.

Friedberg, D., M. Midkiff & J. M. Calvo, (2001) Global versus local regulatory roles for Lrp-related proteins: Haemophilus influenzae as a case study. *J Bacteriol* **183**: 4004-4011.

Friedman, B. M. & R. E. Yasbin, (1983) The genetics and specificity of the constitutive excision repair system of Bacillus subtilis. *Mol Gen Genet* **190**: 481-486.

Glaser, P., M. E. Sharpe, B. Raether, M. Perego, K. Ohlsen & J. Errington, (1997) Dynamic, mitotic-like behavior of a bacterial protein required for accurate chromosome partitioning. *Genes Dev* **11**: 1160-1168.

Graumann, P. L., (2000) Bacillus subtilis SMC is required for proper arrangement of the chromosome and for efficient segregation of replication termini but not for bipolar movement of newly duplicated origin regions. *J Bacteriol* **182**: 6463-6471.

Graumann, P. L., R. Losick & A. V. Strunnikov, (1998) Subcellular localization of Bacillus subtilis SMC, a protein involved in chromosome condensation and segregation. *J Bacteriol* **180**: 5749-5755.

Groch, N., H. Schindelin, A. S. Scholtz, U. Hahn & U. Heinemann, (1992) Determination of DNA-binding parameters for the Bacillus subtilis histone-like HBsu protein through introduction of fluorophores by site-directed mutagenesis of a synthetic gene. *Eur J Biochem* **207**: 677-685.

Grompone, G., M. Seigneur, S. D. Ehrlich & B. Michel, (2002) Replication fork reversal in DNA polymerase III mutants of Escherichia coli: a role for the beta clamp. *Mol Microbiol* **44**: 1331-1339.

Gruber, S. & J. Errington, (2009) Recruitment of condensin to replication origin regions by ParB/SpoOJ promotes chromosome segregation in B. subtilis. *Cell* **137**: 685-696.

Gryczan, T. J. & D. Dubnau, (1978) Construction and properties of chimeric plasmids in Bacillus subtilis. *Proc Natl Acad Sci U S A* **75**: 1428-1432.

Hahn, J., B. Maier, B. J. Haijema, M. Sheetz & D. Dubnau, (2005) Transformation proteins and DNA uptake localize to the cell poles in Bacillus subtilis. *Cell* **122**: 59-71.

Hahn, J., M. Roggiani & D. Dubnau, (1995) The major role of Spo0A in genetic competence is to downregulate abrB, an essential competence gene. *J Bacteriol* **177**: 3601-3605.

Haima, P., S. Bron & G. Venema, (1987) The effect of restriction on shotgun cloning and plasmid stability in Bacillus subtilis Marburg. *Mol Gen Genet* **209**: 335-342.

Hamoen, L. W., A. F. Van Werkhoven, J. J. Bijlsma, D. Dubnau & G. Venema, (1998) The competence transcription factor of Bacillus subtilis recognizes short A/T-rich sequences arranged in a unique, flexible pattern along the DNA helix. *Genes Dev* **12**: 1539-1550.

Hanahan, D., (1983) Studies on transformation of Escherichia coli with plasmids. *J Mol Biol* **166**: 557-580.

Harmon, F. G., J. P. Brockman & S. C. Kowalczykowski, (2003) RecQ helicase stimulates both DNA catenation and changes in DNA topology by topoisomerase III. *J Biol Chem* **278**: 42668-42678.

Harmon, F. G., R. J. DiGate & S. C. Kowalczykowski, (1999) RecQ helicase and topoisomerase III comprise a novel DNA strand passage function: a conserved mechanism for control of DNA recombination. *Mol Cell* **3**: 611-620.

Hirano, M. & T. Hirano, (2002) Hinge-mediated dimerization of SMC protein is essential for its dynamic interaction with DNA. *EMBO J* **21**: 5733-5744.

Hoch, J. A., (1993) The phosphorelay signal transduction pathway in the initiation of Bacillus subtilis sporulation. *J Cell Biochem* **51**: 55-61.

Ireton, K., N. W. t. Gunther & A. D. Grossman, (1994) spo0J is required for normal chromosome segregation as well as the initiation of sporulation in Bacillus subtilis. *J Bacteriol* **176**: 5320-5329.

Jin, D. J. & J. E. Cabrera, (2006) Coupling the distribution of RNA polymerase to global gene regulation and the dynamic structure of the bacterial nucleoid in Escherichia coli. *J Struct Biol* **156**: 284-291.

Kaimer, C., J. E. Gonzalez-Pastor & P. L. Graumann, (2009) SpoIIIE and a novel type of DNA translocase, SftA, couple chromosome segregation with cell division in Bacillus subtilis. *Mol Microbiol* **74**: 810-825.

Kamashev, D. & J. Rouviere-Yaniv, (2000) The histone-like protein HU binds specifically to DNA recombination and repair intermediates. *EMBO J* **19**: 6527-6535.

Kawashima, T., H. Aramaki, T. Oyamada, K. Makino, M. Yamada, H. Okamura, K. Yokoyama, S. A. Ishijima & M. Suzuki, (2008) Transcription regulation by feast/famine regulatory proteins, FFRPs, in archaea and eubacteria. *Biol Pharm Bull* **31**: 173-186.

Kidane, D., B. Carrasco, C. Manfredi, K. Rothmaier, S. Ayora, S. Tadesse, J. C. Alonso & P. L. Graumann, (2009) Evidence for different pathways during horizontal gene transfer in competent Bacillus subtilis cells. *PLoS Genet* **5**: e1000630.

Kidane, D. & P. L. Graumann, (2005a) Dynamic formation of RecA filaments at DNA double strand break repair centers in live cells. *J Cell Biol* **170**: 357-366.

Kidane, D. & P. L. Graumann, (2005b) Intracellular protein and DNA dynamics in competent Bacillus subtilis cells. *Cell* **122**: 73-84.

Kidane, D., H. Sanchez, J. C. Alonso & P. L. Graumann, (2004) Visualization of DNA double-strand break repair in live bacteria reveals dynamic recruitment of Bacillus subtilis RecF, RecO and RecN proteins to distinct sites on the nucleoids. *Mol Microbiol* **52**: 1627-1639.

Kohler, P. & M. A. Marahiel, (1997) Association of the histone-like protein HBsu with the nucleoid of Bacillus subtilis. *J Bacteriol* **179**: 2060-2064.

Koike, H., S. A. Ishijima, L. Clowney & M. Suzuki, (2004) The archaeal feast/famine regulatory protein: potential roles of its assembly forms for regulating transcription. *Proc Natl Acad Sci U S A* **101**: 2840-2845.

Kolling, R., A. Gielow, W. Seufert, C. Kucherer & W. Messer, (1988) AsnC, a multifunctional regulator of genes located around the replication origin of Escherichia coli, oriC. *Mol Gen Genet* **212**: 99-104.

Kolling, R. & H. Lother, (1985) AsnC: an autogenously regulated activator of asparagine synthetase A transcription in Escherichia coli. *J Bacteriol* **164**: 310-315.

Kramer, N., J. Hahn & D. Dubnau, (2007) Multiple interactions among the competence proteins of Bacillus subtilis. *Mol Microbiol* **65**: 454-464.

Krishnamurthy, M., S. Tadesse, K. Rothmaier & P. L. Graumann, (2010) A novel SMC-like protein, SbcE (YhaN), is involved in DNA double-strand break repair and competence in Bacillus subtilis. *Nucleic Acids Res* **38**: 455-466.

Kwan, K. Y., P. B. Moens & J. C. Wang, (2003) Infertility and aneuploidy in mice lacking a type IA DNA topoisomerase III beta. *Proc Natl Acad Sci U S A* **100**: 2526-2531.

Lecointe, F., C. Serena, M. Velten, A. Costes, S. McGovern, J. C. Meile, J. Errington, S. D. Ehrlich, P. Noirot & P. Polard, (2007) Anticipating chromosomal replication fork arrest: SSB targets repair DNA helicases to active forks. *EMBO J* **26**: 4239-4251.

Lee, J., D. R. Tomchick, C. A. Brautigam, M. Machius, R. Kort, K. J. Hellingwerf & K. H. Gardner, (2008) Changes at the KinA PAS-A dimerization interface influence histidine kinase function. *Biochemistry* **47**: 4051-4064.

Lewis, P. J. & A. L. Marston, (1999) GFP vectors for controlled expression and dual labelling of protein fusions in Bacillus subtilis. *Gene* **227**: 101-110.

Lewis, P. J., S. D. Thaker & J. Errington, (2000) Compartmentalization of transcription and translation in Bacillus subtilis. *EMBO J* **19**: 710-718.

Li, W. & J. C. Wang, (1998) Mammalian DNA topoisomerase IIIalpha is essential in early embryogenesis. *Proc Natl Acad Sci U S A* **95**: 1010-1013.

Li, Z., H. Hiasa & R. DiGate, (2005) Bacillus cereus DNA topoisomerase I and IIIalpha: purification, characterization and complementation of Escherichia coli TopoIII activity. *Nucleic Acids Res* **33**: 5415-5425.

Li, Z., H. Hiasa & R. DiGate, (2006) Characterization of a unique type IA topoisomerase in Bacillus cereus. *Mol Microbiol* **60**: 140-151.

Lin, D. C., P. A. Levin & A. D. Grossman, (1997) Bipolar localization of a chromosome partition protein in Bacillus subtilis. *Proc Natl Acad Sci U S A* **94**: 4721-4726.

Liu, L. F. & J. C. Wang, (1979) Interaction between DNA and Escherichia coli DNA topoisomerase I. Formation of complexes between the protein and superhelical and nonsuperhelical duplex DNAs. *J Biol Chem* **254**: 11082-11088.

Lopez, C. R., S. Yang, R. W. Deibler, S. A. Ray, J. M. Pennington, R. J. Digate, P. J. Hastings, S. M. Rosenberg & E. L. Zechiedrich, (2005) A role for topoisomerase III in a recombination pathway alternative to RuvABC. *Mol Microbiol* **58**: 80-101.

Lopez-Torrejon, G., M. I. Martinez-Jimenez & S. Ayora, (2006) Role of LrpC from Bacillus subtilis in DNA transactions during DNA repair and recombination. *Nucleic Acids Res* **34**: 120-129.

Luo, G., I. M. Santoro, L. D. McDaniel, I. Nishijima, M. Mills, H. Youssoufian, H. Vogel, R. A. Schultz & A. Bradley, (2000) Cancer predisposition caused by elevated mitotic recombination in Bloom mice. *Nat Genet* **26**: 424-429.

Manfredi, C., B. Carrasco, S. Ayora & J. C. Alonso, (2008) Bacillus subtilis RecO nucleates RecA onto SsbA-coated single-stranded DNA. *J Biol Chem* **283**: 24837-24847.

Mascarenhas, J., H. Sanchez, S. Tadesse, D. Kidane, M. Krisnamurthy, J. C. Alonso & P. L. Graumann, (2006) Bacillus subtilis SbcC protein plays an important role in DNA inter-strand cross-link repair. *BMC Mol Biol* **7**: 20.

Mascarenhas, J., J. Soppa, A. V. Strunnikov & P. L. Graumann, (2002) Cell cycle-dependent localization of two novel prokaryotic chromosome segregation and condensation proteins in Bacillus subtilis that interact with SMC protein. *EMBO J* **21**: 3108-3118.

Mascarenhas, J., A. V. Volkov, C. Rinn, J. Schiener, R. Guckenberger & P. L. Graumann, (2005) Dynamic assembly, localization and proteolysis of the Bacillus subtilis SMC complex. *BMC Cell Biol* **6**: 28.

Micka, B., N. Groch, U. Heinemann & M. A. Marahiel, (1991) Molecular cloning, nucleotide sequence, and characterization of the Bacillus subtilis gene encoding the DNA-binding protein HBsu. *J Bacteriol* **173**: 3191-3198.

Micka, B. & M. A. Marahiel, (1992) The DNA-binding protein HBsu is essential for normal growth and development in Bacillus subtilis. *Biochimie* **74**: 641-650.

Molle, V., Y. Nakaura, R. P. Shivers, H. Yamaguchi, R. Losick, Y. Fujita & A. L. Sonenshein, (2003) Additional targets of the Bacillus subtilis global regulator CodY identified by chromatin immunoprecipitation and genome-wide transcript analysis. *J Bacteriol* **185**: 1911-1922.

Mondragon, A. & R. DiGate, (1999) The structure of Escherichia coli DNA topoisomerase III. *Structure* **7**: 1373-1383.

Moriya, S., E. Tsujikawa, A. K. Hassan, K. Asai, T. Kodama & N. Ogasawara, (1998) A Bacillus subtilis gene-encoding protein homologous to eukaryotic SMC motor protein is necessary for chromosome partition. *Mol Microbiol* **29**: 179-187.

Mortier-Barriere, I., M. Velten, P. Dupaigne, N. Mirouze, O. Pietrement, S. McGovern, G. Fichant, B. Martin, P. Noirot, E. Le Cam, P. Polard & J. P. Claverys, (2007) A key

presynaptic role in transformation for a widespread bacterial protein: DprA conveys incoming ssDNA to RecA. *Cell* **130**: 824-836.

Newman, E. B., R. D'Ari & R. T. Lin, (1992) The leucine-Lrp regulon in E. coli: a global response in search of a raison d'etre. *Cell* **68**: 617-619.

Nurse, P., C. Levine, H. Hassing & K. J. Marians, (2003) Topoisomerase III can serve as the cellular decatenase in Escherichia coli. *J Biol Chem* **278**: 8653-8660.

Oliveira-Costa, J. P., J. Zanetti, L. R. Oliveira, F. A. Soares, L. Z. Ramalho, F. Silva Ramalho, S. B. Garcia & A. Ribeiro-Silva, (2010) Significance of topoisomerase IIIbeta expression in breast ductal carcinomas: strong associations with disease-specific survival and metastasis. *Hum Pathol* **41**: 1624-1630.

Phillips, Z. E. & M. A. Strauch, (2002) Bacillus subtilis sporulation and stationary phase gene expression. *Cell Mol Life Sci* **59**: 392-402.

Platko, J. V. & J. M. Calvo, (1993) Mutations affecting the ability of Escherichia coli Lrp to bind DNA, activate transcription, or respond to leucine. *J Bacteriol* **175**: 1110-1117.

Platko, J. V., D. A. Willins & J. M. Calvo, (1990) The ilvIH operon of Escherichia coli is positively regulated. *J Bacteriol* **172**: 4563-4570.

Ptacin, J. L., M. Nollmann, E. C. Becker, N. R. Cozzarelli, K. Pogliano & C. Bustamante, (2008) Sequence-directed DNA export guides chromosome translocation during sporulation in Bacillus subtilis. *Nat Struct Mol Biol* **15**: 485-493.

Ratnayake-Lecamwasam, M., P. Serror, K. W. Wong & A. L. Sonenshein, (2001) Bacillus subtilis CodY represses early-stationary-phase genes by sensing GTP levels. *Genes Dev* **15**: 1093-1103.

Raynard, S., W. Bussen & P. Sung, (2006) A double Holliday junction dissolvasome comprising BLM, topoisomerase IIIalpha, and BLAP75. *J Biol Chem* **281**: 13861-13864.

Ricca, E., D. A. Aker & J. M. Calvo, (1989) A protein that binds to the regulatory region of the Escherichia coli ilvIH operon. *J Bacteriol* **171**: 1658-1664.

Ross, M. A. & P. Setlow, (2000) The Bacillus subtilis HBsu protein modifies the effects of alpha/beta-type, small acid-soluble spore proteins on DNA. *J Bacteriol* **182**: 1942-1948.

Sanchez, H., B. Carrasco, M. C. Cozar & J. C. Alonso, (2007a) Bacillus subtilis RecG branch migration translocase is required for DNA repair and chromosomal segregation. *Mol Microbiol* **65**: 920-935.

Sanchez, H., M. C. Cozar & M. I. Martinez-Jimenez, (2007b) Targeting the Bacillus subtilis genome: an efficient and clean method for gene disruption. *J Microbiol Methods* **70**: 389-394.

Sanchez, H., D. Kidane, M. Castillo Cozar, P. L. Graumann & J. C. Alonso, (2006) Recruitment of Bacillus subtilis RecN to DNA double-strand breaks in the absence of DNA end processing. *J Bacteriol* **188**: 353-360.

Sanchez, H., D. Kidane, P. Reed, F. A. Curtis, M. C. Cozar, P. L. Graumann, G. J. Sharples & J. C. Alonso, (2005) The RuvAB branch migration translocase and RecU Holliday junction resolvase are required for double-stranded DNA break repair in Bacillus subtilis. *Genetics* **171**: 873-883.

Seki, M., M. Otsuki, Y. Ishii, S. Tada & T. Enomoto, (2008) RecQ family helicases in genome stability: lessons from gene disruption studies in DT40 cells. *Cell Cycle* **7**: 2472-2478.

Sherratt, D. J., (2003) Bacterial chromosome dynamics. *Science* **301**: 780-785.

Shimamoto, A., K. Nishikawa, S. Kitao & Y. Furuichi, (2000) Human RecQ5beta, a large isomer of RecQ5 DNA helicase, localizes in the nucleoplasm and interacts with topoisomerases 3alpha and 3beta. *Nucleic Acids Res* **28**: 1647-1655.

Shivers, R. P. & A. L. Sonenshein, (2004) Activation of the Bacillus subtilis global regulator CodY by direct interaction with branched-chain amino acids. *Mol Microbiol* **53**: 599-611.

Singh, R. N., (1972) Number of deoxyribonucleic acid uptake sites in competent cells of Bacillus subtilis. *J Bacteriol* **110**: 266-272.

Soppa, J., K. Kobayashi, M. F. Noirot-Gros, D. Oesterhelt, S. D. Ehrlich, E. Dervyn, N. Ogasawara & S. Moriya, (2002) Discovery of two novel families of proteins that are proposed to interact with prokaryotic SMC proteins, and characterization of the Bacillus subtilis family members ScpA and ScpB. *Mol Microbiol* **45**: 59-71.

Strauch, M., V. Webb, G. Spiegelman & J. A. Hoch, (1990) The SpoOA protein of Bacillus subtilis is a repressor of the abrB gene. *Proc Natl Acad Sci U S A* **87**: 1801-1805.

Strauch, M. A., (1993) Regulation of Bacillus subtilis gene expression during the transition from exponential growth to stationary phase. *Prog Nucleic Acid Res Mol Biol* **46**: 121-153.

Suski, C. & K. J. Marians, (2008) Resolution of converging replication forks by RecQ and topoisomerase III. *Mol Cell* **30**: 779-789.

Tadesse, S. & P. L. Graumann, (2006) Differential and dynamic localization of topoisomerases in Bacillus subtilis. *J Bacteriol* **188**: 3002-3011.

Tadesse, S. & P. L. Graumann, (2007) DprA/Smf protein localizes at the DNA uptake machinery in competent Bacillus subtilis cells. *BMC Microbiol* **7**: 105.

Tani, T. H., A. Khodursky, R. M. Blumenthal, P. O. Brown & R. G. Matthews, (2002) Adaptation to famine: a family of stationary-phase genes revealed by microarray analysis. *Proc Natl Acad Sci U S A* **99**: 13471-13476.

Tapias, A., G. Lopez & S. Ayora, (2000) Bacillus subtilis LrpC is a sequence-independent DNA-binding and DNA-bending protein which bridges DNA. *Nucleic Acids Res* **28**: 552-559.

Thaw, P., S. E. Sedelnikova, T. Muranova, S. Wiese, S. Ayora, J. C. Alonso, A. B. Brinkman, J. Akerboom, J. van der Oost & J. B. Rafferty, (2006) Structural insight into gene transcriptional regulation and effector binding by the Lrp/AsnC family. *Nucleic Acids Res* **34**: 1439-1449.

Tse, Y. C., K. Kirkegaard & J. C. Wang, (1980) Covalent bonds between protein and DNA. Formation of phosphotyrosine linkage between certain DNA topoisomerases and DNA. *J Biol Chem* **255**: 5560-5565.

van Sinderen, D., A. Luttinger, L. Kong, D. Dubnau, G. Venema & L. Hamoen, (1995) comK encodes the competence transcription factor, the key regulatory protein for competence development in Bacillus subtilis. *Mol Microbiol* **15**: 455-462.

Vasantha, N. & E. Freese, (1979) The role of manganese in growth and sporulation of Bacillus subtilis. *J Gen Microbiol* **112**: 329-336.

Veaute, X., S. Delmas, M. Selva, J. Jeusset, E. Le Cam, I. Matic, F. Fabre & M. A. Petit, (2005) UvrD helicase, unlike Rep helicase, dismantles RecA nucleoprotein filaments in Escherichia coli. *EMBO J* **24**: 180-189.

Wang, Q., F. G. Albert, D. J. Fitzgerald, J. M. Calvo & J. N. Anderson, (1994) Sequence determinants of DNA bending in the ilvlH promoter and regulatory region of Escherichia coli. *Nucleic Acids Res* **22**: 5753-5760.

Wang, Q. & J. M. Calvo, (1993) Lrp, a major regulatory protein in Escherichia coli, bends DNA and can organize the assembly of a higher-order nucleoprotein structure. *EMBO J* **12**: 2495-2501.

Watt, P. M., E. J. Louis, R. H. Borts & I. D. Hickson, (1995) Sgs1: a eukaryotic homolog of E. coli RecQ that interacts with topoisomerase II in vivo and is required for faithful chromosome segregation. *Cell* **81**: 253-260.

Weinrauch, Y., N. Guillen & D. A. Dubnau, (1989) Sequence and transcription mapping of Bacillus subtilis competence genes comB and comA, one of which is related to a family of bacterial regulatory determinants. *J Bacteriol* **171**: 5362-5375.

Willins, D. A., C. W. Ryan, J. V. Platko & J. M. Calvo, (1991) Characterization of Lrp, and Escherichia coli regulatory protein that mediates a global response to leucine. *J Biol Chem* **266**: 10768-10774.

Wilson, G. A. & K. F. Bott, (1968) Nutritional factors influencing the development of competence in the Bacillus subtilis transformation system. *J Bacteriol* **95**: 1439-1449.

Wilson-Sali, T. & T. S. Hsieh, (2002) Preferential cleavage of plasmid-based R-loops and D-loops by Drosophila topoisomerase IIIbeta. *Proc Natl Acad Sci U S A* **99**: 7974-7979.

Wu, L., C. Z. Bachrati, J. Ou, C. Xu, J. Yin, M. Chang, W. Wang, L. Li, G. W. Brown & I. D. Hickson, (2006) BLAP75/RMI1 promotes the BLM-dependent dissolution of homologous recombination intermediates. *Proc Natl Acad Sci U S A* **103**: 4068-4073.

Wu, L., S. L. Davies, P. S. North, H. Goulaouic, J. F. Riou, H. Turley, K. C. Gatter & I. D. Hickson, (2000) The Bloom's syndrome gene product interacts with topoisomerase III. *J Biol Chem* **275**: 9636-9644.

Wu, L. & I. D. Hickson, (2003) The Bloom's syndrome helicase suppresses crossing over during homologous recombination. *Nature* **426**: 870-874.

Wu, Y. & R. M. Brosh, Jr., (2010) Distinct roles of RECQ1 in the maintenance of genomic stability. *DNA Repair (Amst)* **9**: 315-324.

Yang, J., C. Z. Bachrati, J. Ou, I. D. Hickson & G. W. Brown, (2010) Human topoisomerase IIIalpha is a single-stranded DNA decatenase that is stimulated by BLM and RMI1. *J Biol Chem* **285**: 21426-21436.

Yokoyama, K., S. A. Ishijima, L. Clowney, H. Koike, H. Aramaki, C. Tanaka, K. Makino & M. Suzuki, (2006) Feast/famine regulatory proteins (FFRPs): Escherichia coli Lrp, AsnC and related archaeal transcription factors. *FEMS Microbiol Rev* **30**: 89-108.

Yokoyama, K., S. A. Ishijima, H. Koike, C. Kurihara, A. Shimowasa, M. Kabasawa, T. Kawashima & M. Suzuki, (2007) Feast/famine regulation by transcription factor FL11 for the survival of the hyperthermophilic archaeon Pyrococcus OT3. *Structure* **15**: 1542-1554.

Young, F. E., (1967) Competence in Bacillus subtilis transformation system. *Nature* **213**: 773-775.

Zhang, H. L. & R. J. DiGate, (1994) The carboxyl-terminal residues of Escherichia coli DNA topoisomerase III are involved in substrate binding. *J Biol Chem* **269**: 9052-9059.

Zhu, Q., P. Pongpech & R. J. DiGate, (2001) Type I topoisomerase activity is required for proper chromosomal segregation in Escherichia coli. *Proc Natl Acad Sci U S A* **98**: 9766-9771.